The Tubulin Folding Pathway: Roles of cofactor C/Tbc1 and small GTPase Arl2/Alp41

Risa Mori

University College London

and

Cancer Research UK London Research Institute

PhD Supervisor: Takashi Toda

A thesis submitted for the degree of

Doctor of Philosophy

University College London

September 2012

Declaration

I, Risa Mori, confirm that the work presented in this thesis is my own. Where information has been derived from other sources, I confirm that this has been indicated in the thesis.

Abstract

Supplying a proper amount of correctly folded α/β-tubulin heterodimers is critical for microtubule dynamics. Formation of assembly-competent heterodimers is remarkably complicated at the molecular level, in which the α- and β-tubulins are separately processed in a chaperone-dependent manner. It is known that this sequential step is performed by the tubulin folding cofactor pathway, comprising of a specific set of regulatory proteins - cofactors A to E.

Following detailed biochemical studies in vertebrates, studies have been carried out in *in vivo* models using *S. pombe*, where the pathway is absolutely essential for viability and each component is evolutionarily conserved. The significance of the data and the possibility of the cofactors playing additional roles led us to study Tbc1, the cofactor C orthologue, which we isolated as a high-copy suppressor of α2-tubulin mutants (*atb2-983*). Previous work from others and our own lab indicated that Arl2/Alp41 is a GTP binding protein that would be regulated by the GAP, cofactor C/Tbc1. In order to pursue the *in vivo* roles of Tbc1 and Alp41, we created temperature-sensitive mutants to analyse defective phenotypes, particularly focussing on microtubule structures and dynamics. Interestingly, we have found a range of phenotypes that may be explained by the resulting GTP/GDP state of the G protein. Consistent with Tbc1 being a GAP for Alp41, genetic data supports that Tbc1 negatively regulates Alp41. Biochemical studies have shown that the interactions of these proteins is conserved in fission yeast, and combined with the genetic data we investigated their physiological significance.

In addition, we have identified that Arl2/Alp41 also interacts with cofactor D/Alp1 in a GTP/GDP state dependent manner. This led us to an interesting finding that cofactor D/Alp1 possibly has two opposing roles in the cofactor pathway – to assemble and to disassemble microtubules.

Acknowledgements

I would first like to express my utmost gratitude to my supervisor Takashi for all the support, supervision and guidance, and being patient and understanding with me throughout the last four years. Thanks also go out to the lab members, past and present – Akiko, Aldona, Chiho, Chii Shyang, Hiro, Hirofumi, Isabelle, Kathleen, Kuo-Shun, and Ngang Heok. Thank you all for the technical help, scientific advice, encouragement and fun you shared with me. Special thanks go out to Chii Shyang (aka Daddy) and Kuo-Shun (& Peggy!) for making it so easy to fit into the lab when I first arrived. Daughter was very pleased. And of course, a very big special thanks to Isabelle, for all the scientific and mental support, as well as the many laughs we shared (I will be waiting for that book)!

It wouldn't have been such a fantastic time without all the Yeasties on the floor – thank you to everyone in Frank's, Julie's and Jacky/Paul's labs. It was great to feel a part of this big group of fun-loving people, and to know that there was always someone I could chat to down the corridor. A special mention to my buddies Adrian and Vanessa, for the many hours we spent talking about very important scientific things. My habit of looking around my bench to find bits of paper every day will be a hard one to lose! Thank you also to my year group, especially the "7th floor crew" for the last couple of months!

I must also thank my flatmates Jason and Claire for having to put up with me for so long – I wouldn't have made it without you guys being so comforting and supportive, especially when it meant so much to have a warm (and whacky) home to come home to. A big arigato to Arisa, who also had to put up with me for ages – I'm glad to have shared such fun times with you and I'm sure the experience would have been very different without you on the 6th floor! Also to thank, my wonderful comrade in PhD crime, Ru – for always being there for spontaneous 'discussions'!

Finally I would like to thank my wonderful family, for being so supportive as I went through a time of drastic change and development. Thank you for believing in me, and all their love that helped me through these four years.

Table of Contents

Table of figures

List of tables

Abbreviations

aa	amino acid
bp	base pair
cDNA	complementary deoxyribonucleic acid
CFP	cyan fluorescent protein
DAPI	4',6-diamidino-2-phenylindole
dGTP	deoxyguanosine triphosphate
DNA	deoxyribonucleic acid
dNTP	deoxynucleoside triphosphate
DTT	dithiothreitol
EMM	Edinburgh minimal medium
GAP	GTPase activating protein
GDI	Guanosine nucleotide dissociation inhibitors
GDP	guanosine diphosphate
GEF	Guanine nucleotide exchange factor
GFP	green fluorescent protein
GTP	guanosine triphosphate
H_2O	water
HA	hemagglutinin epitope
hph^r	hygromycin B resistance
IP	immunoprecipitation
IPTG	isopropyl β-D-1-thiogalactopyranoside
kan^r	kanamycin/geneticin resistance
LB	Luria-Bertani
mCherry	monomeric Cherry
mRFP	monomeric red fluorescent protein
MT	microtubule
MTOC	microtubule organising centre
NaOH	sodium hydroxide
nat^r	nourseothricin resistance
OD_{600}	optical density at 600 nm

PBS	phosphate buffered saline
PCR	polymerase chain reaction
PEG	polyethylene glycol
PMSF	phenylmethylsulphonyl fluoride
PVDF	polyvinylidene Difluoride
SDS-PAGE	sodium dodecyl sulfate polyacrylamide gel electrophoresis
SPB	spindle pole body
TBZ	thiabendazole
YE5S	yeast extract with supplements

Chapter 1. Introduction

1.1 The importance of cell division

Any living organism requires the process of cell division, where a cell divides to produce two identical daughter cells. The process is important for every aspect of life – in unicellular organisms it is required for reproduction and proliferation, in which the division creates an entire new organism. In multicellular organisms such as humans, the process is necessary for all stages of life – from embryonic and organ development, to death. Everyday, our bodies are losing millions of cells by cell death which need to be replenished, and cell division enables us to do so. In order for proper cell division to occur, many factors must be accurately controlled and regulated so that the two daughter cells can receive exactly the same genetic material after chromosome segregation. Several mechanisms and even more players are involved in this regulation, and one of the crucial machineries is the cellular cytoskeleton.

1.2 The cytoskeleton

The cytoskeleton, as the name suggests, is the collective name given to the dynamic protein structures that act as a skeleton or cellular scaffolding within the cell. Both eukaryotes and prokaryotes are understood to possess a cytoskeleton, although there are differences between the roles they play and in composition. The eukaryotic cytoskeleton consists of 3 main constituents – the actin microfilaments, intermediate filaments and the microtubules.

The actin microfilaments are thin (approx. 6 nm) linear filaments composed of actin subunits, which generate and resist forces to enable cell-shape maintenance, cell migration and cytokinesis. They utilise ATP hydrolysis to grow, both at the fast-growing barbed end and the slower-growing pointed end. These polarised filaments form either bundles or networks, and together are regulated by several signal transduction mechanisms to respond to the requirements for force generation within the cell. There are many microfilament-associated proteins which work together to regulate

the dynamicity of these structures, participating in activities such as endocytosis, exocytosis and muscle contraction. Microfilaments also act as important 'tracks' for the motility of myosin motors, which bind and walk along the actin filaments in order to transport various cargo and exert cellular tension.

The intermediate filaments are slightly thicker (approx. 10 nm diameter) filaments that traverse the cytosol which are involved in functions such as cell adhesion. They form structures that can withstand tension to support and maintain cell shape. Several proteins together construct the intermediate filaments, including keratins (epithelial cells), lamins (nuclear envelope), neurofilaments (axons), and vimentins (muscle).

1.3 Microtubules

The final and perhaps the most versatile constituent of the cytoskeletal structures is the microtubule. Microtubules are involved in a splendid array of different functions within the cell. Ranging from the most fundamental of activities such as mitosis and cell division, they also play very important roles in intricate regulatory processes such as nuclear positioning. Extensive studies have also shown involvement in polarised growth, cell migration, intracellular trafficking and maintenance of cell integrity.

The rigid structure of the microtubule has a diameter of approximately 25 nm, and is composed of α/β tubulin heterodimers that collectively form a unidirectional linear protofilament (Fig.1.1). The heterodimers are arranged in a head-to-tail configuration, generating an overall polarity with the α-tubulin at the minus end and the β-tubulin at the fast growing plus end. The minus end is usually stably anchored, as opposed to the plus end which dynamically switches between growth and shrinkage. Thirteen of these protofilaments collectively form a microtubule, as they associate with each other in a lateral parallel manner (Inoue and Salmon, 1995). The whole structure forms a cylindrical shape, with a hollow cylindrical centre. Microtubules can then be organised into various structures, such as bundles or meshed networks.

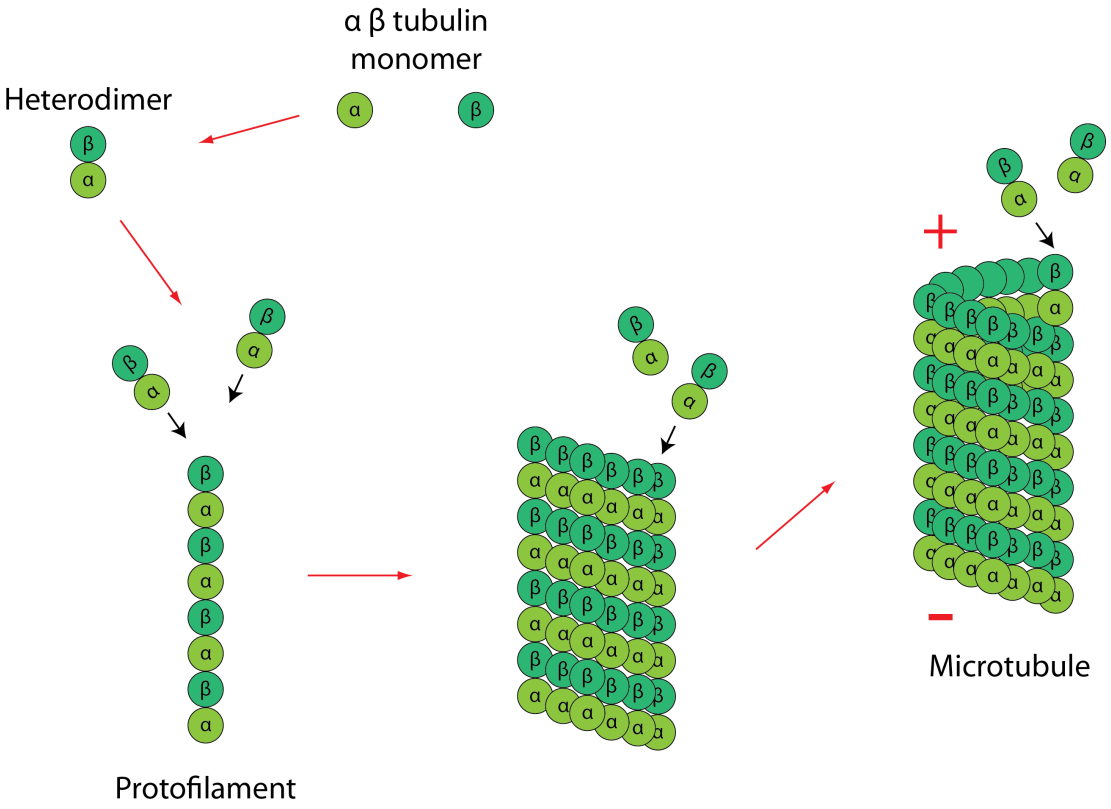

Figure 1.1 Microtubule formation

α- and β- tubulin monomers are initially folded into a heterodimer, which is then incorporated into a protofilament. Thirteen protofilaments laterally associate and form a microtubule. Heterodimers are readily incorporated into the dynamic plus end of the microtubule, giving it polarity.

Microtubule formation is initiated by a process called nucleation, requiring the function of the MTOC (microtubule organising centre) and γ-tubulin. γ-tubulin, together with various other components, form the γ-tubulin ring complex – a scaffold in which the α/β heterodimers can begin to polymerise. In vertebrate cells, microtubules nucleate mainly from the centrosomes, which also act as microtubule anchoring structures and stabilise their minus ends. However, although it was believed during the early years of microtubule research that all the microtubules were nucleated from the centrosome, more recent work led to an advance in this idea that there are some non-centrosomal microtubules which are not focused at the centrosome. These microtubules are able to be less restricted spatially and structurally, allowing a diverse range of cell shapes and morphologies – this can be seen for example in mammalian cells, which have different cell shapes depending on their function.

So how are these non-centrosomal microtubules formed in the first place? There are several suggested mechanisms (Keating and Borisy, 1999) – they may be nucleated at the centrosome and then released so that they can be transported to wherever its fate lies (Keating et al., 1997), they may be cytoplasmically assembled (Yvon and Wadsworth, 1997), they may derive from a broken microtubule that had already been formed (McNally and Vale, 1993, Vorobjev et al., 1997), or they are nucleated from other distinct sites such as in chromatin induced assembly (Heald et al., 1997). The proposed mechanisms unveiled a whole new understanding of microtubule nucleation, and the field remains an active area of research.

1.3.1 Tubulin

The fundamentals of microtubule biogenesis rely on tubulin monomers. Aside from the α-, β- and γ- tubulin which are well known, there have been other tubulins identified such as the δ-, η-, ε- and ζ-tubulins, which are more species specific and less established (Ruiz et al., 1987; Dutcher and Trabuco, 1998; Chang and Stearns, 2000; Ruiz et al., 2000). Although there are some diversities amongst the species, in most organisms the different tubulins are made up of multigene families which contain various isoforms (Hall and Cowan, 1985).

The human α-tubulin proteins include TUBA1A-C, TUBA1C, TUBA3C-E, TUBA4A and TUBA8. β-tubulin proteins include TUBB, TUBB1, TUBB2A-C, TUBB3, TUBB4, TUBB4Q and TUBB6. The two γ-tubulin proteins are TUBG1 and TUBG2. The various proteins, together with the range of post-translational modifications that they can undergo, create diversity between the tubulins for their appropriate functions.

The different tubulin isoforms have emerged as a hot-topic of study due to its disease implications. Tubulins and microtubules are closely associated with neurodevelopment. The crucial process of axon extension and neuronal migration after asymmetric cell division of neuronal progenitors are enabled by the microtubules providing a scaffold for this intracellular transport. Disruptions in these processes can lead to cortical malformation disorders (Barkovich et al., 2012).

For example, mutations within the α-tubulin isoform TUBA1A was shown to cause lissencephaly/pachygyria – a developmental disease that forms abnormal folds on the brain surface (Keays et al., 2007; Poirier et al., 2007). The mutation results in reduced efficiency in the α-tubulin interactions with the CCT-complex (see Chap.1.6.2), as well as the inability for the folding intermediate to interact with the cofactors in the tubulin folding pathway (see Chap.1.8, Tian et al., 2008). On the other hand, mutations in the β-tubulin gene *TUBB2B* causes asymmetric polymicrogyria, where neuronal over-migration occurs due to defects in the pial membrane. The wide variation of neuronal conditions caused by tubulin defects mirrors the diversity of function that microtubules have, and there is much left to discover regarding neuronal malformation disorders and the developmental pathways.

1.3.2 Microtubule dynamics

One of the most characteristic features of microtubules is their dynamicity. Microtubules can either elongate or shorten responding to the requirements within the cell, and this regulation occurs in a tightly regulated intricate manner. The processes of growth and shrinkage are separated by the states in which the microtubule switches from growth to shrinkage – catastrophe, and from shrinkage to growth – rescue. These

events together make up the processes of dynamic instability (Mitchison and Kirschner, 1984; Desai and Mitchison, 1997).

Microtubules elongate by polymerisation, where additional GTP-bound α/β-tubulin heterodimers are incorporated into the plus end. Between this addition and the hydrolysis of GTP by β-tubulin, a GTP cap is formed on the microtubule. However as soon as this cap is lost, the end undergoes depolymerisation, where the heterodimers are lost by dissociation (Desai and Mitchison, 1997). The α-tubulin also has a nucleotide, but in contrast to the β-tubulin, it cannot be hydrolysed. The plus end of the microtubule elongates dynamically, and extends throughout the cytoplasm as it grows. The minus end is also able to elongate, although the rate is much slower than that of the plus end. The minus end is usually anchored at the microtubule organising centre (MTOC), or has a cap to stabilise the end.

1.3.3 Microtubule associated proteins (MAPs)

This dynamicity of microtubules is regulated by various mechanisms, and one of them is the existence of microtubule-associated proteins (MAPs). There are several types of MAPS which have different effects on the microtubule. Tau is a stabilising MAP found mostly in neurons with mutations in this protein leading to neurodegenerative diseases known as tauopathies. Notably, multiple mutations in *tau* cause frontotemporal dementia with parkinsonism-17 (FTDP-17) by promoting tau aggregation in the CNS (Vogelsberg-Ragaglia et al., 2000). Conversely, destabilising MAPs also exist, which include microtubule severing factors such as katanin, spastin and fidgetin (Zhang et al., 2007). There are also MAPs that destabilise by inducing depolymerisation – some motor proteins from the kinesin-13 family triggers catastrophe from both ends of the microtubule by inducing a conformational change in the tubulin (Ems-McClung and Walczak, 2010).

The plus-end-tracking +TIP proteins are an extensively studied group of MAPs. As the name suggests, these proteins track the growing plus end to control various aspects of microtubule dynamics and regulation. Since the first +TIP was published in 1999 –

CLIP1, an endosome-microtubule linker protein (Perez et al., 1999), a plethora of proteins were reported as +TIPs. There are currently more than 20 different families, all of different sizes, functions and structures. A well established group is the End-Binding (EB) family, consisting of family members that possess: an N-terminal CH domain that binds microtubules, a C-terminal dimerisation domain, and the EBH (EB homology) domain (Hayashi and Ikura, 2003; Honnappa et al., 2005; Komarova et al., 2005; Slep et al., 2005; Weisbrich et al., 2007). EB1 itself can promote microtubule growth by suppressing catastrophe events, but since then there have been more emerging properties (Komarova et al., 2009). These EB proteins are localised to the plus end by recognising the GTP-cap or conformation (Maurer et al., 2012), where they recruit and interact with several +TIPs – the EBH domains recognise the Ser-X-Ile-Pro (SXIP) motif which is shared by several of the +TIP proteins (Honnappa et al., 2006). As a platform for other +TIP proteins, they induce several functions – MCAK can induce catastrophe as a depolymerising +TIP (Newton et al., 2004), whereas CLASP can promote rescue events by recruiting tubulin (Al-Bassam et al., 2010). Other +TIP families include the CAP-GLY proteins, TOG proteins and motor proteins.

On the contrary there are proteins that localise specifically to the minus end. Recently a minus-end 'cap' named Patronin has been identified which protects the minus ends from depolymerisation (Goodwin and Vale, 2010, Meunier and Vernos, 2011). This protection mechanism was also found in mammalian cells, where the human orthologue Nezha anchors non-centrosomal minus ends to the adherens junction within epithelial cells (Meng et al., 2008).

1.3.4 Tubulin modifications

After incorporation into the microtubule, tubulin heterodimers can undergo multiple post-translational modifications (PTMs). The purpose of these modifications are believed to be to generate a 'tubulin code', which allows various microtubule associated factors to interact with microtubules in order to carry out their function (Westermann and Weber, 2003; Verhey and Gaertig, 2007).

The range of PTMs that can occur include acetylation, glutamylation, polyglutamylation, glycylation, polyglycylation and detyrosination (reviewed in Janke and Bulinski, 2011). With the exception of acetylation, the tubulin modifications occur on the C-terminal tails of the α- and β- tubulin. These acidic 'tails' lie on the exposed external surface of the microtubule, and carry regions which give the tubulin diversity to define the tubulin isoform (Sullivan and Cleveland, 1986).

There are several different enzymes involved in the modification of these tubulin tails, specific to the type of modification they induce. One of the first PTMs to be discovered was tyrosination/detyrosination. The addition of tyrosines to the C-terminus of α-tubulin was seen first in 1975, which was found to be a reversible process (Arce et al., 1975; Hallak et al., 1977). In fact the detyrosination of the C-terminus Tyr sets off a tyrosination-detyrosination cycle, in which the adding back of the Tyr returns the tubulin to its nascent state. The enzyme that tyrosinates the tubulin – Tyr ligase (TTL) was the first tubulin modification enzyme to be purified and cloned (Raybin and Flavin, 1977; Schroder et al., 1985; Ersfeld et al., 1993), whereas the detyrosination carboxypeptidase enzyme still remains unknown. Detyrosination stabilises the tubulin, reducing the ability of depolymerising factors such as the kinesin-13 motors to interact with the tubulin. On the other hand, the presence of the tyrosine allows the binding of factors such as CLIP-170 at the plus end via its GLY-CAP motif (Peris et al., 2006).

Another example includes two deacetylating enzymes – histone deacetylase 6 (HDAC6) (Hubbert et al., 2002; Matsuyama et al., 2002) and sirtuin 2 (SIRT2) (North et al., 2003), which deacetylate α-tubulin. Acetylation can also occur, where the Lys40 on α-tubulin and Lys252 on β-tubulin are acetylated by several acetyltransferases. Acetylation is thought to be important in axonemal tubulin and cilia formation, differentiation, and ER-mitochondria interaction and is well studied due to its disease implications (Perdiz et al., 2011).

An increasing number of PTM enzymes have been identified since the first modification was studied. The diversity of the function of microtubules rely on these specialised modifications, and allow processes such as intracellular trafficking, cilia/flagella

assembly, and importantly, regulation of dynamics and mitosis. However it has been reported that certain organisms such as yeasts do not share these tubulin modification processes. For instance, fission yeast only possess the tyrosinated form of α-tubulin, hence it does not have a carboxypeptidase that is able to carry out this detyrosination (Alfa and Hyams, 1991). Instead, fission yeast has other methods of regulation which enable microtubule regulation – such as cell cycle stage dependent regulation.

1.3.5 Functions of microtubules in mitosis

During the different stages of the cell cycle, microtubules are able to reorganise in a dynamic fashion in order to adapt to the required function. One of the most important functions of microtubules is to reorganise into the mitotic spindle. During mitosis, the mitotic spindle is crucial for the segregation of chromosomes into two daughter cells.

Once the cell is ready to divide, the interphase microtubule network disassembles, and the centrosomes nucleate microtubules from the opposite ends of the cell (Belmont et al., 1990). After nuclear envelope breakdown, tightly regulated and organised microtubules form a bipolar spindle that is able to align and segregate the chromosomes. There are many types of microtubules nucleated during the different stages of mitosis – the anti-parallel spindle microtubules, the astral microtubules and the kinetochore-fibres (Fig.1.2).

Astral microtubules are only present in the moment immediately before and during mitosis. Astral microtubules are also nucleated at the centrosome, but they remain unattached to the kinetochore – their function is to work in concert with the actin skeleton to regulate spindle orientation. Nucleating in a radial manner from the centrosome, they interact with the cell cortex in order to determine the orientation in regards to the entire cell, and together with dyneins they are able to push the centrosome into the desired position for mitosis (Rosenblatt, 2005). This is important in cells that undergo asymmetric cell division such as *Drosophila melanogaster* neuroblasts (Knoblich, 2010). However astral microtubules are not essential for mitosis (Khodjakov et al., 2000).

On the other hand the anti-parallel inter-polar microtubules are dynamic and the most abundant microtubules in the bipolar spindle. Each centrosome emanates microtubules from the opposing poles, and the microtubules interact in an anti-parallel configuration in the centre of the spindle. Various MAPs and kinesin motor proteins generate a bundle from the plus ends of these anti-parallel microtubules to form the central spindle, which initiates the positioning of the actomyosin contractile ring and cytokinesis (reviewed by Glotzer, 2009). They are also necessary for chromosome congression – they interact with the chromosomes through the chromokinesins (Vanneste et al., 2011) or via kinetochore interactions (Cai et al., 2009).

The other microtubules that are crucial for the actual process of chromosome segregation are the kinetochore (K) fibres. They are assembled from mechanisms that still remain unclear, and attach the chromosomes to the spindle poles in preparation for segregation. They are formed from a bundle of 20-40 microtubules (Rieder, 1981; McEwen et al., 1997), and attach to the outer kinetochore through the KMN complex (KNL1, Mis13, Ndc80 complex) which creates the link between the force generated through microtubule polymerisation and depolymerisation to segregate the kinetochores.

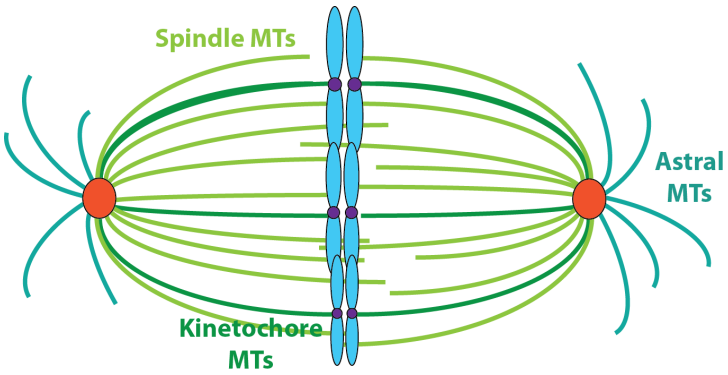

Figure 1.2 Microtubule types in mitosis

There are several microtubule types formed during mitosis. The spindle microtubules are formed from the opposing centrosomes (shown in orange), which also emanate astral microtubules which interact with the cell cortex for spindle orientation. Kinetochore microtubules are crucial for chromosome segregation – generating the force required in the segregation process.

1.3.6 Functions of microtubules in interphase

Interphase microtubules are thought to be more cell-type specific (Wadsworth and McGrail, 1990), depending on what organism is being described. Only existing at interphase, these microtubules are disassembled as soon as mitosis is initiated. However extensive studies in fission yeast have shown that they exhibit several important functions during interphase.

In yeasts, interphase microtubules form anti-parallel bundles which are initiated from sites on the nuclear envelope. Formed from 5-7 microtubules per bundle (Hoog et al., 2007), they dynamically grow and shrink, extending towards the cell tips of *S. pombe,* overlapping with other interphase microtubules. Once they have reached the cell ends, they become curved and bend with the compression, slowing the rate of its growth (Drummond and Cross, 2000). After a pause of around 60-90 seconds, they undergo catastrophe and shrink to the cell middle (Sagolla et al., 2003). The depolymerisation occurs only once the microtubules reach the polar cortex of the cell and not the lateral cortex, which maintains the lateral orientation of the microtubules along the long axis (Brunner and Nurse, 2000; Grallert et al., 2006). There are also proteins that are involved in the regulation of individual microtubules such as Amo1 (Pardo and Nurse, 2005), a nucleoporin protein that is involved in the interaction between the microtubules and the nucleus.

This polarised organisation of interphase microtubules is maintained by the sliding of the microtubules along one another enabled by the minus-end-directed kinesin motor Klp2 (Carazo-Salas et al., 2005; Janson et al., 2005). Bundling is achieved by the protein Ase1 (Loiodice et al., 2005; Yamashita et al., 2005). The individual microtubules undergo this cycle of polymerisation and depolymerisation, until the cell reaches G2/M transition and the interphase microtubules disassemble in preparation for mitosis.

There are various functions associated with interphase microtubules in fission yeast. This ranges from nuclear positioning (Tran et al., 2001) to spindle orientation (Vogel et al., 2007; Daga and Nurse, 2008). They are also important in transporting cell-end

factors to the cell tips (Feierbach et al., 2004; Martin et al., 2005), acting as tracks for various motor proteins to deliver the cargo to the cell tips. It also establishes the cell shape, with defects in interphase microtubules resulting in T-shaped, curved or branched cells (for examples see cofactor mutants, Chap.1.7).

1.4 Fission yeast as a model organism

The fission yeast *Schizosaccharomyces pombe* is a unicellular ascomycete fungus. Fission yeast only have three chromosomes of 5.7, 4.7 and 3.5Mb in size, with 5144 genes in the entire genome (Wood et al., 2002; Rhind et al., 2011; Bitton et al., 2011). Many genes and their related mechanisms are conserved from fission yeast to higher eukaryotes, including mitosis and cell cycle regulation.

There are several advantages of using fission yeast as a model organism. First and possibly the most important is its ease of genetic manipulation. Homologous recombination occurs at a very high frequency in fission yeast, making it readily prone to integrating DNA fragments of interest into its genome at a specific locus. This makes endogenous gene tagging, gene fusions, deletions, or replacement simple with a high success rate. Compared to mammalian knockdowns, there is less background in a fission yeast deletion strain, and the availability of various vectors required to enable these modifications mean that experiments using different gene expression levels etc. are very simple to design.

Also available in the fission yeast research community is a comprehensive database and associated tools. The whole genome has been sequenced, with the recent introduction of databases such as the deletion library covering 99% of the genome (Kim et al., 2010; Spirek et al., 2010), the ORFeome for determining cellular localisation (Matsuyama et al., 2006, (Matsuyama et al., 2006; Hayashi et al., 2009) and for the comparative functional genomics of the entire fission yeast clade (Rhind et al., 2011). These are all very useful tools, and allow comprehensive research on the organism.

Another practical advantage is their ease of maintainence and fast growth rate – one generation only takes 3 hours in rich media. Their distinct and easily observable life cycle means that various aspects of it can be manipulated for growth (e.g. by altering their growth conditions by switching media or temperature). Fission yeast is a heterothallic organism, meaning that in media lacking nitrogen sources, the h^- and h^+ cells are able to mate and form a diploid zygote which undergoes meiosis and sporulation. In rich media, they will undergo mitosis and vegetative growth where they remain haploid. The ease of mating also allows simple strain construction and observation of genetic interactions. In comparison to budding yeast, fission yeast do not duplicate their genome, and their division by fission is similar to mammals compared to budding seen in *S. cerevisiae* .

1.4.1 The fission yeast cell cycle

The cell cycle is the repeating process where the cell duplicates its chromosomes in order to divide them into the two identical daughter cells. This process is strictly monitored and regulated so that proper division can occur. Defective cell division will lead to a wide range of effects, including cancer. Cancer can be caused by several malfunctions of cell division, but the most important is the loss of cell cycle control (reviewed in Hanahan and Weinberg, 2011) where uncontrolled cell proliferation can cause the development of tumours and metastasis.

The cell cycle is divided into 4 phases – G1, S, G2 and M. During G1, the cell can synthesise enzymes and proteins required for the subsequent processes, and grow in size. During S phase, DNA ‘synthesis’ occurs, and during the second ‘gap’ at G2 phase, the cells grow further in preparation for the consequent M phase – mitosis.

Mitosis itself consists of five stages – prophase, in which chromosome condensation occurs; prometaphase, where nuclear envelope breakdown occurs; metaphase, in which the sister chromatids are captured by the microtubules at the kinetochore structures and are aligned to the centre of the cell; anaphase, in which the attached sister chromatids separate from the middle of the cell to the opposing poles of the cell; and finally

telophase, the final stage after separation in which the spindle microtubule will disassemble and the nuclear envelope forms around the newly segregated chromosomes. Following this, cytokinesis ensues, when the two cells are cleaved into separate entities, producing two daughter cells. The daughter cells then either each enter G1 to repeat the process again, or enter a quiescent state called the G0 phase, in which the cells are metabolically active but do not undergo any more proliferation. This depends on either the environmental conditions that the cell is subjected to, or the various signals that inform the cell if it is appropriate to divide. Once the conditions are suitable again, the cell will re-enter G1 and undergo cell division.

The fission yeast cell cycle also follows this pattern, however the proportion of each of the stages is different to higher eukaryote cells. As Fig.1.3 shows, they spend approximately 70% of their cycle in G2 phase, and the rest in M, G1 and S phase. During the long G2 phase, the fission yeast cell will grow to an appropriate size in order for mitosis to be initiated. A haploid fission yeast cell measures 4μm wide, but the length varies depending on the cell cycle stage. During G2 it will grow from a length of 7μm to the maximum of 14 μm. Once this length has been achieved mitosis ensues.

An important feature of fission yeast mitosis is that they do not breakdown their nuclear envelope – they undergo closed mitosis, as opposed to higher eukaryotes that undergo open mitosis in which complete nuclear envelope breakdown is seen (Ding et al., 1997).

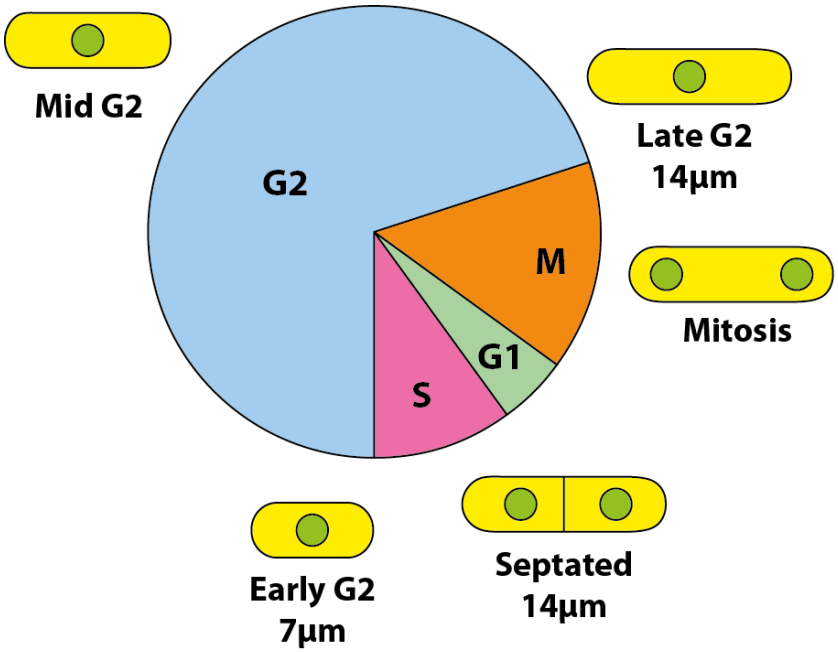

Figure 1.3 The fission yeast cell cycle

Fission yeast cells spend 70% of the cell cycle in G2 phase. M, G1 and S phase makes up the rest of the cell cycle. The cells gradually elongate until they reach the length of cell division. Green circles show the nucleus.

1.4.2 Microtubule organisation in the fission yeast cell cycle

Fission yeast cells have four tubulin genes – the two α-tubulin genes *nda2*$^+$ and *atb2*$^+$; the β-tubulin gene *nda3*$^+$; and one γ-tubulin gene *gtb1*$^+$ (Yanagida, 1987; Horio et al., 1991; Stearns et al., 1991; Horio and Oakley, 1994). γ-tubulin is found in the MTOCs where nucleation occurs of microtubules. Much of the regulation of microtubules is conserved between fission yeast and higher eukaryotes, with the only obvious difference being the lack of post-translational modification in fission yeast as discussed earlier.

The organisation of microtubules during the different cell stages is shown in Fig.1.4. During interphase, the microtubules are distributed only in the cytoplasm, forming bundles consisting of anti-parallel microtubules that are nucleated from the perinuclear region and extending to the cell cortex. As the SPB (the fission yeast equivalent of the centrosome) duplicates, they nucleate microtubules that extend to form the mitotic spindle. During prometaphase this spindle is very short, forming a small bridge between the two SPBs. Whilst the spindle elongates the interphase microtubules start to disassemble, and disappear by the time metaphase is reached. During metaphase the spindle elongates to reach across the nucleus, and microtubules are extended from the SPB into the cytoplasm forming the astral microtubules (Hagan and Yanagida, 1995; Hagan and Hyams, 1996; Mata and Nurse, 1997). This angle and length of astral microtubule formation is suggested to maintain the conformation of the spindle, and as anaphase B is reached the spindle elongates until the divided nuclei reach the cell tips. This elongation of the spindle is highly dynamic, with polymerisation and depolymerisation occurring for each individual microtubule. The spindle midzone is also formed at this time which occurs as anti-parallel microtubules are bundled by Ase1 (Sagolla et al., 2003). As the spindle breaks down, microtubules are newly nucleated from the outer face of the SPB and eMTOC (equatorial MTOC) which form the post-anaphase array by the function of the medial ring (Hagan and Hyams, 1988; Heitz et al., 2001), which leads the nuclei back to the centre of the cell. As cytokinesis occurs and septation concludes, the chaperone Rsp1 removes the eMTOC and there are no more microtubules nucleated from the middle of the cell. The microtubules then reorganise

into an array of interphase microtubules as the cell undergoes the division cycle again (Zimmerman et al., 2004).

The advantage of using the fission yeast system in order to study microtubules is the ease of visualisation. In comparison to mammalian cells which have a dense and intricate meshwork of microtubules, it is simply easier to visualise microtubules as they only contain a number of distinct bundles that can be followed over time. Advances in microscopy have enabled the details of fission yeast microtubules to be studied, including end-tracking and the measuring of dynamics. In this study I have taken advantage of this ease of microtubule analysis in order to observe microtubule phenotypes in my various mutants.

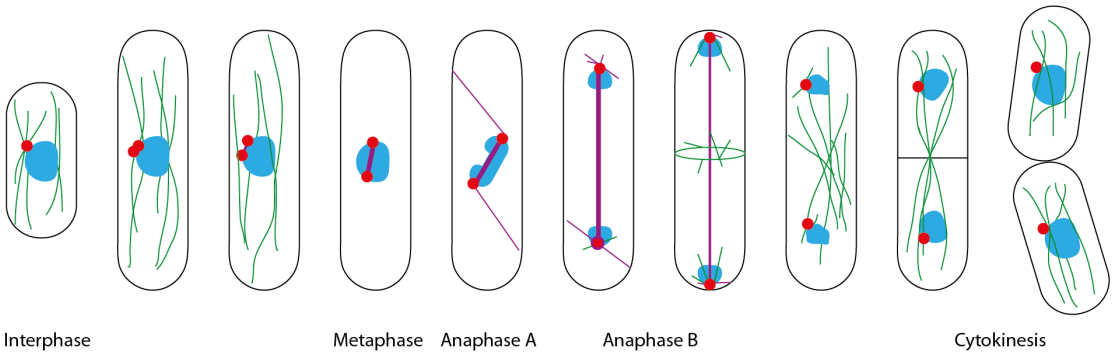

Figure 1.4 Microtubule organisation in the fission yeast cell cycle

Figure adapted from (Hagan, 1998). Cytoplasmic interphase microtubules (shown in green) form only within interphase cells which disappear by the time metaphase is reached. Nuclear spindle (shown in purple) forms after separation of the SPB (shown in red) and elongate through anaphase. The medial ring forms at the cell centre as the spindle starts to breakdown and the post anaphase array assembles. After cytokinesis the cell divides into two and the cells undergo the same process once more.

1.5 GTPases and their regulation

The small GTPases, or otherwise known as small G proteins, are small guanine nucleotide binding proteins between 20-25 kDa which cycle between an inactive GDP-bound state and an active GTP-bound state. When in their active GTP-state, they can interact with their effector proteins to induce downstream signalling events. This cycle between the inactive and active state is intricately regulated by a specific set of proteins which can assist this change of conformation (Fig.1.5). The first set of proteins are the guanine nucleotide exchange factors (GEFs), which trigger the release of the bound GDP for replacement with the more abundant GTP within the cell. On the contrary, the other set of proteins – the GTPase activating proteins (GAPs), assist the hydrolysis of the GTP by providing an essential catalytic group. Another set of proteins – the guanosine nucleotide dissociation inhibitors (GDI), as seen in Rho and Rabs, prevent exchange of the nucleotide, maintaining it in the active or inactive state whilst in complex with the G protein. Once this dissociates, nucleotide exchange can resume once again.

The most well studied small G-protein family is the Ras superfamily, which consists of at least 154 members which are classified into 5 different families – the Ras, Rho, Rab, Arf and Ran families (Wennerberg et al., 2005). These proteins regulate an array of cellular processes, from cell membrane-mediated signal transduction, nuclear import, to exocytosis. In order to cope with such a vast number of G proteins and cellular functions, there are equally as many GEFs and GAPs to enable specificity of signalling. Both GEFs and GAPs are multi-domain proteins with domains that interact with the protein of interest.

1.5.1 GEFs

GEFs are crucial for the exchange between GDP to GTP because of the high affinity of the small G proteins for GDP/GTP nucleotide. This means that the dissociation rate of the nucleotides are slow, with half-lives of one or more hours. This low speed cannot match the requirement of the GDP/GTP exchange which should occur within minutes.

In order to accelerate this process for efficient GDP/GTP exchange, GEFs are required (Vetter and Wittinghofer, 2001).

GEFs aid this dissociation process by reducing the nucleotide affinity in the nucleotide binding site. This triggers the release of the nucleotide and this binding site can therefore be filled with another nucleotide. The actual factor influencing the GDP to be replaced with GTP is not the GEF itself – the nucleotide binding site of the G protein has the same affinity for both GDP and GTP, so this exchange only occurs because of the high cellular concentration of GTP compared to GDP. Between this exchange, it has been shown with Ran and its GEF RCC1, that the interaction of the G protein with the GEF reduces the affinity for the nucleotide, and similarly the interaction with the nucleotide reduces the affinity for the GEF. This allows exchange between the two nucleotides (Vetter and Wittinghofer, 2001).

On a more molecular level, the nucleotide is bound to the G-protein between the switch 1 and switch 2 region, which together with the Phosphate binding P-loop interact with a magnesium ion and phosphates, which enable the high affinity binding between the nucleotide and the G protein. GEF binding triggers conformational changes in the phosphate binding switch regions and the P-loop, which sterically blocks the binding of the magnesium ion essential for the high-affinity binding. This renders the phosphate groups to be released, which in turn releases the bound nucleotide so that it can be replaced with the new nucleotide. This allows efficient exchange.

1.5.2 GAPs

GTP hydrolysis on the G protein is slow. In order to accelerate this process to the speed and efficiency that is required for various cellular processes, GAPs are required. The mechanism of GAP function is via several processes. Firstly, the interaction with the GAP lines up the water molecule to the γ-phosphate opposite to the nucleotide for efficient nucleophilic attack. This mechanism was first shown in the Ras-RasGAP complex (Scheffzek, 1997), where the Ras-GAP stabilised the glutamine 61 residue of the Ras, lining it up for efficient attack by the water. The binding also blocks the water

from binding to the active site. This glutamine residue is known to vary amongst the various GAPs, with the Rap-RapGAP interaction occurring without the glutamine, instead with an asparagine taking over its function. (Daumke et al., 2004).

Another effect of GAP binding is the introduction of the arginine finger, an essential arginine residue that 'points' into the phosphate binding site to stabilise the transition state by neutralising the negative charge at the γ-phosphate. This arginine is essential for GAP function – in several cases where this arginine is replaced with another residue, the GAP function is lost and GTP hydrolysis is slowed down considerably.

GAPs and their interactions with the G-protein are regulated by interactions with proteins or lipids, binding second messengers, or post-translational modifications.

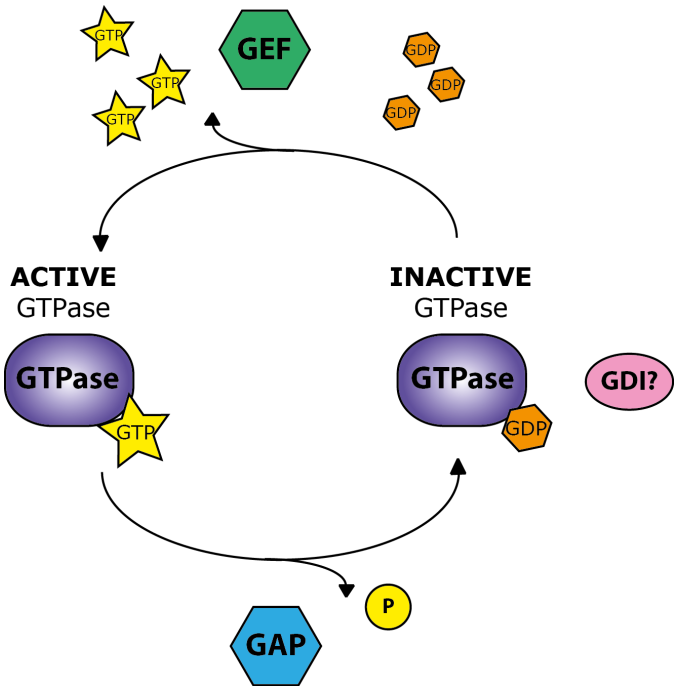

Figure 1.5 The nucleotide cycle

The GTPase is converted from the active GTP bound form to the inactive GDP form and vice versa in a cycle aided by GAP and GEF proteins. The GDI maintains the GTPase in the inactive state.

1.6 Protein folding and chaperonins

In the cell, there are numerous proteins of different size and function. In order to allow this diverse range to be available, proteins must be folded into different conformations. Tubulins are known to undergo a very complex process of folding reactions that have not been observed in other proteins. This is made possible by a specific set of chaperones.

1.6.1 Molecular chaperones

New macromolecular structures are constantly being folded or assembled in the cell. To enable this synthesis to occur, there are helper proteins termed molecular chaperones which aid these complex processes. Molecular chaperones often tend to be associated with protein folding processes, but are also involved in other processes as demonstrated by the first study to use the term 'molecular chaperone' in 1978, in which the formation of nucleosomes from histone and DNA were assisted by the chaperone nucleoplasmin (Laskey et al., 1978).

A molecular chaperone is defined as a protein that interacts with and assists proteins to achieve the functionally active conformation, but does not become part of the final structure. The molecular chaperones involved in protein folding allow flexibility of its function. There are numerous possible conformations that a protein chain are able to form, and molecular chaperones are required for efficient and quick folding to happen (Anfinsen, 1973).

The speed of protein folding depends on various factors such as size of the protein – smaller proteins will fold within microseconds, as opposed to larger multi-domain proteins taking up to hours (Kubelka et al., 2004). This complex folding process can be a complicated task. In addition, when this folding is slow in a crowded cellular environment, protein aggregation can occur, which can lead to various cellular malfunctions causing conditions such as dementia and Parkinson's disease. Therefore it

is crucial for this process to be assisted, maintaining the proteins in a soluble and conformationally flexible state.

Molecular chaperones are classified into several classes depending on their structure and function (reviewed in Hartl et al., 2011). One of the most well studied of these classes are the heat-shock proteins (HSPs). They are named so, as their function is upregulated under stress conditions such as elevated temperatures. This can cause increased aggregation as well as misfolding. Of these classes, the HSP70s, HSP90s and the HSP60 chaperonins promote folding through ATP and cofactor-regulated binding and release cycles. Other chaperones will assist folding of newly made proteins, or transport across membranes such as in the mitochondria and endoplasmic reticulum (Araki and Nagata, 2011).

1.6.2 Chaperonins and the CCT-complex

The chaperonins make up one of the classes of the molecular chaperones. They have a distinct toroidal structure, each ring consisting of multiple subunits. Folding by chaperonins depends upon ATP hydrolysis, and by creating a favourable environment for the protein to fold, they reduce chances of aggregation and misfolding.

Chaperonins interact with the unfolded protein in two stages – first they form a binary complex with the unfolded protein intermediate in an ATP independent manner (Martin et al., 1991). Subsequently, ATP hydrolysis occurs and there is a conformational change in the chaperonin to release the protein with the assistance of another cochaperonin (Gao et al., 1992; Saibil et al., 1993).

There are two groups of chaperonins – group I chaperonins consist of those found in bacteria, such as the well studied GroEL and GroES chaperonins. The second group are found in the eukaryotic cytosol and archaea. Amongst these chaperonins is the CCT complex (chaperonin containing TCP-1 otherwise known as c-cpn), which is closely associated to cytoskeletal proteins. It consists of a double barrelled oligomer with 8 subunits - α, β, γ, δ, ε, ζ, η and θ which are arranged in a position in the chaperonin

ring (Liou and Willison, 1997). Both tubulin (Llorca et al., 2000) and actin (Llorca et al., 1999) interact first with the CCT complex to be able to reach their native state before folding. It was observed that recombinant β-tubulin purified from microtubules was able to form a binary complex with the CCT complex. In addition, some of the subunits are able to behave monomerically, for example as a MAP (Roobol et al., 1999).

This initial capture of α- and β- tubulin by the CCT complex can be seen at the beginning of the tubulin heterodimer folding pathway, as shown in Fig.1.6. When this pathway was first investigated *in vitro*, the discovery of additional chaperones initiated the study of a whole new set of chaperones that were specific to the folding of tubulin.

1.7 The tubulin folding cofactor pathway *in vitro*

The tubulin folding cofactor pathway was first established *in vitro* by several studies carried out by Cowan and colleagues. The study had been initiated by evidence that a cytoplasmic chaperonin which existed as an 800 kDa multi-subunit toroid formed a binary complex with unfolded β-actin. When incubated with ATP, native state β-actin was released, suggesting that the chaperonin was directly involved in the folding of the actin. When it was discovered that this chaperonin contained TCP-1, which was shown to be involved in tubulin biogenesis in rabbit reticulocyte lysates (Yaffe et al., 1992), it was examined to see if the purified cytoplasmic chaperonin could fold α- or β- tubulin *in vitro* (Gao et al., 1993).

Folding assays were carried out with denatured tubulin polypeptides as target proteins, to determine if the cytoplasmic chaperonins would sufficiently fold tubulin. The results showed that indeed the chaperonins were able to form a binary complex with either tubulin, but unexpectedly, this was not sufficient to release the native peptides upon incubation with GTP or GDP. As both tubulins are GTP-binding proteins, the native polypeptides were expected to be released when GTP was added to the folding reaction. However this was clearly not sufficient, and additional factors appeared to be required – in order to identify these cofactors, fractions from rabbit reticulocyte lysate was added to the folding assays with unfolded α- or β- tubulin. The two cofactors that were

discovered to be necessary for this folding were named cofactors A and B. This concept was totally novel, as it showed that although the same cytoplasmic CCT complex was able to facilitate folding of β-actin and also tubulin, a specific set of separate cofactors were required in addition to fold and release α- and β- tubulin. Upon purification of the cofactors *in vitro*, the interactions were confirmed, and this became the first report that novel chaperonins that were structurally unrelated to GroES were identified as being required for tubulin folding (Gao et al., 1994). Cofactor B was shown to interact with α-tubulin, whilst cofactor A binds β-tubulin.

An additional component was deemed necessary in the folding reaction of β- tubulin with the CCT components and cofactor A present, and this was identified to be cofactor D. Simultaneously, two further proteins – cofactors E and C, were also identified as being necessary for the folding of β-tubulin in its native state (Tian et al., 1996).

The study concluded that each of the cofactors had slightly different roles within the cofactor pathway. Cofactor A was able to capture the intermediate-state β- tubulin after its interaction with the CCT complex to form a stable complex. However it was not deemed as being absolutely necessary for the folding reactions carried out *in vitro*, suggesting that cofactor A plays an important role but only functions as a reservoir in which a steady amount of partially folded β-tubulin subunits can be maintained before being transferred to cofactor D.

On the contrary, cofactors C, D and E are all thought to be essential for the folding pathway. Cofactor D captures the β-tubulin after its interaction with cofactor A, and this cofactor D-β-tubulin complex can bind to cofactor E. Cofactor C is then able to interact with this complex to induce GTP hydrolysis to trigger the release of native heterodimers (Fig.1.6).

Taken together, the identification of the cofactors involved in the β-tubulin pathway had been solved. However, not much was understood regarding the details of the α-tubulin pathway. The cofactors mentioned above could only very inefficiently fold α-tubulin,

which suggested that there were other cofactors involved for this process. This was found to be cofactor B (Tian et al., 1997) – which was isolated again via *in vitro* folding assays using native bovine brain tubulin when it showed that efficient α-tubulin folding was achieved by this cofactor. Interestingly, when the amino acid sequence of this cofactor was analysed, it was found to share the CLIP-170 GLY-CAP motif with cofactor E, also thought to be involved in the α-tubulin pathway. The CLIP-170 domain consists of tandemly repeated motifs that are able to bind the EEY on microtubules. Cofactor B was able to increase the yield of native α-tubulin generated from the tubulin folding experiments, by capturing the intermediate state α-tubulin after generation by the CCT complex reaction. By forming a complex it enables the maintenance of an α-tubulin pool, but it is not able to by itself release native α-tubulin. However the ability for it to interact with cofactor E suggests that cofactor B delivers α-tubulin to cofactor E for further processing.

The idea that cofactor C was involved in bringing together the two parallel arms of the α- and β-tubulin pathway was confirmed by studies suggesting that this 'supercomplex' had GTPase activity. GTP hydrolysis is a key feature of the β-tubulin, and its importance in the tubulin folding pathway has been studied to great depth. Firstly, it was shown that GTP hydrolysis as well as the interactions among the cofactors was crucial for the efficient folding of native tubulin. This was only achieved when all three cofactors were present – cofactors C, D and E. It was known that the combination of these three cofactors was able to trigger a GTP hydrolysis reaction (Tian et al., 1997; Tian et al., 1999). This was confirmation that the cofactors can act as GAPs for the tubulins, which in turn are GTPases. The tubulin itself actually carries out the hydrolysis of the GTP, and the cofactors were stimulating this reaction.

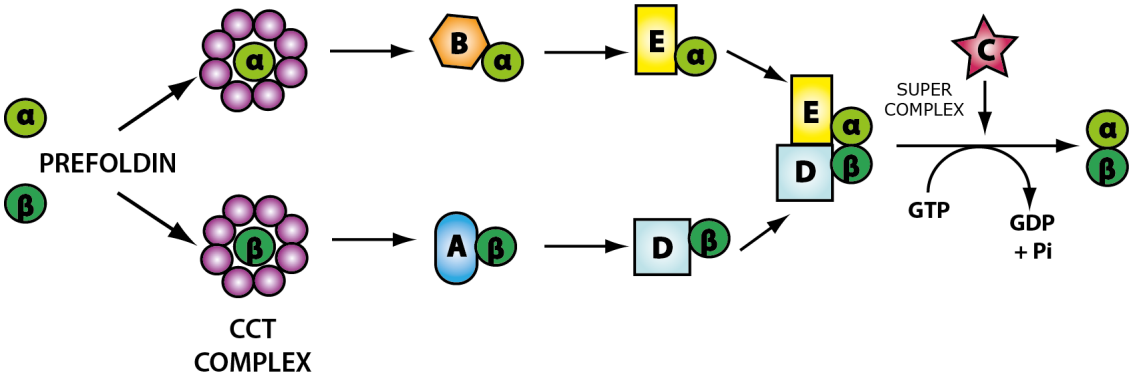

Figure 1.6 The tubulin folding pathway model

Native α- and β- tubulin monomers are first captured by the CCT complex as described in Chap.1.6.2. After release, the α- tubulin monomer is captured by cofactor B, which then delivers it to cofactor E. On the β-tubulin arm of the pathway, the β-tubulin monomer is captured by cofactor A which is then replaced by cofactor D. The two parallel pathways converge and with the introduction of cofactor C, GTP hydrolysis occurs, triggering the release of the newly folded α/β tubulin heterodimer for addition to the plus end of the microtubule.

1.8 The tubulin folding cofactor pathway in fission yeast

1.8.1 The 'altered polarity' genes

Following on from the *in vitro* tubulin cofactor pathway model established by Cowan and colleagues, studies in their biological functions *in vivo* were initiated in the fission yeast system by Takashi Toda's laboratory.

The fission yeast orthologues of the tubulin folding cofactors had been identified as hits in a screen carried out for temperature sensitivity mutants with defects in cell morphology (Radcliffe et al., 1998; Hirata et al., 1998) and mitochondria distribution (Yaffe et al., 1996). A subset of mutants that were defective in cell polarity included the alp genes (altered polarity) – 15 loci including *alp1-alp15* that showed bent or curved morphologies. Of these 15 loci, it was identified through genetic analysis that *alp2* was allelic to one of the α-tubulin genes *atb2*, and *alp12* to the β-tubulin encoding *nda3* (Radcliffe et al., 1998). Both these mutants showed a morphological and microtubule defect at the restrictive temperature, showing that the balance between α- and β- must be maintained within the cell. Therefore mutants showing defects in this tubulin is crucial for the cell, as an excess of either tubulin or an inbalance between them is toxic to the cell.

Table 1 shows the tubulin cofactors and their orthologues in different species.

Homo sapiens	*S. pombe*	*S. cerevisiae*
Cofactor A	Alp31	Rbl2
Cofactor B	Alp11	Alf1
Cofactor C	Tbc1	Cin2
Cofactor D	Alp1	Cin1
Cofactor E	Alp21	Pac2
Arl2	Alp41	Cin4

Table 1 Tubulin folding cofactors and their orthologues
Proteins labelled in red identify those that were investigated in depth in this study.

1.8.2 Alp1^{D}

Amongst those genes, *alp1* was picked-up as a frequently mutated locus within these polarity mutants. Upon observation at the restrictive temperature, the *alp1* ts mutant *alp1-1315* showed bent morphology and nuclear displacement (Hirata et al., 1998). Analysis of the amino acid sequence of Alp1^{D} showed that it encoded the orthologue to human cofactor D, as well as showing sequence homology to the *C. elegans* orthologue F16D3.4, bovine cofactor D, and budding yeast Cin1. Appropriately, *alp1-1315* showed unstable microtubules when incubated at the restrictive temperature. Other microtubule defects such as nuclear and septum displacement was also observed, which are commonly observed phenotypes amongst mutants in microtubule regulation. In addition, Alp1^{D} was suggested to be a MAP, as it co-localised and co-sedimented with microtubules, and its lethality upon overexpression could be rescued by the overexpression of β-tubulin. This study led to the notion that the tubulin cofactors are indeed essential for cell division and may act as microtubule regulators as well as playing crucial roles in tubulin heterodimer folding.

1.8.3 Alp11^{B} and Alp21^{E}

Following this study, the remaining cofactor homologues in fission yeast were also identified and studied. The orthologues of cofactor B and E – *alp11* and *alp21*, respectively, were also subsequently identified. These two cofactor homologues were also shown to be essential for cell viability, consistent with the other homologues.

alp11-924, the ts mutant for the cofactor B homologue, showed branched or bent cell morphology after 8 hours at 36°C. Together with the previously observed phenotypes such as misplaced septa and nuclei, no microtubules were seen in these mutants after staining for microtubules. Additionally, aggregated mitochondria staining was seen – another phenotype common amongst tubulin mutants (Yaffe et al., 1996). *alp21*, the fission yeast orthologue of cofactor E, was initially isolated as the multicopy suppressor of the *alp11-924* ts mutant. Disruption of this gene also showed similar morphology defects and temperature sensitivity.

The products of *alp11* and *alp21* were shown to physically interact with α-tubulin by immuno-precipitation, which strongly suggested their involvement in the tubulin cofactor pathway. To confirm this, their interactions with the only other known cofactor, $Alp1^D$, was tested. The outcome showed data consistent with the model pathway that Cowan and colleagues had derived from their *in vitro* examinations – $Alp21^E$ interacts with both $Alp1^D$ and $Alp11^B$. However $Alp11^B$ cannot bind $Alp1^D$. This is consistent with the model that suggests that the α-tubulin monomer initially binds with $Alp11^B$, and then $Alp21^E$, which then all comes together for $Alp1^D$ and $Alp21^E$ to form a supercomplex with the so far unidentified cofactor C (see Fig.1.6). The fact that $Alp11^B$ cannot bind to $Alp1^D$ also is consistent, as $Alp11^B$ is on the 'α-tubulin arm' of the pathway, as opposed to $Alp1^D$ which is on the 'β-tubulin arm'. Further experiments observing the cofactors and their interaction with β-tubulin shows that neither $Alp11^B$ or $Alp21^E$ on the 'α-tubulin arm' can bind with β-tubulin.

With the knowledge that the overexpression of $Alp1^D$ is toxic to the cell (Hirata et al., 1998), $Alp11^B$ was also overexpressed using the inducible *nmt1*-promoter (Maundrell, 1990). Data showed that in fact $Alp11^B$ was also toxic to the cell, although $Alp21^E$ was not. The lethality of excess $Alp11^B$ was rescued by the co-overexpression of α-tubulin.

This study from Hirata also showed the first evidence of $Alp1^D$ being different to the other cofactors in the pathway. The functional hierarchy of the cofactors had not been established in the *in vitro* model pathway, therefore multicopy plasmids of each of the different cofactors were transformed into each of the cofactor mutants to observe any possible recue. The resulting data showed that an excess of $Alp1^D$ was able to rescue the temperature sensitivity of both *alp11* and *alp21* ts mutants, but overexpression of either of these cofactors was not sufficient to rescue the *alp1* ts mutant. This striking data suggested that $Alp1^D$ was acting downstream of the other cofactors rather than in parallel with $Alp21^E$. This meant that it was likely that $Alp1^D$ was not only required for the β-tubulin tubulin pathway but also for the α-tubulin path.

A key finding in these studies was the effect of the mutants on the tubulin levels within the cell. The ts mutants *alp1-1315* and *alp11-924* showed a decrease in the α-tubulin

level at the restrictive temperature. An overexpression of Alp11^{B}, but not Alp21^{E}, was able to rescue this decreased α-tubulin level of *alp11-924*. On the other hand in *alp1-1315*, the levels of Alp11^{B} were found to be much higher in comparison to wild-type cells whereas the level of α-tubulin was lower. Both these effects were rescued by the overexpression of Alp1^{D} by plasmid. As expected, the levels of β-tubulin were not affected in either of these mutants. Taken together, it suggests that Alp1^{D} and Alp11^{B} are involved in the maintenance and stability of α-tubulin monomers within the cell, and that Alp11^{B} levels are regulated by Alp1^{D}.

Further investigation of the *alp11-924* mutant revealed that the mutation had resulted in a truncated version of the protein (Radcliffe and Toda, 2000), and the structure of the protein was identified together with the regions that were important for maintenance of tubulin molecules. The importance of Alp11^{B} in maintaining the α-tubulin levels in the cell can be explained by the coiled coil region located at the middle region of the protein. Truncations mutants lacking this domain showed reduced levels of α-tubulin in the cell, as well as disrupted interaction with the monomers. Alp11^{B} also contains a glycine-rich tubulin interacting EEY binding GLY-CAP domain at the C-terminal, which appears to show importance in microtubule maintenance, as without it microtubules appear highly unstable (Radcliffe and Toda, 2000). This is thought to be because of its importance in the interaction of Alp11^{B} with α-tubulin.

1.8.4 Alp31^{A}

Now that the α-tubulin pathway had been solved, the next step was to investigate the β-tubulin pathway. This was addressed with the consequent study of *alp31* (Radcliffe et al., 2000a), the orthologue of cofactor A, which was shown to have a role in the β-tubulin pathway in parallel to cofactor B in the α-tubulin pathway. Surprisingly, it appeared that Alp31^{A}, unlike the other fission yeast cofactors, was nonessential for cell viability. The deletion mutant showed no temperature sensitivity or sensitivity to microtubule drugs, but a proportion of the cells showed a defect in morphology similar to the other cofactor mutants. In addition, the *alp31* deletion mutant was synthetic lethal

with the *nda3* mutants, suggesting its involvement in the β-tubulin folding pathway. Similar to the other cofactors, overexpression of Alp31^{A} was toxic to the cell, resulting in defective microtubules as well as bent morphology. Upon observation of Alp31^{A} and its physical interactions with the other cofactors or α- and β- tubulin, it was shown that Alp31^{A} did not bind to either Alp1^{D} or Alp11^{B}, nor either of the tubulins. This was strikingly different to the properties of Alp11^{B}, which was supposedly acting in parallel to Alp31^{A} on the α-tubulin pathway. Also, there was no difference seen in the β-tubulin levels in the mutant of *alp31*. As mentioned earlier, the mutants of *alp1* and *alp11* had both shown a reduction in α-tubulin levels. If we were expecting the cofactors on the β-tubulin pathway to share similar features, we would observe a difference in these levels. However this was not seen in the deletion mutant of *alp31*. Taken together with its non-essentiality, this suggested that Alp31^{A} requirement within the cell is not as stringent as the other cofactors – or that the importance of Alp31^{A} may lie in microtubule integrity rather than the balance of the tubulin monomers within the cell.

However this would mean that the α- and β-tubulin pathways may not be so'parallel' after all. An explanation for this phenomenon could be the difference in nature between the α- and β- tubulin monomer – perhaps the β-tubulin monomer is more capable of undergoing folding on its own and is only assisted by Alp31^{A}. This also highlights the established fact that level of α-tubulin is more strictly regulated by the cofactors, and that the excess of β-tubulin is more disruptive to the cell than that of α-tubulin (Hiraoka et al., 1984; Toda et al., 1984).

1.8.5 Alp41

As described above, Toda and colleagues have identified and studied in detail the fission yeast homologues of the tubulin cofactors. However, there were still some players missing. A homologue of cofactor C had not been identified, and it was still elusive if there were any other players in the pathway. In the meantime, a screen in budding yeast isolated three new genes that showed supersensitivity to the anti-microtubule drug benomyl – CIN1, CIN2 and CIN4 (Stearns et al., 1990). Independently, these genes were also isolated in a screen for genes that showed an

increased rate of chromosome instability (Hoyt et al., 1990), with mutants showing loss of microtubules. Of these three genes, the fission yeast orthologue of CIN4 was identified and named Alp41. Domain analysis revealed that it contained domains that were hallmarks for GTP binding, including GLDHAGK, WDIGGQ and NKQD (Radcliffe et al., 2000b). Alp41 was found to be essential, and the terminal morphology of lethal deletion mutants showed a branched and bent morphology similar to that of the other cofactor mutants. Similar to the other cofactors, genetic interaction studies of *alp41* showed that the over expression of $Alp1^{D}$ was able to suppress the lethality of *alp41* deletion mutants, suggesting its possible roles in relation to the tubulin folding pathway, most probably upstream of $Alp1^{D}$. However not much more was identified regarding this protein, no conditional mutations were available and its actual functions within the pathway remained elusive.

1.8.6 Finding an orthologue of cofactor C

Although the fission yeast orthologues of cofactor A, B, D and E had been identified and studied, there still remained one cofactor that had not been identified – cofactor C. Cofactor C is thought to play its role in the final steps of the tubulin folding pathway, where the α- and β- tubulin pathways converge and the α/β tubulin heterodimer, cofactor D and cofactor E come together to form a supercomplex. This complex is completed with the introduction of cofactor C, and only then can GTP hydrolysis occur to allow the release of the heterodimer (Fig.1.5). Without the identification of this final cofactor, the complete *in vivo* pathway and the functional hierarchy could not be established.

However in 2006, a screen was carried out by Toda and colleagues for fission yeast mutants that demonstrated defects in spindle-kinetochore interaction – this study would later lead to the identification of the fission yeast orthologue of cofactor C. The main finding of the screen was the isolation of an *atb2* mutant, *atb2-983,* with its mutation at V260I, a residue that locates in the interacting interface between α- and β- tubulin. This was a new type of *atb2* mutant, which showed a different and unexpected phenotype to that of the more conventional α-tubulin mutants like those previously mentioned

(Radcliffe et al., 1998). Unlike the predecessors, *atb2-983* showed apparently wild-type microtubules during interphase and mitosis that showed no difference from wild-type microtubules. However when the dynamics of these microtubules were observed, they showed slower growth and shrinkage rates, as well as demonstrating a high rate of chromosome mis-segregation. In order to elucidate the details of this mutant, a multi-copy suppressor screen was carried out to find any potential interactors, and within the hits that rescued these phenotypes, SPAC328.08C was found. An orthologue search on this gene suggested that this gene could be the fission yeast orthologue of cofactor C, which we named Tbc1 (tubulin binding cofactor C-1).

1.9 The TBCC proteins in humans

1.9.1 The conserved TBCC domain

There is a family of proteins found in eukaryotes that carry a conserved domain called the TBCC domain. In humans, three TBCC domain containing proteins are found – the tubulin folding cofactor C, RP2 and TBCCD1. The domain is named after its conservation with one of these proteins – cofactor C, or TBCC. This domain, found at the C-terminus of cofactor C, contains a sequence which is established as the 'hallmark' of the TBCC protein family. Although it remains unpublished, the structure of this domain within cofactor C has been elucidated by Saito, K et al. in 2007 (PDB ID: 2YUH). The N-terminal domain of cofactor C was also crystallised by Garcia-Mayoral et al. in 2008 (PDB ID: 2L3L) as shown in Fig.1.7.

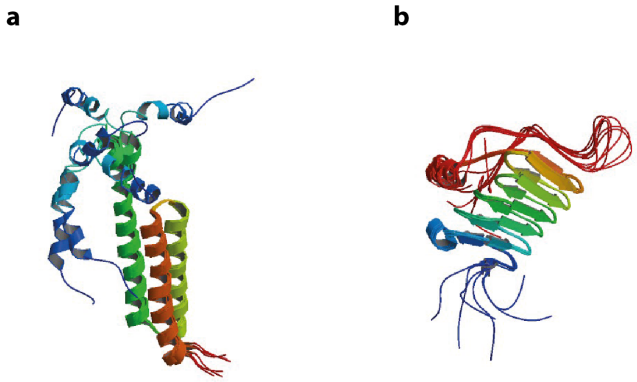

Figure 1.7 The crystal structure of human cofactor C TBCC

The (a) N-terminal and (b) C-terminal domains of human cofactor C was crystallised by Garcia-Mayoral et al (2001, PDB ID: 2L3L) and Saito et al (2008, PDB ID: 2YUH), respectively. This allowed identification of the domains as described below.

The sequences of cofactor C and RP2 share 29% identity and 53% similarity over a domain of around 200 amino acids (Bartolini, 2002). Together with the TBCC domain, structural studies have shown that these three proteins also share two CARP domain, which are found in CAP proteins (cyclase-associated proteins). The known domains of these proteins are shown in Fig.1.8.

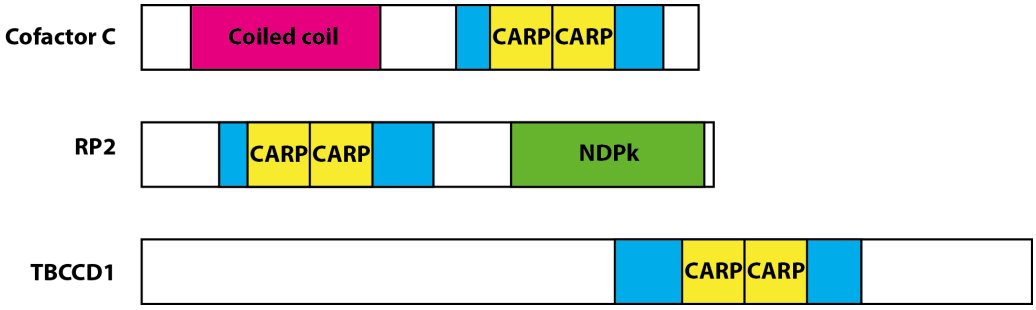

Figure 1.8 Structure of TBCC domain containing proteins

Known domains are shown in coloured boxes. The TBCC domain is shown in blue, with the CARP repeats in yellow. The CARP domain is found in CAP (cyclase-associated proteins). The Alpha module shown in magenta suggests an interaction domain. The nucleotide diphosphate kinase (NDPk) domain, shown in green, is a phosphocarrier domain.

Following the study of the human proteins, further phylogenetic analysis of the TBCC domain containing proteins were carried out in several eukaryotic organisms. This was initiated in the parasite *Trypanosoma brucei.* In an in-depth proteomic analysis of the *Trypanosoma brucei* flagellum, a protein was identified encoding the TBCC domain (Stephan et al., 2007). This triggered a study of several phylogenetically diverse eukaryotic organisms in order to find the proteins that contained this conserved TBCC domain. Following this study it was established that all these proteins were able to be distinguished into three distinct groups, or clades. The different clades were identified by the organism and the protein that had the conserved TBCC domain. The first clade contained the proteins from a diverse range of organisms, including the tubulin folding cofactor C proteins both from human and yeast. The fission yeast cofactor C candidate (discussed in Chapter 3) has also been found placed in clade 1 according to its sequence. Clade 2 only contained the organisms that are able to form cilia and flagella. Clade 3 then contains all the proteins that were not able to be placed in either clade 1 or clade 2, from both flagellated and non-flagellated eukaryotes. The characteristic of clade 3 proteins is that they do not contain some of the key features of the TBCC domain, such as the arginine finger, which is a residue that is thought to be crucial for the activities of both cofactor C and RP2.

1.9.2 The “C-like” protein TBCCD1

In fact, the roles of the proteins within clade 3 of these proteins have only recently been studied. The first role to be identified was in the TBCCD1 homologue - *ASQ2,* in the green alga *Chlamydomonas reinhardtii* (Feldman and Marshall, 2009). Mutants of this gene had defects in centriole linkage which resulted in cells with defects in centriole number control as well as positioning. The protein was found to localize in the region between the centrioles and the nuclear envelope, and some on the centrioles themselves. Mutants also showed a defect in spindle orientation, although there is no major defect in spindle formation. The study highlights the possible role of *ASQ2* in spindle positioning as a result of the regulation of centriole number and positioning.

The role of TBCCD1 in centrosome regulation was also confirmed in mammalian cells where human TBCCD1 was characterized (Goncalves et al., 2010). TBCCD1 was found to localise at the basal bodies as well as the centrosome in a microtubule independent fashion, suggesting that it was an integral centrosome component. RNAi induced depletion caused a defect in the placement of the centrosome in relation to the nucleus, which in turn resulted in cell cycle delay, reduced primary cilia assembly and interestingly, defects in the Golgi apparatus. Of its many roles, microtubules are important, together with motor activity, for the organising and positioning of the Golgi apparatus close to the nucleus (Rios and Bornens, 2003). Also playing a role in this regulation are the various microtubule anchoring proteins that allow the Golgi apparatus to be steadily localised within the cell centre. The resulting disorganisation and displacement of the Golgi apparatus led to the conclusion that TBCCD1 may in fact act as a component of the pericentriolar matrix.

1.9.3 RP2 and its G protein Arl3

The human RP2 gene encodes a 350 amino acid protein that is ubiquitously expressed in human tissues. Mutations in the gene are shown to be responsible for between 15-20% of X-linked retinitis pigmentosa (XLRP), the most severe form of retinitis pigmentosa in which progressive retinal degeneration occurs (Schwahn et al., 1998).

Upon investigation of the possible function of RP2 and how it causes XLRP, its sequence similarity – 30.4% identity over 151 amino acids (Schwahn et al., 1998), with tubulin folding cofactor C was scrutinised. Moreover, the two proteins also shared the structural domains as mentioned previously in section 1.9.1, suggesting that there is functional conservation between the two proteins. The function of cofactor C as a player of the tubulin folding pathway had been established in studies mentioned in Chap.1.7, its crucial role being as a GAP of tubulins as part of the supercomplex. It had been confirmed that RP2, sharing the arginine finger vital for GAP activity, was able to stimulate the GTPase activity of native tubulin much like cofactor D and cofactor C (Bartolini, 2002), suggesting that RP2 may indeed also have a G protein that it regulates. This R118 residue that is conserved in cofactor C is an amino acid that is mutated in

retinitis pigmentosa patients, signifying the possible importance of the GAP activity in RP2 function and cofactor C.

In the meantime, Arl2 in mammalian cells had been identified as a homologue of CIN4 (Bhamidipati et al., 2000), a budding yeast gene working in close regulation with the other cofactors in the budding yeast (Hoyt et al., 1990) tubulin folding pathway (Hoyt et al., 1997). As Arl2 was able to interact with cofactor D and regulate the GAP activity of cofactors C, D and E, its possible involvement in the tubulin folding pathway had been suggested.

This possible role of Arl2 led to the investigation of the other Arl proteins and their possible roles. The Arl (ARF-like) family consists proteins identified as Ras-related small G proteins (Clark et al., 1993). Named 'ARF-like' due to their high sequence similarity with the ARF proteins, they share approximately 40 to 60% similarity. However they are not functional homologues with the ARF proteins, as they are not able to function as a cofactor in the cholera-toxin catalysed ADP ribosylation of $G\alpha_s$ (adenylate cyclase) which is the unique feature of the ARF proteins (Tamkun et al., 1991; Amor et al., 2001).

The Arl protein family all share functional and sequence similarity, so when searching for a potential interactor of RP2, the other Arl members were investigated. Interaction studies with expressed Arl proteins and RP2 showed that Arl3, in its GTP bound form, binds most stably to RP2 in a myristoylation dependent manner (Bartolini, 2002; Evans et al., 2005). The crystal structure of RP2 was solved (Kühnel et al., 2006) and subsequently the interaction between RP2 and Arl3 was also crystallised, identifying the important binding regions (Veltel et al., 2008a) as shown in Fig.1.9. In addition, RP2 was found to have a GAP domain, and showed GAP activity for Arl3. Moreover, when the residues that were commonly mutated in retinitis pigmentosa patients were introduced into the structure, including mutations in the arginine finger, GAP activity was lost. This suggested that the GAP activity of RP2 was important for its function and resultant disease when defective.

In cultured cells, RP2 predominantly localises to the plasma membrane, targeted by myristoylation and palmitoylation of its N-terminal (Chapple et al., 2000). This localisation is thought to be essential for its function in the retina. Immunofluorescent labelling showed that RP2 localised on the plasma membrane of the rod and cone photoreceptors by post-translational modifications by myristoylation and palmitoylation (Chapple et al., 2003); and Arl3 in the microtubule structures including the connecting cilium, suggesting that it is a MAP (Grayson et al., 2002). The connecting cilium is a specialised microtubule structure, and defects in formation cause retinal degeneration, suggesting that mutations in RP2 and Arl3 cause patient phenotypes by disrupting cytoskeleton-membrane links.

Further studies have revealed more information about RP2 and Arl3, and their function related to cilia in photoreceptors and other cells. RP2 was shown to localise at the cilia basal body in human retinal epithelial (RPE) cells and in the cilia of renal epithelial cells (Evans et al., 2010). This identification of RP2 in renal epithelial cells complemented the studies where Arl3 knock-out mice showed ciliary defects in the kidney as well as liver and pancreas (Schrick et al., 2006, Hurd et al., 2010).

This localisation pattern of RP2 at the centriole, basal body and ciliary apparatus of photoreceptor cells, as well as at the Golgi, plasma membrane and the periciliary ridge (Evans et al., 2010; Hurd et al., 2010; Hurd et al., 2011), suggests that RP2 is involved in the endomembrane to ciliary base movement of proteins and then consequently intraflagellar transport (IFT) into the cilium (Follit et al., 2006). Loss of RP2 GAP activity resulted in disruption of the IFT machinery as well as fragmentation of the Golgi network, strongly suggesting that the GAP activity of RP2 and its regulation of Arl3 is crucial for Golgi cohesion and for the transport of proteins to the base of the photoreceptor for consequent IFT (Follit et al., 2006; Evans et al., 2010)

The effectors of Arl3 also give us an insight into the function of RP2 (Linari et al., 1999; Van Valkenburgh et al., 2001; Veltel et al., 2008b). Phosphodiesterase 6 delta (PDE6δ) and uncoordinated 119 protein (Unc119) are both proteins involved in regulation of the membrane association of lipid-modified proteins together with Arl3

(Ismail et al., 2012; Schwarz et al., 2012). They form a ternary complex, in which together they traffic cargo to the membrane (Veltel et al., 2008b). In the model proposed for this trafficking, the myristoylated cargo proteins bind to the orthologue of Unc119, Unc119b, in the cytoplasm and the cargo is trafficked to the cilium. The Unc119 then binds to the membrane-bound Arl3-GTP, which triggers the release of the myristoylated cargo protein into the cilium, or around the basal body ready for transport into the cilium. RP2 then hydrolysis the GTP bound to Arl3, and releases the Unc119b from Arl3.

Affinity pull-down of retinal lysates has recently found a novel interactor of RP2 (Schwarz et al., 2012) – the rod transducing beta subunit (Gβ1). GTP-bound Arl3 was shown to displace Gβ1 from its interaction with RP2. This suggests that Gβ1 may also be undergoing the same process as for PDE6δ and Unc119. The undefined GEFs and GAPs may be regulating the regulation of these various effectors within this pathway. This model involving RP2 and Arl3 in the crucial protein transport mechanism within the photoreceptors sheds light on the importance of these proteins within the cell and the implications of defective protein function.

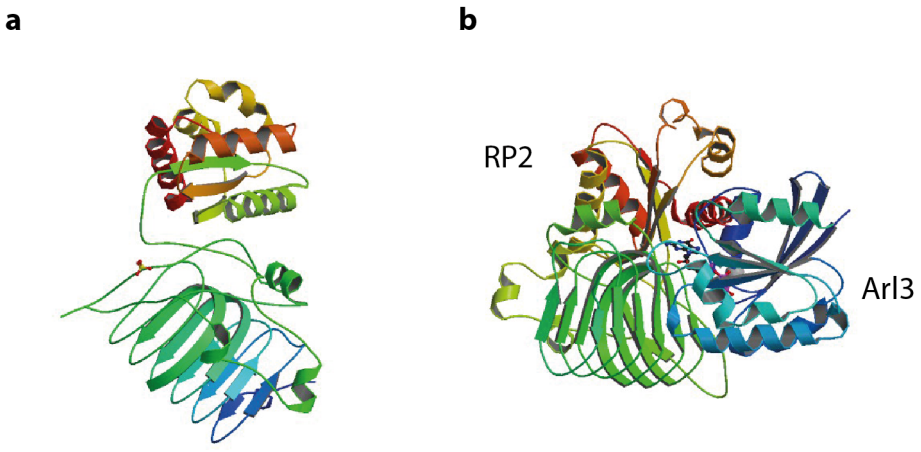

Figure 1.9 Structure of RP2 and its interaction with Arl3

(a) shows crystal structure of RP2, PDB ID: 2BX6 (Kühnel et al., 2006). (b) shows RP2 and its interacting partner Arl3 bound to GppNHp, PDB ID: 3BH6

1.9.4 Cofactor C and Arl2

As introduced in Chap.1.9, Arl2 was first identified as a member of the Arl (ARF-like) family of proteins (Clark et al., 1993). Compared to that of the ARF proteins, Arl protein functions are less understood. (Veltel et al., 2008a).

In order to elucidate the possible functions of the Arl proteins, potential interacting factors of Arl2 were investigated. The first partner found was BART (binding to Arl2), the 19 kDa bovine brain protein which specifically interacted with Arl2-GTP. BART was found to be ubiquitously expressed in human and mouse tissues. The BART-Arl2 interaction has been crystallised (Zhang et al., 2009), which in turn revealed a novel binding mode different from the other ARF proteins. The affinity and specificity of the interaction suggested that it was an effector of Arl2, especially as it showed no GAP activity for Arl2 (Sharer and Kahn, 1999). Consequent studies on the Arl2-BART interaction, including insights into its crystal structure (Fig.1.10) revealed some possible functions of the two proteins – it was found that together, they were able to enter mitochondria and bind with a mitochondria-specific protein (Sharer, 2001). Functions were also seen in the retention of STAT3, a member of the signal transducers and activators of transcription within the nucleus, suggesting a nuclear role in addition (Muromoto et al., 2008). In a recent study it was also suggested that BART has implications in cancer, where it was shown that BART was an inhibitor of GTP-bound Arl2, which itself acts as a RhoA inhibitor by inducing the rearrangement of the actin cytoskeleton and inducing cancer cell invasion (Taniuchi et al., 2011). More evidence was reported linking Arl2 and cancer by Beghin and colleagues who showed that levels of Arl2 regulated microtubule dynamics and cell cycle control within breast tumour cells. Low levels of Arl2 in cells showed reduced contact inhibition and increased cluster formation, increasing its proliferative advantage. On the contrary increased Arl2 levels showed less aggressive cells with enhanced necrosis (Beghin et al., 2007; Beghin et al., 2009; Zhou et al., 2010).

Another known interactor of Arl2 is PDEδ - a regulatory subunit of PDE6 in the murine system. This interaction was seen to be dependent on GTP, with the introduction of PDEδ stabilising GTP binding of Arl2. This interaction was seen for both Arl2 and its

related protein Arl3 (Hanzal-Bayer et al., 2005; Ismail et al., 2011). The crystal structure of this interaction is shown in Fig.1.10.

There are also other cell-type specific evidence of Arl2 function reported – The human UNC119 protein was shown to interact with Arl2 in photoreceptors (Kobayashi et al., 2003; Mori et al., 2006; Ismail et al., 2012). The crystal structure of this interaction is shown in Fig.1.10 In the parasite Trypanosoma brucei, loss of Arl2 function led to inhibited cleavage furrow formation, accumulating multinucleated cells as a result of defective cytokinesis (Price et al., 2010).

In addition to these roles of Arl2 in connection with BART and PDEδ function, there has been evidence that Arl2 plays a role in microtubule related functions. The *C. elegans* homolog *evl-20* was shown to be involved in regulation of cytoskeletal dynamics. The loss of *evl-20* function causes cell division defects in development caused by abnormal cytokinesis, and disruption of cortical and astral microtubules (Antoshechkin and Han, 2002).

One of the interesting microtubule related functions suggested is the ability of Arl2 to regulate the tubulin folding cofactors. Cowan and colleagues showed that the tubulin GAP activity of cofactors C, D and E on β-tubulin was downregulated with the introduction of Arl2 (Bhamidipati et al., 2000). Importantly, it was also shown that Arl2 interacts with cofactor D, preferentially and more efficiently in its GDP bound form. In addition, the destructive effect of the overexpression of cofactors D and E were prevented by the presence of Arl2. Additional binding partners – the protein phosphatase 2A (PP2A) proteins were later identified (Shern et al., 2003), suggesting that there may be more interactors of Arl2 that are yet to be identified. Interestingly, this study also found that whilst in complex with PP2A, Arl2 could not bind to GTP and that keeping cofactor D within this complex inhibited its action compared to if it was free. Additional functions of Arl2 and cofactor D in epithelial cells have also been reported (Shultz et al., 2008), as regulating the disassembly of the apical junctional complex – which is involved in the maintainance of cell-surface polarity and epithelial monolayer cell-cell contacts.

As a small G protein, it is assumed that Arl2 may have a GAP and/or GEF aiding its function and GDP/GTP exchange. A potential candidate suggested is ELMOD2 – a protein containing the ELMO domain which was found to have GAP function on Arl2 in experiments using purified bovine testis proteins. This was surprising, as ELMOD2 did not contain the canonical ARF-GAP signature, and therefore a possible alternative function is suggested for this interaction. The specificity of this interaction remains unclear, with a possibility of the ELMO proteins playing a wider role in GTPase regulation (Bowzard et al., 2007). It has since then be shown that ELMOD2 is involved in antiviral response in idiopathic pulmonary fibrosis (Pulkkinen et al., 2010).

In addition to these known interactors of Arl2, there is potentially more proteins that may interact with Arl2, regulating its function or working downstream as the effector of this multi-tasking G protein. The potential also remains of more GAPs and/or GEFs to be identified. One of these possible interactors is the tubulin binding cofactor C (see Chap.1.7), which is a candidate pursued in this current study.

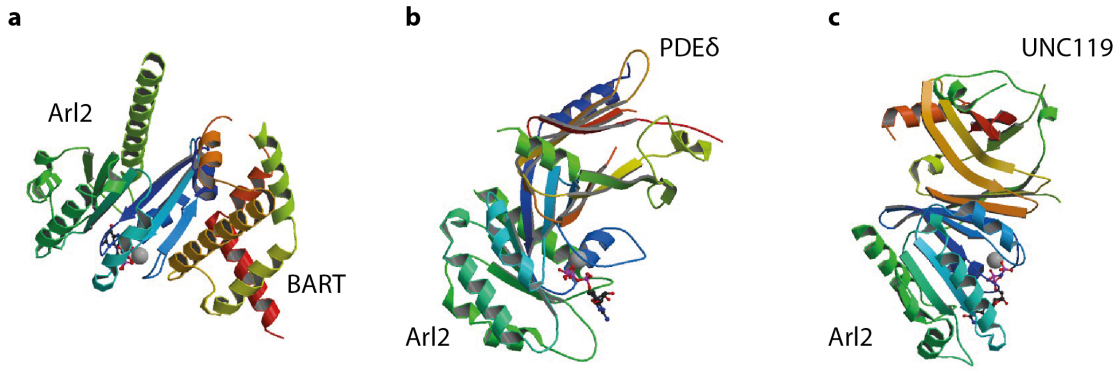

Figure 1.10 Structure of Arl2 and its interacting partners

Interactions between Arl2 and its known interacting partners are shown. (a) Arl2 and BART, PDB ID: 3DOE (Zhang et al., 2009) (b) Arl2 and PDEδ, PDB ID: 1KSG (Hanzal-Bayer et al., 2002) and (c) Arl2-GppNHp and UNC119, PDB ID: 4GOK (Ismail et al., 2012). These structures will help in elucidating and understanding any additional interactors of Arl2.

1.10 Aim of Study

Several aspects of microtubules have been studied in great detail, with a vast amount of knowledge being accumulated regarding aspects such as structure, dynamics, MAPs and tubulin modifications. However it is striking that a process as fundamental as the tubulin folding cofactor pathway has not yet been fully understood. The tubulin heterodimer is the basic building block of the microtubule, and the correct folding of the α- and β-tubulin monomer into this heterodimer must be accurately and correctly achieved in order for proper microtubule biogenesis. The fact that cell tackles this heterodimer formation by such a complex pathway with so many players and stages of regulation is intriguing, and suggests the importance of this process.

Cowan and colleagues had proposed a tubulin folding pathway from *in vitro* data that has been shown by tubulin folding experiments using purified tubulin and the various cofactors. However this has not been studied in great depth *in vivo*. Toda and colleagues have previously worked on the cofactor pathways in the fission yeast *S. pombe*, but a complete pathway could not be defined due to the lack of the tubulin cofactor C orthologue. Studies in fission yeast had already shown some discrepancies with the model pathway, mainly from the rescue experiments carried out by the various cofactor mutants. It was clear that Alp1 overexpression was sufficient to rescue the ts mutants of *alp11* and *alp21* (Radcliffe et al., 1999), and that *alp31* was not essential in the fission yeast system (Radcliffe et al., 2000a). Fig.1.7 highlights this difference – the *in vitro* model pathway showed all the cofactors of having equal importance in a parallel fashion, but this may not be the case *in vivo*.

Therefore, I set out to find and confirm the fission yeast orthologue of cofactor C. In addition, there was an additional protein of unknown function that had been identified as playing a role in microtubule regulation – Alp41, which I aimed to place in the pathway. In order to do this I constructed and analysed mutants of these 2 proteins, to gain a more detailed understanding of the activity of cofactor C and its function in the pathway. With the knowledge that cofactor C was suggested to have GAP activity, and Alp41 being a possible G protein, I assessed if cofactor C was indeed a GAP for Alp41.

Another unanswered question was if there were any other interactors of Alp41. Through searching for possible binding partners of Alp41, I assessed what functions it may be playing downstream of the microtubule pathway.

To observe these microtubule defects, I used the fission yeast system. The simplicity of genetic modification and ease of assessing microtubules made the organism the ideal model to study these questions in. Together with biochemical techniques, I was able to identify what the missing links were in the tubulin folding pathway, by functionally characterising cofactor C in fission yeast and its related protein Alp41. By identifying another binding partner of Alp41, I also added an extra role to one of the cofactors within the pathway.

Taken together, I propose a model for how the interactions of these cofactors together regulate the very fundamentals of microtubule biogenesis.

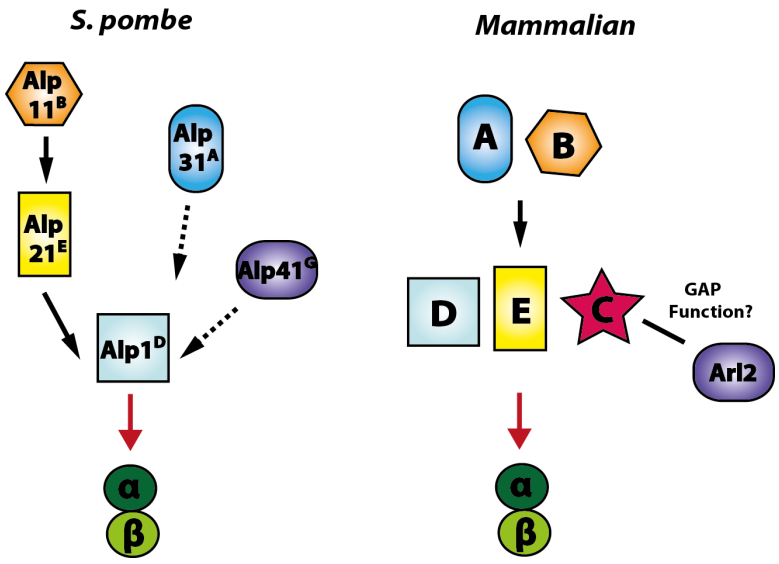

Figure 1.11 The tubulin folding pathway: Fission yeast V.S. Mammalian

The model of the mammalian tubulin cofactors based on the *in vitro* data suggest that they function in a parallel fashion. Fission yeast genetics show that Alp1(D) overexpression is able to rescue mutants of Alp11(B), Alp21(E) and Alp41. This suggests that Alp1(D) plays a more downstream role and may be involved in more than one function within the pathway.

Chapter 2. Materials & Methods

2.1 Fission yeast growth and maintenance

Fission yeast cells were grown in standard conditions (Moreno et al., 1991). Table 2 shows various media used for cell culture. Unless otherwise stated, strains were cultured in rich YE5S media. For selection, media with various added drugs were used (Table 3). For overexpression using the *nmt* promoters, cells were grown in minimal media with the required supplements plus thiamine, washed out using a filtration pump, and further grown in minus thiamine conditions for approximately 16-32 hours as necessary.

Media	Added Components
YE5S	0.5% Difco yeast extract, 3% dextrose, 250 mg/ml amino acids (uracil, adenine, histidine, lysine, leucine)
EMM	14.7 mM potassium hydrogen phthalate, 15 mM Na2 HPO4 , 93.5 mM NH4 Cl, 2% w/v glucose, salt stock, vitamin stock, mineral stock
MEA	3% Difco yeast extract, 75 mg/ml amino acids (uracil, adenine, histidine, lysine, leucine)
YFM	YE5S with 15% glycerol
LB (for *E.coli*)	170 mM NaCl, 0.5% w/v yeast extract, 1% w/v bactotryptone, pH7.0

Table 2 Growth media and added components

Drug	Added components and concentration
Hygromycin B	YE5S + 300 μg/ml hygromycin B (Roche)
Kanamycin	YE5S + 100 μg /ml Geneticin (G418) (Sigma)
ClonNAT	YE5S + 100 μg /ml nourseothricin (Werner Bio-agents)
Aureobasidin A	YE5S + 0.5 μg /ml aureobasidin (Takara Bio)
Phloxine B	YE5S + 7.5 μg /ml Phloxine B (Sigma)

Table 3 Drugs added to media for cell growth

2.2 Fission yeast transformation

50 ml of host strain was cultured over night and collected by centrifugation at 3,000 G for 3 mins. The cells were washed twice in LiAc/TE, and gently mixed after the addition of 7.5 μl salmon sperm DNA. 10 μl of PCR product or 1 μl of plasmid DNA was added (approx. 200 ng DNA) and the sample rotated on a slow shaker for 10mins. 260 μl of 40% PEG solution was added and the sample shaken at 30°C for 1 hour or 27°C for 2 hours for temperature sensitive mutants. The sample was then heat shocked at 42°C for 10 mins, the cells were washed with YE5S and shaken with 500 μl fresh YE5S for 1.5 hours. The cells were then plated onto YE5S plates and incubated at 27°C or 30°C for approximately 20 hours. The plates were then replica plated using Whatman Paper onto selective plates and incubated for a further 3-7 days until colony growth was observed.

2.3 Gene tagging and manipulation

For endogenous gene tagging, the one-step PCR-based method was used (Bahler et al., 1998) using long oligonucleotides approximately 100 base pairs in length. Oligonucleotides were designed to carry approximately 80 base pairs of homology flanking the sequences adjascent to the insertion site at the endogenous locus of the target gene, with an added 20 base pairs of homology to the insertion cassette from the template plasmid (See Chap.2.20). For gene tagging with various tags such as GFP, 3HA, 3pk, etc, the pFA6a template plasmid series was used, which contained a selection marker – kan^r, nat^r or hph^r (Sato et al., 2005). Once the PCR product was obtained, it was cleaned up by ethanol precipitation and then transformed into a wild-type strain. The integrants were selected using selective plates containing the appropriate drug, and the tagging confirmed by colony PCR.

2.4 Isolation of temperature sensitive mutants

The essential gene of interest (*tbc1* or *alp41*) was tagged with a hygromycin (hph^r) selection cassette using tagging methods previously described in the previous section. The fragment was then amplified by PCR. These fragments were then randomly mutagenised using "error prone PCR", using unbalanced dNTP conditions (2.5 mM 10x dGTP in comparison to the others (0.25 mM)) and Vent DNA polymerase (New England Biolabs Ltd.). These conditions had been designed to maximize the rate of mutagenesis. The PCR product was then ethanol precipitated and transformed into the wild-type 513 strain and plated onto YE5S plates. After 20 hours at 27°C the plates were replicated onto YE5S+hygromycin plates and incubated for another 3 days until colonies had formed. These plates were then replicated further onto YE5S plates containing phloxine B. The phloxine B dye is used in yeasts to distinguish between live and dead cells. The dye is incorporated by all the cells, but metabolically active cells can remove the dye and therefore appear colourless (white). However cells that are dead are not able to remove this dye so they will stain dark pink/red on the plate. Replica plated plates were incubated at 27°C and 36°C. After 1-3 days of incubation, these plates were observed for colonies that were growing as white colonies at the permissive temperature and were either dark pink/red or dead at the higher temperatures.

The screen was repeated until around 8000 colonies had been screened, and the temperature sensitive mutant candidates picked up and restreaked. These cells were also observed under the microscope to check if the morphology looked defective compared to wild-type cells. After initial screening, the strains were backcrossed with a wild-type strain to ensure that there was proper integration of the randomly mutagenized gene and that the defects were not caused by off-site mutations. The strains that showed the same sensitivity on the phloxine B plate and the resistance plate were deemed as temperature sensitive mutants.

2.5 Random Spore Analysis

Various strains used within this study were constructed by mating and subsequent random spore analysis. The two strains of interest with opposite mating types, h^+ and h^-, were grown on MEA plates overnight. The two strains were then mixed and incubated for a further day. Once the formation of asci had been confirmed under the microscope, the cells were taken and placed in 100 μl of 0.5% SHP solution (Biosepra) and mixed vigorously for cell wall digestion. After incubation at 27°C for a minimum of 3 hours, 43 μl of 100% ethanol was added and the cells vigorously shaken for 20 mins on a mechanical shaker in order to eliminate the cells that had not sporulated. The spores were then pelleted and washed with 1 ml distilled water and serial dilutions of 10^{-1} to 10^{-5} cells plated on YE5S plates which were incubated at 27°C until colonies could be observed. Once the colonies had grown, these plates were replicated onto appropriate plates for selection.

2.6 Genomic DNA extraction from fission yeast cells

1.5 ml of saturated cell culture was collected by centrifugation and the supernatant removed. To this pellet, 100 μl of Yeast Cell Lysis colution (EPICENTRE MasterPure Yeast DNA Purification Kit) was added and vortexed for thorough mixing. The cells were then incubated at 65°C for 15 mins for lysis, and the samples placed on ice for 5 minutes. 50 μl of MPC Protein Precipitation Reagent was added and the sample vortexed for 10 seconds. The cell debris was pelleted by centrifugation for 10 mins at 13,000 G, and the supernatant transferred to a new tube. 500 μl of isopropanol was added and mixed thoroughly by inversion. The DNA was then pelleted by centrifugation at 13,000 G for 10 mins. The supernatant was discarded and the pellet washed with 500 μl of 70% ethanol. The ethanol was removed and the DNA pellet suspended in 30 μl of distilled water.

2.7 Sequencing

Sequencing for mutations in the ts mutants and for general confirmation of constructs were carried out by the Cancer Research UK London Research Institute in-house sequencing facility using the Applied Biosystems 3730xl DNA Analyser.

2.8 Serial dilution spot assay for temperature and TBZ sensitivity

The strain of interest was grown to exponential growth. The cell density per ml was measured using the KX-21N cell counter (Sysmex Corp) and adjusted to obtain $2x10^7$ cells per ml. 10 fold serial dilutions were prepared up to $2x10^2$ cells per ml in a 96 well plate. The cells were then spotted onto YE5S plates using a 48-pin replicator. The plates were incubated at various temperatures and then images taken after 2-3 days of growth.

2.9 Fluorescence microscopy and quantification

The DeltaVision-SOftWoRx system (Olympus and Applied Precision Co.) was used for obtaining all fluorescence microscopy data. The images were acquired using an Olympus IX70 PlanApo 100x, NA 1.4, oil immersion objective. The imaging software used was softwoRx 3.3.0, with the Coolsnap HQ (Roper Scientific) camera. The cells were cultured to exponential phase and then collected by centrifugation. They were then re-suspended in 100 μl of growth media and 10 μl pipetted onto an agarose pad. The agarose pads were prepared by adding 800 μl of melted 2% agarose in growth media to the rubber chamber. Cells on the pad were then covered by a glass cover slip and the agarose pad placed onto a glass slide. The glass slide was then used for observation under the microscope. 15 sections were taken along the Z-axis, at 0.2 μm intervals. The images were further processed using deconvolution and then projected into a single projection with the maximum intensity algorithm. The images were then processed by Adobe Photoshop CS4 and CS5.

2.10 Hoechst and MitoTracker staining

15mins before observation, 200 μl of exponential cell culture was taken and 1 μl of Hoechst solution added (to a final concentration of 5 μg/ml). The sample was incubated in the dark, shaking, for 15 mins. Following incubation the cells were collected by centrifugation, washed 3 times in culture media and then observed on the slide.

The same procedure was carried out for Mitotracker staining – a final concentration of 100 mM of Mitotracker solution was added to the cells for incubation.

2.11 Protein extraction

2.11.1 Alkaline extraction

In the cases where a high purity sample was not necessary, for instance when checking the expression of a protein or to confirm tags, the alkaline fast extraction method was used. Cells from an exponential culture were collected by centrifugation and 1 ml collected in a tube and washed with 1 ml of distilled water. The pellet was resuspended in 1ml of 0.3N NaOH and incubated at room temperature for 10 mins. The cells were then pelleted by centrifugation at 4000 G for 3 mins and the supernatant removed carefully. 100 μl of Laemmli buffer was added and vigorously mixed by vortexing. The sample was then boiled for 5 mins at 95°C and then placed on ice. The sample was then loaded onto an SDS-PAGE gel.

2.11.2 Extraction by glass beads

When a more pure protein sample was required, the protein was extracted using mechanical breaking by glass beads. 50ml of cells were collected from an exponential culture by centrifugation at 3500 G for 5 mins. The pellet was then re-suspended in 100 μl extraction buffer and 100 μl of acid-washed glass beads was added. The lid was sealed and the tubes shaken at 4°C in a FastPrep FP120 shaker at setting 6.0 for 25 seconds, 3 times. The protein extracts were then separated from the cell debris and the

beads by centrifugation at 13,000 G for 5 mins. The protein concentration was then determined by the Bradford assay (Bio-Rad).

2.12 Immunoblot analysis

The protein samples were boiled in Laemmli buffer for 5 mins and loaded onto SDS-PAGE gels (4-12% tris-acetate Criterion XT gradient gel from Bio-Rad) and the resolved proteins transferred onto Immobilion PVDF membrane (Millipore) by wet transfer at 4°C overnight at 30V, or at room temperature for 1 hour at 100V. 10% skimmed milk in PBS was used to block the membrane for 1 hour at room temperature or at 4°C overnight. Primary antibody in 5% milk/PBS was added to the membrane and incubated for 1 hour at room temperature or overnight at 4°C. The membrane was washed with 0.1% PBST for 10 mins, 3x, and the secondary antibody in 5% milk/PBS or Immunoshot was added and incubated for 1 hour at room temperature. The membrane was further washed with 0.1% PBST for 5 mins, 3x. For detection of the bound membrane, the ECL chemilluminescence kit (GE Healthcare Co.) was used and the film exposed for the appropriate time and developed. Table 4 shows the antibody concentrations used for all the antibodies used in this study.

Antibody	Clonality	Species	Concentration (for Immuno-blot)	Cat. No
Anti-pk	monoclonal	mouse IgG2	1:1000	ABD Serotec, MCA1360GA
Anti-Flag (M2)	monoclonal	mouse IgG1	1:1000	Sigma, F-3165
Anti-HA	monoclonal	mouse IgG1	1:1000	Babco, MMS-101P
Anti-GFP	monoclonal	mouse IgG1	1:1000	Rochem 11814460001
Anti-Myc	monoclonal	mouse IgG1	1:1000	Babco, MMS-150R
TAT-1 (anti-alpha tubulin)	monoclonal	mouse IgG1	1:2000	Sigma T-5168

Table 4 List of primary antibodies used for immuno-blot analysis

2.13 Immunoprecipitation

Protein extract was prepared using the glass bead method. A minimum of 3mg of protein extract was used per sample. Less protein can be extracted from cells that have been cultured in EMM, so a larger volume of cells were cultured in this case. The extract was added to protein A or G dynabeads (Invitrogen) bound with the appropriate antibody and incubated at 4°C for 1.5 hours on a rotating shaker. The beads were then washed 5x with wash buffer and 15µl of 1x Laemmli buffer added to the beads. The sample was then boiled for 5 mins, spun down at 13,000 G for 1 minute and the sample loaded onto an SDS-PAGE gel. Once the proteins had been resolved, an immunoblot was performed to detect the protein.

2.14 Expression and purification of recombinant proteins

Recombinant Alp41 and Tbc1 proteins were expressed in *E.coli* and purified for use in peptide array analysis. The various forms of Alp41 (wild-type, Q70L, T30N, T47A) and Tbc1 constructs were cloned into the pET28a vector containing a 6-HIS tag. The protein was expressed in *E. coli* (BL-20) by incubation at 19°C overnight upon 1 mM IPTG induction in 2 litres of culture. The cells were pelleted by centrifugation at 8,000 G for 30 mins at 4°C and 10 ml of lysis buffer added. The sample was mixed vigorously and incubated at 4°C on ice for a further hour. After incubation the cells were sonicated for 7 seconds with 30 second intervals 7 times or until the sample was no longer viscous. The sample was then spun down at 14,800 G for 20 mins at 4°C and the supernatant collected and added to a Ni-NTA agarose column (QIAGEN). The column was rotated for an hour and the flow-through collected. After 4 washes with wash buffer, elution buffer was passed through the column and 10 fractions collected. Laemmli buffer was added and the samples loaded onto an SDS-PAGE gel. Once the proteins had been resolved, the gel was incubated with coomassie blue solution (40% methanol, 10% glacial acetic acid, 0.05% Coomassie brilliant blue) for 30 mins at room temperature or over night. Destaining buffer (40% methanol, 10% glacial acetic acid, 0.05%) was then used to destain the gel ready for observation.

2.15 Peptide Array Assay

The peptides were synthesised and spotted onto a cellulose membrane at 2 amino acid residue increments, 20 residues per spot. The membrane was activated by 1 hour incubation at room temperature in solution with 50% ethanol and 10% glacial acetic acid. It was then briefly washed in PBST x3, and 20 μg protein in PBST added to incubate on a shaker overnight at 4°C. The membrane was then washed once in PBST, and then blocked with 3% milk in PBST. After blocking, primary antibody in 3% milk/PBST was added to the membrane and incubated for an hour at room temperature, and then washed x3 in PBST, followed by addition of secondary antibody in 3% millk/PBST. The membrane was then washed x3 in PBST and then the blot detected by the ECL kit.

2.16 Yeast 2-Hybrid screening

The yeast two-hybrid screen is a technique to screen for and detect protein-protein interaction. A host yeast strain is required which contains an inducible promoter fused to reporter genes which enable a detectable response to the interactions (Fig.2.1). The system used in this study utilised a HIS3 reporter which is known to be sensitive to weaker interactions.

The gene of interest (*alp41*) was cloned into the pGBKT7 bait plasmid. The pGBKT7 plasmid contains the GAL4 DNA binding domain, Kan resistance cassette for selection in *E. coli,* and TRP1 for *S. cerevisiae* selection. This plasmid was then transformed into the AH109 wild-type *S. cerevisiae* strain.

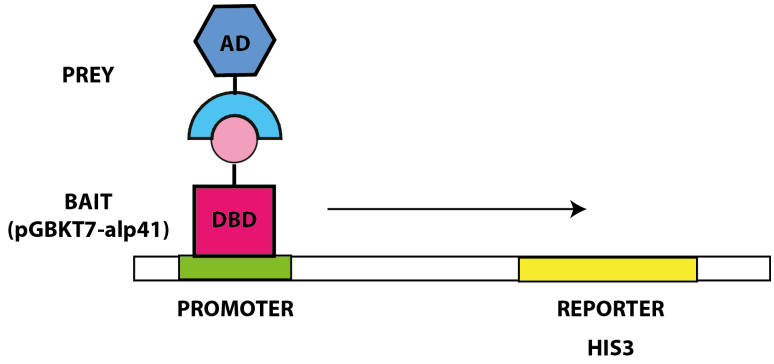

Figure 2.1 Yeast 2-Hybrid screening

The downstream reporter gene is activated upon binding of a transcription factor to the upstream promoter. The transcription factor is split into two – the DNA binding domain carrying the bait (shown in pink), and the activating domain (shown in blue). Only when the two parts interact is there activation of transcription and reporter activity observed. This allows the host strain to become resistant to HIS, which is therefore used for the selection process. The underlying reporter activity (i.e. how efficient this selection is basally) must be identified to eliminate false positives. If there is growth seen and HIS selection is leaky, 3AT can be added to eliminate the background activity to identify the true positives.

2.16.1 Transformation into *S. cerevisiae*

50 ml of AH109 cell culture was grown overnight, and the OD_{600nm} adjusted the to OD_{600nm}= 0.3-0.5 after one generation of growth for cell recovery. The cells were collected by centrifugation and washed with 1ml TEL buffer, and resuspended in 50 µl TEL buffer (100mM Tris-HCl, 1mM EDTA, 1M LiAc). 200 µg of plasmid DNA and 2 µl of boiled salmon sperm DNA was added to the cells and mixed gently. After 5 mins incubation at room temperature, 300 µl of TELP buffer (100mM Tris-HCl, 1mM EDTA, 1M LiAc, 50% PEG) was added and the sample vortexed for 10 seconds. This was then incubated in a shaker at 27°C for 3 to 4 hours. After incubation, the cells were heat shocked for 15mins at 42°C, and then pelleted and washed in 1 ml 1M sorbitol. Of this sample, 100 µl of sample was plated on various selection plates. After around 2 days, colonies grew, and these strains were restreaked. The selection plates are shown below:

2.16.2 Checking the reporter activity of pGBKT7-*alp41*

As mentioned, the HIS3 reporter system can be leaky. This leakiness can be overcome by the careful use of 3AT (3-aminotriazole) which suppresses the chances of false positives. However if the concentration of 3AT is too high, then true positives may also be suppressed, so a suitable concentration must be determined in order to have enough sensitivity but to decrease the false positives. In order to do this, the underlying reporter activity of the pGBKT7-*alp41* must be determined. This was done by spotting each strain on YGN plates with no histidine and various concentrations of 3AT. A plate with added histidine was also used for a positive control. After growth, the spots were observed – the minimum concentration at which the strain does not grow was used in the following experiments for selection. The concentration of 3AT is gene dependent. In the case of *alp41*, there was no obvious reporter activity – the cells did not grow even when there was no 3AT added. Therefore no 3AT was necessary for further selection.

2.16.3 Transformation of *S.pombe* library

The *S. pombe* cDNA library, a gift from Julie Cooper's lab, was transformed into the AH109 strain containing pGBKT7-Alp41. A large scale transformation was carried out, with 40ml of cells being used per transformation and 30 μg of library DNA being added to an overall sample of 7 ml TELP. After heat shock the cells were incubated at 30°C for recovery, and plated onto two different plates – with or without histidine. The plates were incubated at 30°C for up to 10 days and the colonies picked and restreaked onto minus histidine plates. These were continuously re-streaked fresh and the persistent clones picked as candidates. These restreaked plates were replicated onto selection plates.

2.16.4 Isolation of plasmids from *S.cerevisiae* transformants

In order to recover the plasmids that potentially contain the interactor of the gene of interest, 10ml of the strain was grown to saturation and collected by centrifugation. The pellet was resuspended in 1 ml distilled water and after washing, the pellet was

resuspended in SZ buffer (0.92 M Sorbitol, 110 mM Na-citrate, 70 mM EDTA) with added beta-mercaptoethanol and zymolyase. This was incubated for 1 hour at 37°C and then SDS-TE (20% SDS, 100 mM Tris-HCl, 10 mM EDTA) added. This was mixed and incubated for 10 mins at 60-65°C. 150 μl of potassium acetate was added to the sample and incubated on ice for 1 hour. The debris was then pelleted by centrifugation at 12,000G for 15mins, 4°C. The supernatant was transferred to a fresh tube and cleaned by the Wizard DNA Clean-Up system (Promega). The plasmid was eluted in 50 μl of kit buffer. This was then transformed into super-competent *E.coli* and the resulting plasmid purified by mini-prep. These plasmids were digested with the enzyme HINDIII in order to eliminate multiple plasmids etc.

2.16.5 Transformation of plasmids and elimination of false positives

The AH109 strain containing pGBKT7 alone and pGBKT7-*alp41* were transformed with the above plasmids. The transformants were spotted onto plates with histidine, no histidine and no histidine plus varying concentrations of 3AT if necessary. The strain in which there was growth only for the strain containing *alp41* on minus histidine plates was picked up as interactors.

The plasmids that had been transformed into these strains were then sequenced and then aligned with the *S. pombe* genome to determine what genes had been identified as interactors by the screening. The genes were found on the database and determined if they could be physiological interactors.

2.17 Solutions and buffers

Solution	Added components
TE	10 mM Tris-HCl, pH7.5, 1 mM EDTA
TAE	0.08 M Tris acetate, pH7.5, 2 mM Na2EDTA
LiAc/TE	100 mM lithium acetate pH7.4, 10 mM Tris-HCl pH7.4, 1 mM EDTA pH8.0
LiAc/TE/40% PEG3640	LiAc/TE + 40% polyethylene glycol 3640 (Sigma)
Transfer buffer	39 mM glycine, 48 mM Tris-base, 20% methanol
PBS	170 mM NaCl, 3 mM KCl, 10 mM Na2HPO4, 2 mM KH2PO4
PBST	PBS + 0.1% Tween-20
2x Laemmli sample buffer	125 mM Tris-HCl pH6.8, 50% glycerol, 4% SDS, 0.02% bromophenol blue, 100 mM DTT
Extraction buffer (yeast protein extraction)	0.5M Hepes, 0.5M NaF, 1M Na-b-glycerophosphate, 250mM EGTA, 250mM EDTA, 10% Triton X-100, PIC, 100mM PMSF
IP buffer	50 mM Tris.HCl pH 7.4, 1 mM EDTA pH 8.0, 150 mM NaCl, 0.05% NP-40, 10% glycerol
Wash buffer (IP)	IP buffer plus 1M DTT, 750mM PNPP, PIC, 100mM PMSF
Lysis buffer (*E.coli*)	50mM Hepes, 250mM NaCl, 10% glycerol, 5mM beta-mercaptoethanol, 0.5% TritonX-100, 1mM PMSF, PIC, 40mM Imidazole
Wash buffer (*E.coli*)	as above but with 60mM Imidazole
Elution buffer (*E.coli*)	as above but with 250mM Imidazole

Table 5 Tables of buffers and solutions

2.18 Fission yeast plasmids used in this study

Name	Gene
pREP1-Alp41	*alp41*$^{+}$
pREP1-Alp41-T47A	*alp41*
pREP1-Alp41-T30N	*alp41*
pREP1-Alp41-Q70L	*alp41*
pREP1-Alp41-F50A	*alp41*
pREP1-GFP-Alp41-T47A	*alp41*
pREP1-GFP-Alp41-T30N	*alp41*
pREP1-GFP-Alp41-Q70L	*alp41*
pREP1-Alp1	*alp1*$^{+}$
pREP1-GFP-Alp1	*alp1*$^{+}$
pREP1-TBCC	human cofactor C
pREP1-RP2	human RP2

Table 6 Table of plasmids

2.19 Strains used in this study

Name	Genotype
513	*h⁻ leu1 ura4*
CHP428	*tbc1::kan^r pAL(tbc1$^+$) leu1 ura4 his7 ade6*
RM03	*h⁻ kan^r-nmt1-GFP-tbc1$^+$ leu1 ura4*
RM036	*h⁻ tbc1-1-hph^r leu1 ura4*
RM052	*h⁻ tbc1-9-hph^r leu1 ura4*
RM057	*h⁻ tbc1-11-hph^r leu1 ura4*
RM058	*h⁻ alp41-1-hph^r leu1 ura4*
RM064	*h⁻ alp41-5-hph^r leu1 ura4*
RM068	*h⁻ alp41-7-hph^r leu1 ura4*
RM070	*h⁻ alp41-8-hph^r leu1 ura4*
RM072	*h⁻ alp41-9-hph^r leu1 ura4*
RM082	*h⁻ alp41-14-hph^r leu1 ura4*
RM085	*h⁻ tbc1$^+$-FLAG-kan^r leu1 ura4*
RM089	*h$^+$ tbc1$^+$-3pk-kan^r leu1 ura4 his2*
RM099	*h⁻ alp41$^+$-3pk-kan^r leu1 ura4*
RM128	*h⁻ kan^r-nmt1-GFP-alp41$^+$ leu1 ura4*
RM131	*h$^+$ kan^r-nmt1-GFP-alp41$^+$ leu1 ura4 his2*
RM140	*h$^+$ alp21$^+$-FLAG-kan^r leu1 ura4 his2*
RM176	*h⁻ alp1$^+$-3pk-kan^r leu1 ura4*
RM188	*h⁻ alp21$^+$-3pk-kan^r leu1 ura4*
RM287	*h⁻ leu1 ura4 +pREP1*
RM289	*h⁻ leu1 ura4 +pREP1 (human cofactor C)*
RM291	*h⁻ leu1 ura4 +pREP1 (human RP2)*
RM293	*h⁻ tbc1-1-hph^r leu1 ura4 +pREP1*
RM295	*h⁻ tbc1-1-hph^r leu1 ura4 +pREP1 (human cofactor C)*
RM297	*h⁻ tbc1-1-hph^r leu1 ura4 +pREP1(RP2)*
RM299	*h⁻ tbc1-11-hph^r leu1 ura4 +pREP1*
RM301	*h⁻ tbc1-11-hph^r leu1 ura4 +pREP1 (human cofactor C)*
RM303	*h⁻ tbc1-11-hph^r leu1 ura4 +pREP1(RP2)*
RM318	*h⁻ kan^r-nmt1-GFP-alp41$^+$ alp1$^+$-3pk-hph^r leu1 ura4*
RM347	*h⁻ alp41-14-hph^r sid4$^+$-mRFP-kan^r aur^r-GFP-atb2$^+$ leu1 ura4*
RM356	*h⁻ tbc1-11-hph^r alp41-14-nat^r leu1 ura4*
RM357	*h⁻ tbc1-11-hph^r alp41-9-nat^r leu1 ura4*
RM376	*h⁻ tbc1-11-hph^r SV40-GFP-atb2$^+$ leu1 ura4*
RM385	*h⁻ alp21$^+$-FLAG-nat^r leu1 ura4*
RM395	*h⁻ alp1$^+$-3pk-kan^r alp21$^+$-FLAG-nat^r leu1 ura4*
RM398	*h⁻ tbc1::kan^r pAL(tbc1$^+$) alp41-14-nat^r leu1 ura4 his7 ade6*
RM429	*h⁻ tbc1$^+$-3HA-hph^r leu1 ura4*
RM440	*h⁻ kan^r-nmt1-GFP-alp41$^+$ alp1$^+$-3pk-hph^r tbc1$^+$-3HA-nat^r leu1 ura4*
RM443	*h⁻ tbc1$^+$-3HA-hph^r alp1-3pk-kan^r alp21$^+$-FLAG-nat^r leu1 ura4*
RM469	*h⁻ tbc1$^+$-3HA-nat^r kan^r-nmt1-GFP-alp41$^+$ leu1 ura4*
RM473	*h⁻ tbc1$^+$-3HA-hph^r alp21$^+$-FLAG-nat^r leu1 ura4*
RM475	*h⁻ tbc1$^+$-3HA-hph^r alp1$^+$-3pk-kan^r leu1 ura4*
RM477	*h⁻ alp41-14-hph^r sid4$^+$-mRFP-kan^r aur^r-GFP-atb2$^+$ cut11$^+$-CFP-nat^r leu1 ura4*
RM480	*h⁻ sid4$^+$-mRFP-kan^r aur^r-GFP-atb2$^+$ cut11$^+$-CFP-nat^r leu1 ura4*
RM496	*h⁻ leu1 ura4 +pREP1-alp1$^+$*

RM497	*h⁻ leu1 ura4 +pREP1-GFP-alp1⁺*
RM498	*h⁻ leu1 ura4 aur^r-mCherry-atb2⁺*
RM515	*h⁺ leu1 ura4 his2 kan^r-nmt1-GFP-alp1⁺*
RM520	*h⁻ leu1 ura4 aur^r-mCherry-atb2⁺ +pREP1-GFP-alp1⁺*
RM521	*h⁻ cut11⁺-RFP-nat^r aur^r-GFP-atb2⁺ leu1 ura4 +pREP1*
RM523	*h⁻ cut11⁺-RFP-nat^r aur^r-GFP-atb2⁺ leu1 ura4 +pREP1-alp41⁺*
RM525	*h⁻ cut11⁺-RFP-nat^r aur^r-GFP-atb2⁺ leu1 ura4 +pREP1-alp41-Q70L*
RM527	*h⁻ cut11⁺-RFP-nat^r aur^r-GFP-atb2⁺ leu1 ura4 +pREP1-alp41-T30N*
RM529	*h⁻ cut11⁺-RFP-nat^r aur^r-GFP-atb2⁺ leu1 ura4 +pREP1-alp41-T47A*
RM540	*h⁻ alp41-8-hph^r leu1 ura4 pREP1-alp41+*
RM541	*h⁻ alp41-8-hph^r leu1 ura4 pREP1-alp41 Q70L*
RM542	*h⁻ alp41-8-hph^r leu1 ura4 pREP1-alp41-T30N*
RM543	*h⁻ alp41-8-hph^r leu1 ura4 pREP1-alp41-T47A*
RM544	*h⁻ alp41-7-hph^r leu1 ura4 pREP1-alp41⁺*
RM546	*h⁻ alp41-7-hph^r leu1 ura4 pREP1-alp41-Q70L*
RM548	*h⁻ alp41-7-hph^r leu1 ura4 pREP1-alp41-T30N*
RM549	*h⁻ alp41-7-hph^r leu1 ura4 pREP1-alp41-T47A*
RM550	*h⁻ alp41-14-hph^r leu1 ura4 pREP1-alp41⁺*
RM552	*h⁻ alp41-14-hph^r leu1 ura4 pREP1-alp41-Q70L*
RM554	*h⁻ alp41-14-hph^r leu1 ura4 pREP1-alp41-T30N*
RM555	*h⁻ alp41-14-hph^r leu1 ura4 pREP1-alp41-T47A*
RM565	*h⁻ alp41-7-hph^r leu1 ura4 pREP1*
RM567	*h⁻ alp41-8-hph^r leu1 ura4 pREP1*
RM571	*h⁻ alp41-14-hph^r leu1 ura4 pREP1*
RM596	*h⁻ alp41-5-hph^r aur^r-GFP-atb2⁺ leu1 ura4*
RM598	*h⁻ alp41-7-hph^r aur^r-GFP-atb2⁺ leu1 ura4*
RM600	*h⁻ alp41-8-hph^r aur^r-GFP-atb2⁺ leu1 ura4*
RM628	*h⁺ alp41-8-hph^r tbc1-11-nat^r leu1 ura4 his2*
RM637	*h⁻ leu1 ura4 +pREP41-GFP-alp41⁺*
RM638	*h⁻ leu1 ura4 +pREP41-GFP-alp41-Q70L*
RM639	*h⁻ leu1 ura4 +pREP41-GFP-alp41-T47A*
RM641	*h⁻ tbc1⁺-3HA-hph^r leu1 ura4 +pREP41-GFP-alp41⁺*
RM643	*h⁻ tbc1⁺-3HA-hph^r leu1 ura4 +pREP41-GFP-alp41-Q70L*
RM644	*h⁻ tbc1⁺-3HA-hph^r leu1 ura4 +pREP41-GFP-alp41-T47A*
RM646	*h⁻ alp1⁺-3pk-hph^r leu1 ura4 +pREP41-GFP-alp41⁺*
RM650	*h⁻ tbc1⁺-3HA-nat^r alp1⁺-3pk-hph^r leu1 ura4 +pREP41-GFP-alp41⁺*
RM652	*h⁻ tbc1⁺-3HA-nat^r alp1⁺-3pk-hph^r leu1 ura4 +pREP41-GFP-alp41-Q70L*
RM653	*h⁻ tbc1⁺-3HA-nat^r alp1⁺-3pk-hph^r leu1 ura4 +pREP41-GFP-alp41-T47A*
RM717	*h⁻ leu1 ura4 +pREP1-alp41⁺*
RM719	*h⁻ leu1 ura4 +pREP1-alp41-Q70L*
RM721	*h⁻ leu1 ura4 +pREP1-alp41-T30N*
RM723	*h⁻ leu1 ura4 +pREP1-alp41-T47A*
PR6	*h⁻ alp11-924 leu1 ura4*

Table 7 Table of strains used in this study

2.20 Oligonucleotides used in this study

For mutagenesis of *tbc1*$^+$ for ts mutant isolation

RM04-Tbc1-5'

CGTTGTTGTTAAGGAATGGA

RM05-Tbc1-3'

GGGAATTGAGTGTTTTAGGT

For mutagenesis of *alp41*$^+$ for ts mutant isolation

RM11-Alp41-5'

CCCTGTTGCATGGTATGATG

RM12-Alp41-3'

TCTGGAAGTACATAGTCAGC

C-terminal tagging of *tbc1*$^+$

RM35 - tbc1 CtagF

AGCATCCTATTTTGGATTTTACTTGGGCACGCTCTGACCCGTCTCCACATTTT

CGTATCACTAGTGACCTTTTTGACGCTCGGATCCCCGGGTTAATTAA

RM36 - tbc1 CtagR

GAAACAAGGAATCTCAAAGGATTTACTGATATAATCGACTTGGTGGTAAGA

TGGATGGATGACATGAATGATTAGAAAGGGAATTCGAGCTCGTTTAAAC

C-terminal tagging of *alp41*$^+$

RM37-Alp41-CtagF

TAACGGGCCTTAATATCAAAGACGCGATAAGCTGGCTTGCTAATGATCTAA

AGGAGATTAAGTTGGGAACTATTGATTATCGGATCCCCGGGTTAATTAA

RM38-Alp41-CtagR

AGACCTGTAAGTGATCTTTATTAATGAGAAGCCTAAATAACAATATTTTAGG

AAACACATGACAAGCTATTTAATTCGACGAATTCGAGCTCGTTTAAAC

C-terminal tagging of *alp1*$^+$

RM39-Alp1-CtagF

CAGTATCTCAAAACGCAACTTTTGTTAAACAGCTAAGGAATATAATACAGA
AACAAATAGATAAACTGATAGCTGATCGACGGATCCCCGGGTTAATTAA
RM40-Alp1-CtagR
GTGTTCCTTTTATGGACATCAATTTAGTACTACATAAGCACGAACTGTTTTG
GCTAAAAATTTGAGATTATTCACCAGATGAATTCGAGCTCGTTTAAAC

C-terminal tagging of *alp21*$^{+}$

RM41-Alp21-CtagF
GAGACGACCAAAAGCGTCTCTTTGAACTCCCTTTTACTTGTACTTTTATCGA
TGTATATGCAAAGGAAAGTGGAAACGTCCGGATCCCCGGGTTAATTAA
RM42-Alp21-CtagR
TTAATAATTTTATAATTGTGTCGAACCGATTAAATAACTTAGAGGCACTTTT
CATATATGGTATATACATGGAATTAGTAGAATTCGAGCTCGTTTAAAC

N-terminal tagging of *tbc1*$^{+}$

RM43 Tbc1-N-tag F
GATCATTGAACACAGCATAACGTACTGTGATTTAATTTTGCATATATAACGG
GTGTTTTAGTTCTAATTTAAAAGGAAAAGAATTCGAGCTCGTTTAAAC
RM44 Tbc1-N-tag R
AACAGACCTTTCGATATGAACGAAATTGCAGATGTAAATAAACCCATACCT
TTTCTCAATTCGACGAACTTTTCAGACATTTTGTATAGTTCATCCATGC

N-terminal tagging of *alp41*$^{+}$

RM46 alp41-N-tag F
TTAAGCCCTTGTTGAGTAACGCAATGCAAGGCAAATTCATCGCATATTTTCT
TATTTCTTGGTTACTCTACTATTGAGAAGAATTCGAGCTCGTTTAAAC
RM47 alp41-N-tag R
TTTGAATCATCTTACAGTAACAAAACCCTGACTTCTCGTTCCTTTAGCTTTTG
CTGTCTCAAAATAGTCAATAATCCCATTTTGTATAGTTCATCCATGC

Sequencing of *tbc1* mutants

RM20-CofC-seq-1: TGGAATATTATCATGAGGCAT

RM21-CofC-seq-2: ATAATTTTCATTTCAAGGCAC
RM22-CofC-seq-3: TCTGAAAAGTTCGTCGAATT
RM23-CofC-seq-4: TAGATTTGACACGAAGGCTT
RM24-CofC-seq-5: ATAACGCTACAAAATGCAAC
RM25-CofC-seq-6: GCCCTTCTTTTGATTGATTA

Sequencing of *alp41* mutants
RM26-Alp41-seq-1: AAGTTGATAGCTTAAGCCCTT
RM27-Alp41-seq-2: TGTTGAACGAGGATGTAAGTA
RM28-Alp41-seq-3: AAATGTGAATTATCTTAACATGC
RM29-Alp41-seq-4: ATCCGAGTAATCGTAAGAATC

For expression of recombinant Tbc1 protein
RM32 Tbc1 prot- exp-5' 2
AAAGAATTCAATTTCTTACCAAATTATATAAATCC
RM33 Tbc1 prot-exp-3' 2
AAACTCGAGTTGGTGACACGATAC

For expression of recombinant Alp41 protein
RM13-Alp41-protexp-5'
AAAGAATTCATGGGATTATTGACTATT
RM14-Alp41-protexp-3'
AAACTCGAGTTAATAATCAATAGTTCC

Mutagenesis of Alp41
SDRM Q70L
GGGGACATTGGGGGGCTGAAAACGCTA
SDRM Q70L comp
TAGCGTTTTCAGCCCCCCAATGTCCCC

SDRM T30N
GGGGGTTGGATAATGCAGGTAAAAACACAATTTTGAAGTGCC

SDRM T30N comp

GGCACTTCAAAATTGTGTTTTTACCTGCATTATCCAACCCCC

SDRM T47A

GAAGTTTCGCCTGCCTTTGGCTTTCAAAATTCGAACGC

SDRM T47A comp

GCGTTCGAATTTGAAAGCCAAAGGCAGGCGAAACTTC

Chapter 3. Isolation of temperature sensitive mutants of *tbc1*

3.1 *S. pombe* Tbc1 is the orthologue of human cofactor C

Having picked up a candidate for the fission yeast homologue of tubulin binding cofactor C from the previously mentioned screen (Asakawa, 2005), I first confirmed that SPAC328.08c was indeed the orthologue by a range of biochemical, genetic and sequence analysis techniques. Once it had been confirmed, we decided to name the gene '*tbc1*', tubulin binding cofactor c-1, which is the name used throughout this study. In order to identify the function of Tbc1, I isolated temperature sensitive mutants of this essential gene and observed its phenotype. Deducing from the suggestion that it plays a role in the tubulin folding pathway, I also studied the microtubule phenotypes in these mutants.

3.1.1 There are sequence similarities between Tbc1 and the human homologues

First, a sequence comparison was carried out in order to determine if the candidate was conserved with the human cofactor C. Fig 3.1 shows the alignment between Tbc1 and the cofactor C orthologues in various organisms including *Drosophila melanogaster* and the budding yeast *Saccharomyces cerevisiae*. Regions of conservation can be seen throughout the protein, spanning from the N-terminus to the C-terminus. There are specific regions where the sequences are more conserved between the yeasts, however many of the regions that are conserved between the human and fly sequence are also conserved in the fission yeast Tbc1. The region of homology is also highly concentrated in the C-terminus of the protein, where the characteristic CARP domain is found in the human cofactor C.

Moreover, Fig 3.2 shows the sequence homology between the fission yeast Tbc1 and the 3 human related proteins – cofactor C, RP2 and TBCCD1. Tbc1 shares 24% identity with human cofactor C, 31% identity with RP2 and 30% with TBCCD1. As introduced

earlier in Chap 1.9, the three human proteins share a common region called the TBCC domain. This region is indeed conserved within Tbc1, as well as the C-terminus coiled coil domain. In addition, we found in its sequence the conserved Arginine finger – a feature shared by both TBCC and RP2 that is crucial for GAP activity. The Arginine finger is labelled in blue. This arginine finger and its surrounding regions are thought to be essential for GAP activity, and therefore the conservation of this region allowed me to speculate that there may be a similar function in Tbc1. This will be pursued later in this study.

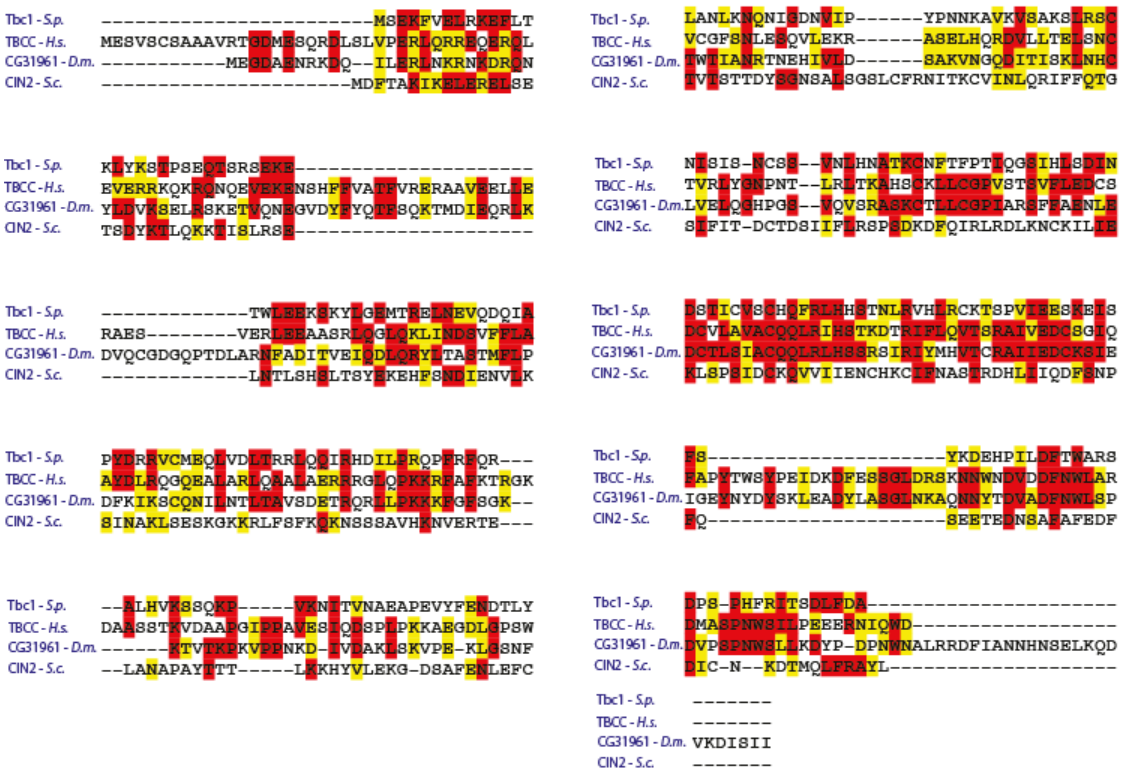

Figure 3.1 Sequence alignment of Tbc1 and its homologues in different organisms

The genome sequence of Tbc1 and its homologues in *H. sapiens*, *D. melanogaster* and *S. cerevisiae* were aligned using the ClustalW2 program as a base and then adjusted by hand. Residues marked in red show exact conservation, while yellow marks the residues with similar amino acid properties.

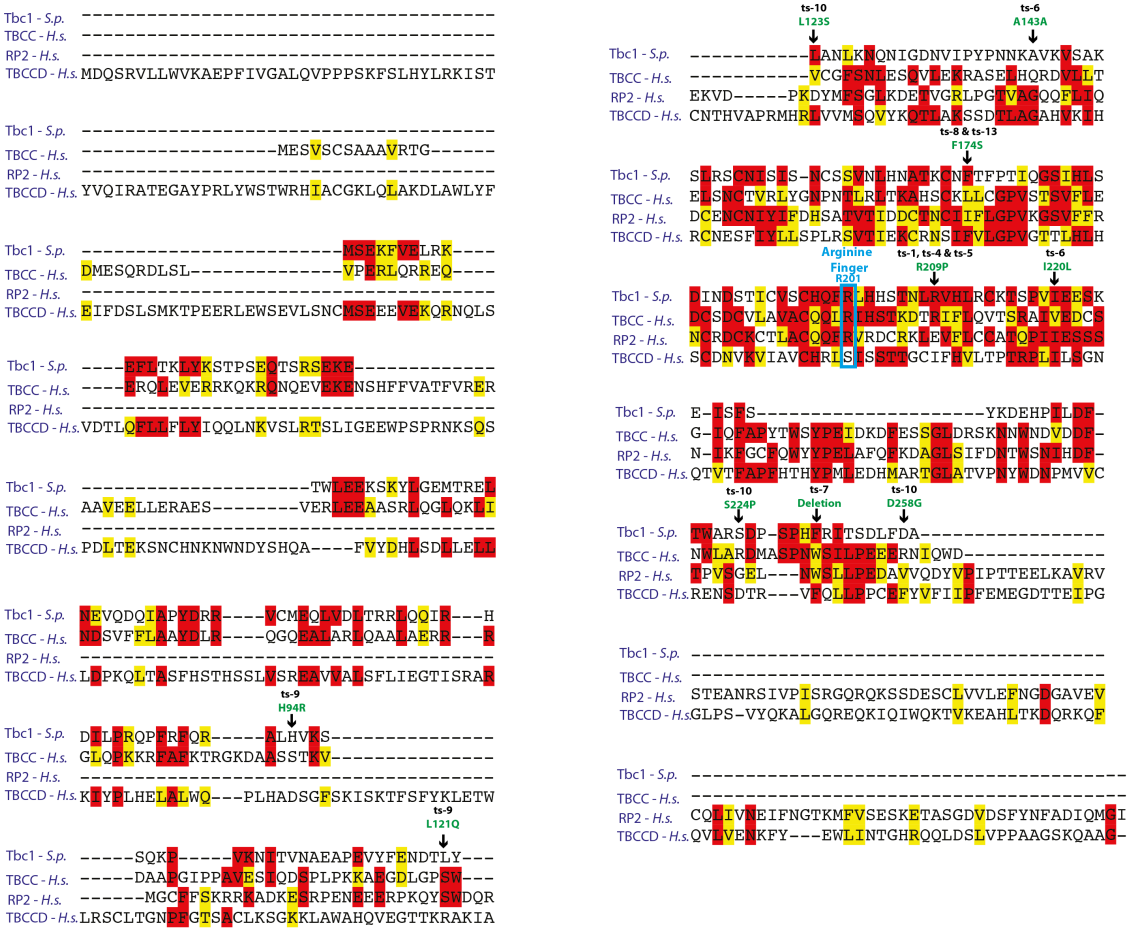

Figure 3.2 Sequence alignment of Tbc1 and its human homologues

The genome sequence of *S. pombe* Tbc1 was aligned with its human orthologues TBCC (cofactor C), RP2 and TBCCD using ClustalW2 as a base and then adjusted by hand. The blue label marks the R201 Arginine finger – a crucial motif in Cofactor C and RP2 that gives it its characteristic GAP activity. Residues marked with red show exact conservation, while yellow marks the residues with similar amino acid properties. Mutations of the temperature sensitive mutants isolated (see Chap.3.3) are indicated in green.

3.1.2 Tbc1 interacts with the proteins in the supercomplex

The high sequence conservation and the similarities in the domain structure allowed me to hypothesise with confidence that Tbc1 was indeed the fission yeast homologue of human tubulin cofactor C. To confirm this functionally, I assessed if it was able to do the most important function of tubulin cofactor C – to form a complex with Alp1 and Alp21 – the yeast homologues of cofactor D and E, respectively. The three cofactors form a supercomplex at the final stage of the pathway, where they bring together the α- and β- tubulin monomers to form the heterodimer (see Fig.1.6). The orthologue of cofactor C would therefore be expected to interact with the other two cofactors. I tested this by immuno-precipitation (IP), using strains in which Alp21 was tagged at its C-terminus with 3FLAG under the control of its own promoter. Tbc1 was similarly tagged with 3HA and Alp1 with 3pk. The protein was extracted from the triple tagged strain, along with two control strains (a single tagged strain and a double tagged strain – see figure for more details) and incubated with beads coupled with antibody for 3pk or FLAG. Fig. 3.3a shows that Alp21-3Flag and Tbc1-3HA both co-immuno-precipiated with Alp1-3PK. In extracts where Alp21 and Tbc1 were present but untagged, no signal was detected, confirming the specificity of the interactions. This not only allowed us to confirm that Alp21 and Alp1 were able to interact, but also that Tbc1 was able to interact with Alp1. To confirm that Tbc1 was also able to interact with Alp21, the reciprocal IP was carried out where both Alp1-3pk and Tbc1-3HA co-immuno-precipitated with Alp21-3FLAG. Fig. 3.3b shows clear bands for membranes blotted with both HA and 3pk antibodies. In conclusion, fission yeast Tbc1 was able to interact with both Alp1 and Alp21, therefore confirming that it is involved in the tubulin folding pathway and that it had the ability to form the supercomplex at the final stage.

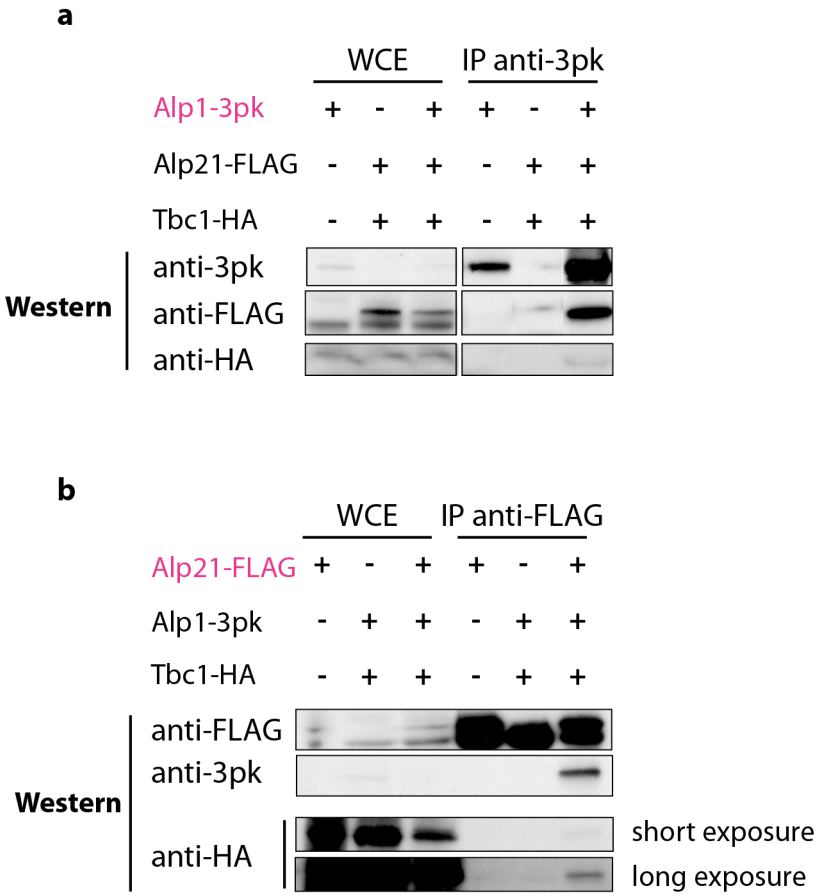

Figure 3.3 Tbc1 and its interaction with Alp21 and Alp1.

Reciprocal co-IPs between Alp1-3PK, Alp21-3Flag and Tbc1-3HA. (a) immunoblot from IP against Pk. (b) immunoblot from IP against FLAG. 2 different exposures are shown for panel (b) for clarity. In both blots, the first lane shows the single tagged strain and the second lane the double tagged strain. The final lanes on the far right show the result from the triple tagged strain. 5 mg of protein was used for each IP. WCE (whole cell extract), 0.01% of IP, 30µg.

3.1.3 Tbc1 cannot be tagged on the N-terminus

In order to observe the localisation of Tbc1, I tagged it at the N-terminus with GFP using pFA6a-*nmt1-GFP*. This *nmt* promoter series allows conditional overexpression of the tagged gene of interest by altering the growth conditions – addition of thiamine to the growth media allows surpression of the promoter turning it OFF, whereas the lack of thiamine turns the promoter ON and allows overexpression. Conventionally, the cells would be grown in minimal media plus thiamine conditions overnight, the thiamine washed out and then further incubated for over 16 hours for substantial overexpression to be seen. Initially I had attempted to tag Tbc1 with GFP using the endogenous promoter at the C-terminus, however no signal was seen under the microscope. Therefore I tried tagging the N-terminus, replacing the original promoter with a stronger *nmt* promoter.

Upon comparing the cell growth on plus and minus thiamine plates, we found no difference between the two conditions (Fig.3.4). In addition we saw completely normal growth under both conditions, comparable to the wild-type cell growth also shown on the plates. Equally, there was no signal detected upon observation under the microscope. This suggests either that the overexpression of Tbc1 was not toxic to the cell, or on the contrary that the construct was somehow not expressing GFP properly. Another possibility is that the *nmt1* promoter 'leaked' – to which it is prone. If the repression is not perfect there may have not been any difference between the two conditions, both in growth and signal observation.

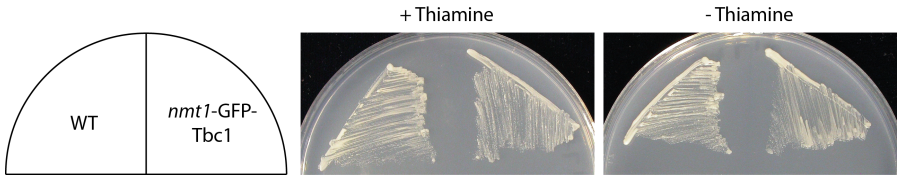

Figure 3.4 Overexpression of Tbc1 in wild-type cells

Wild-type cells expressing Tbc1 at its endogenous level (left) or over-expressing GFP-Tbc1 under the control of the strong *nmt1* promoter (right). Integrants were streaked onto EMM plates with (OFF) or without (ON) thiamine and incubated for 2 days at 27°C.

3.2 The tubulin cofactors and their stoichiometry

The interaction of Tbc1 with Alp1 and Alp21 was true to the *in vitro* model that had been derived from the human cofactors data. However what is not clear from the *in vitro* model is the precise stoichiometry of the cofactors – and therefore in what sort of balance the cofactors play their role. This was addressed by tagging Alp1, Alp21 and Tbc1 as well as G protein Alp41 (which will be discussed later in Chapter 4) with the same 3pk epitope at the C-terminus, which allowed each of the proteins to be produced under their native promoter. Whole cell extracts were prepared from each of these strains and the same amount (30 μg) ran on an SDS-PAGE gel. After separation by gel electrophoresis, the protein was transferred to membrane which was blotted for 3pk using an anti-V5 antibody (Clontech). Tubulin was used as a loading control and separately immuno-detected using an anti-α-tubulin antibody. In the experiment shown in Fig 3.5, two independent strains for each of the tagged cofactors were used. Each of the bands show a similar intensity apart from Alp1, which shows a fainter band compared to the other cofactors. This difference in intensity would suggest that quantitatively, there are fewer Alp1 molecules in the cell compared to the other cofactors that are in a 1:1 ratio with one another. This proposed that maybe there is a difference between Alp1 and the other cofactors in the fission yeast system. Previous results from our laboratory suggests that Alp1 plays a more major role than the other cofactors, as seen in the genetic interactions between the mutants of each of the cofactor proteins – Alp1 overexpression was able to rescue each of the other cofactor mutants. This difference in stoichiometry between Alp1 and the different cofactors, together with the genetic interaction data, strengthens the idea that the hierarchy of cofactors may be different in fission yeast (Fig.1.8).

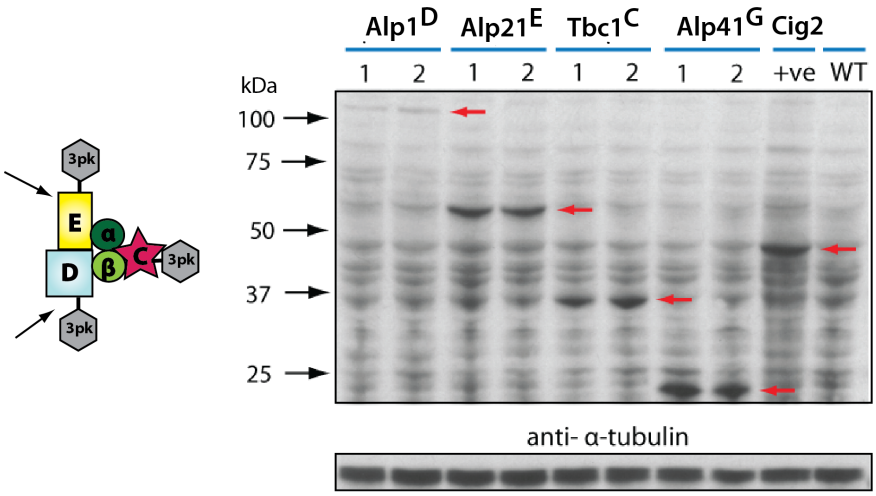

Figure 3.5 Stoichiometry of tubulin cofactors

30 μg of protein extract from cells with various tubulin cofactors tagged with 3pk was run on an SDS-PAGE gel and blotted with anti-V5 antibody. Red arrows show the band that corresponds to the protein size of the tagged protein (Alp1=126.5 kDa, Alp21=58.5 kDa, Tbc1=30.0 kDa, Alp41=21.2 kDa, positive control Cig2=42.4 kDa. Two independent strains labelled 1 and 2 were used for each protein. As a positive control, Cig2-3pk was used, and a wild-type strain for the negative control. α-tubulin is shown as a loading control.

3.3 Isolation of *tbc1* temperature sensitive mutants

Tbc1 is essential in fission yeast (Kim et al., 2010). Therefore it is not possible to construct a deletion mutant of this gene as the cells will be dead before observation. Therefore it is conventional in fission yeast biology to create temperature sensitive mutants – mutants that will grow normally and show the wild-type phenotype when incubated at the permissive temperature of 27°C, but a defective phenotype at the restrictive temperature of 36°C. Mutants are isolated by random mutagenesis, and selected upon drug resistance and temperature sensitivity. Fig.3.6 shows a schematic of the isolation procedure.

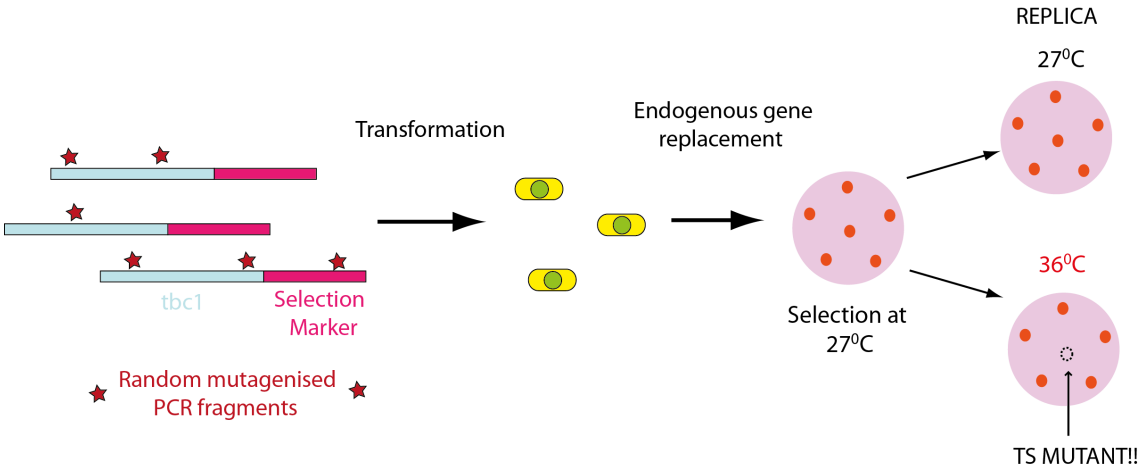

Figure 3.6 Temperature sensitive mutant isolation

The target gene was subjected to random mutagenesis by unbalanced PCR reaction. PCR fragments were then transformed into wild-type fission yeast cells for endogenous gene replacement to occur. Transformants were replica plated onto YE5S plates containing hygromycin and phloxine B, which were then incubated at the permissive temperature of 27°C or at the restrictive temperature of 36°C. The clones that grew on 27°C but did not on 36°C were picked and restreaked for further analysis.

3.4 Characterisation and analysis of *tbc1* temperature sensitive mutants

Three independent sets of screening were carried out, which allowed approximately 9000 colonies to be screened. In total, 11 candidate mutants were isolated for further investigation. In order to remove the mutants that could be showing temperature sensitivity due to additional extragenic mutations, these strains were all backcrossed with a wild-type strain. All candidates showed co-segregation of mutant phenotype with hygromycin resistance, indicating that the ts phenotype was due to the intragenic gene mutation in the *tbc1* locus.

The summary of the 11 isolated mutant strains are shown in Fig 3.9. Initially, the mutants were characterized and classified by temperature sensitivity, sensitivity to the anti-microtubule drug thiabendazole (TBZ), and cellular morphology.

3.4.1 Temperature sensitivity

First, temperature sensitivity was observed in more depth by the serial dilution spot test. This assay allows a detailed comparison to be made between the growth of mutant alleles at the various temperatures. Fig. 3.7 shows the 11 candidates spotted onto YE5S plates containing phloxine B, which stains dead cells bright red (see Materials and Methods). $5x10^4$ cells were spotted on the first lane, followed by four 10-fold dilutions. A control wild-type strain was also spotted in the same manner for comparison of growth. These plates were incubated at various temperatures ranging from 27°C to 36°C and observed three days later.

Although there was a variation in the degree of sensitivity, most of the strains did not grow well at 36°C. Alleles such as *tbc1-2, tbc1-3, tbc1-6, tbc1-7* and *tbc1-9* showed a milder sensitivity at the slightly lower temperature of 34°C, with *tbc1-2* and *tbc1-6* also showing a less ts red colony formation at 36°C. Upon observation under the light microscope, the morphology of these mutants were all similar – with the characteristic bent and branched shape also seen in the other cofactor mutants (Hirata et al., 1998;

Radcliffe et al., 1998; Radcliffe et al., 1999; Radcliffe and Toda, 2000). However the degree of the phenotype also varied, similar to the temperature sensitivity. The two results correlated, suggesting that the more severe the temperature sensitivity, the more severe the morphological phenotype (See also Fig.3.9).

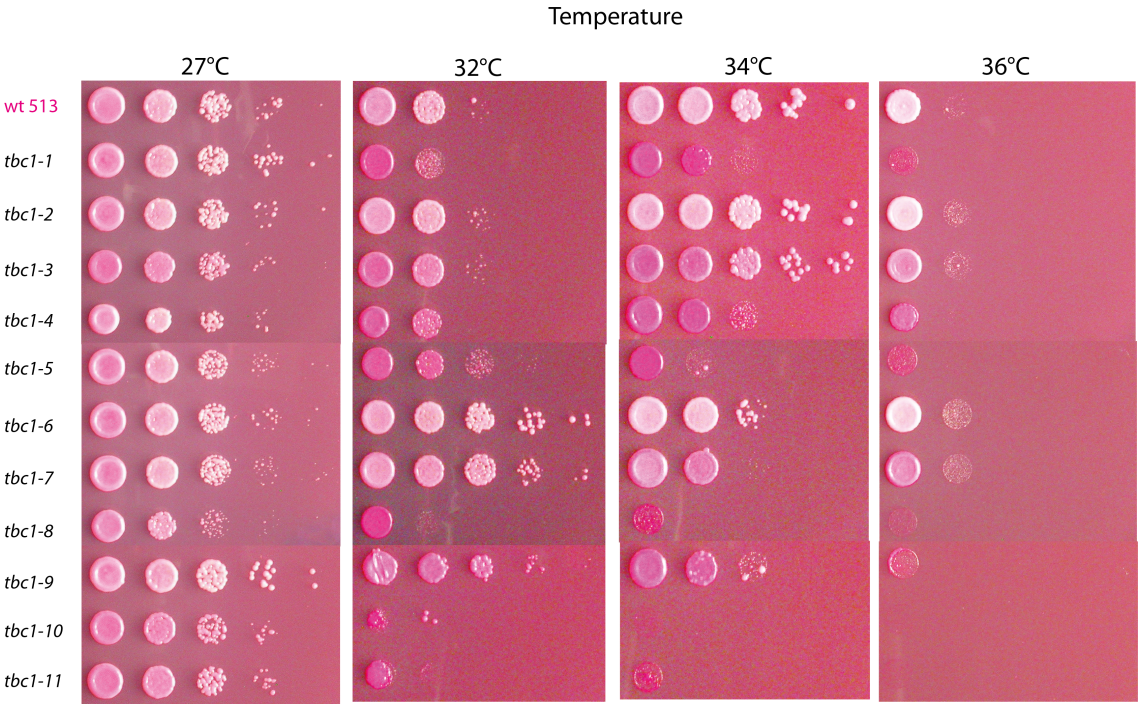

Figure 3.7 Serial dilution spot test for temperature sensitivity for all *tbc1* ts candidates

The 11 candidates isolated in the screening of 9000 clones were tested for temperature sensitivity by spot test. All plates were made with rich YE5S media with added phloxine B. Plates were incubated for 3 days in the temperatures shown. Pink colour indicates normal growth, dark red colour indicates cell death and therefore temperature sensitivity.

3.4.2 Thiabendazole sensitivity

A spot test was also carried out to compare TBZ sensitivity. TBZ, or thiabendazole, is a microtubule depolymerising agent commonly used to determine microtubule defects in yeast. Mutants usually associated with microtubule function show an increased sensitivity or resistance to this drug compared to wild-type cells. YE5S plates with increasing concentrations of TBZ were used, with Fig.3.8 showing plates with 10 or 15 μg/ml TBZ, which were the concentrations where the mutants showed a stark phenotype. These plates were incubated at 27°C for 2 days. The mutant candidates showed varying sensitivity to the drug (see also Fig.3.9). As expected, the sensitivity of the mutant to TBZ tended to correlate with the temperature sensitivity of the mutants. *tbc1-2, tbc1-3* and *tbc1-6* which showed milder temperature sensitivity also showed more resistance to TBZ.

Taken together, the temperature and TBZ sensitivity shows that Tbc1 may indeed play a significant role in the tubulin cofactor pathway and therefore microtubule function. The similarity of phenotype to the other cofactor pathway mutants also suggest that there may be some interplay between Tbc1 and the other cofactors.

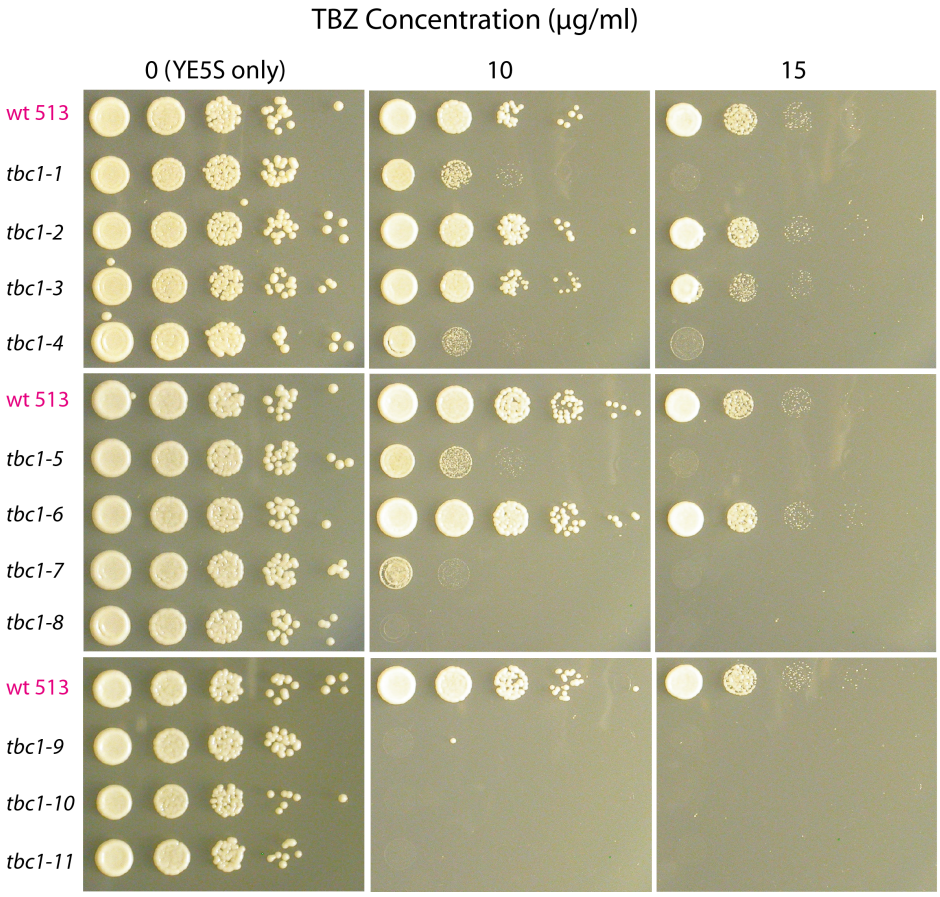

Figure 3.8 Serial dilution spot test for TBZ sensitivity for all *tbc1* ts candidates

All ts candidates were spotted onto YE5S plates containing 10 or 15 µg/ml of TBZ. The plates were incubated at 27°C for 2 days. Wild-type *tbc1* strain was also spotted to enable comparison.

3.4.3 Sequencing of *tbc1* mutants

In order to determine which domain of the protein may be affecting the temperature or TBZ sensitivity, the candidate mutants were sequenced. The known domains of human cofactor C include a N-terminal spectrin central repeat-like coiled coil region and a C-terminal RP2/CAP-like TBCC domain that contains the conserved GAP region (Grynberg et al., 2003). The human orthologues cofactor C, RP2 and TBCCD1 all contain the so called TBCC domain, which is also conserved in Tbc1. Fig.3.9 shows the mutations revealed by sequencing, which are also highlighted in Fig.3.2 to show conservation of mutated residues. Notably, a high proportion of the mutants only had single point mutations within the gene, indicating how easily the *tbc1* gene would be affected by single mutations and how severe the result of these can be. It was also striking that there were no mutations found in the N-terminal for the 11 alleles isolated. All the mutations were seen either after the coiled-coil region, either in the unidentified region or in the TBCC domain which contains the conserved GAP region. This suggests that either the N-terminus is difficult to mutate because it is crucial for function, or that if there were any mutations it would not result in such severe temperature sensitivity. It is unclear which of these two reasons result in the lack of N-terminal mutants, but it does show that the C-terminal TBCC domain is highly likely to affect the sensitivity of these mutants.

Interestingly, three of the mutants - *tbc1-1*, *tbc1-4* and *tbc1-5*, contained exactly the same mutation at R209P. As a result, these mutants similarly showed high sensitivity to both temperature and TBZ. This arginine may be significant because of its proximity to the arginine finger – the residue that is crucial for the activity of cofactor C and RP2 as a GTPase activating protein (GAP). The region around this domain is crucial for GAP function – in which the arginine finger 'points' into the GTP binding pocket of the G protein. Defects in this area would result in the possible loss of GAP function as well as defective microtubule function.

tbc1-8 and *tbc1-11* also carry the same mutation at F174S and have similar phenotypes. These two strains showed both high sensitivity to temperature and TBZ, as well as

severe morphology defects. This mutation was in the middle of the RP2-CAP-like TBCC domain. Much like the arginine finger, it is predicted that defects in this motif may disrupt GAP function of this protein.

tbc1-9 and *tbc1-10* both carried multiple mutations, H94R and L121Q, and L123S, S244P and D258G, respectively. Taking into account the previous data, it would be likely that the mutations that are in the RP2-CAP like TBCC domain would be causing the temperature sensitivity in these mutants.

The two alleles *tbc1-2* and *tbc1-3* were found to contain no mutations after sequencing and consequently eliminated from the mutant strains after backcrossing.

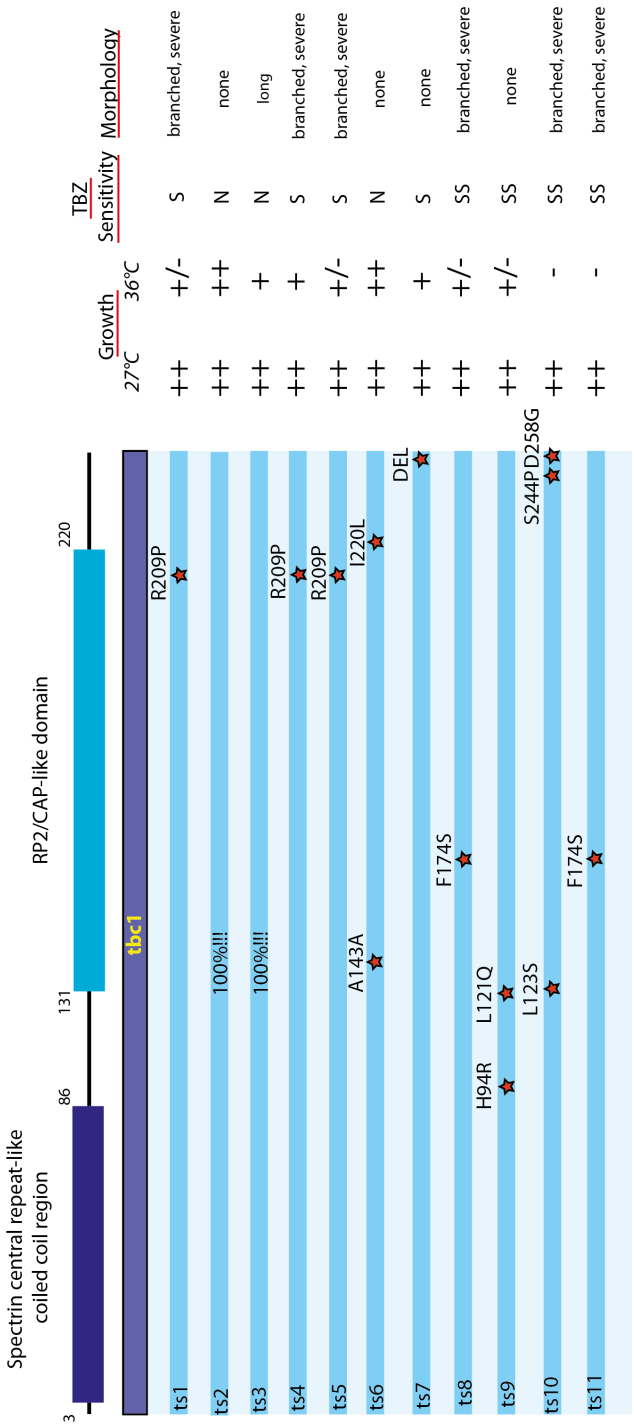

Figure 3.9 Summary of characteristics of *tbc1* ts candidates

The eleven ts mutant candidates were sequenced and the mutation sites shown in the scheme. The known domains of Tbc1 are shown and labelled. Growth at 27°C and 36°C are indicated – '-' indicates no growth at all, '+/-' indicates moderate growth, '+' indicates normal growth and '++' shows significant growth. TBZ sensitivity is described as 'S' for sensitive, 'SS' for significantly sensitive, and 'N' for normal. The morphology observed for cells of each of the candidates is listed on the far right.

3.4.4 Growth curve

The above data showing growth defects in mutants were all observed on plates. In order to further analyse how and when the growth defects appear, I plotted a growth curve which followed their growth in media over several hours. Cells were subcultured in YE5S media overnight and split into two flasks diluted to the early exponential phase concentration of $2x10^6$ cells ml^{-1}. The cell concentration was measured every hour for 6 hours. The results were then plotted onto a graph as shown in Fig.3.10 (upper panel). The wild-type cells continued to increase in number, and in 6 hours the concentration increased to around $1.2x10^7$ cells ml^{-1}. *tbc1-1* and *tbc1-11* however showed slower rate of growth from around 4 hours, with the end cell number being lower than $1.0x10^7$. On the other hand *tbc1-9*, which showed only moderate temperature sensitivity, continued to increase in cell number similar to the wild-type strain.

Many microtubule mutants that show a mitotic phenotype will start to show a decrease in growth in one or two cell cycles, so it was interesting that the *tbc1* mutants do not seem to show a growth defect for the majority of the time span tested. Therefore, an independent experiment was carried out to assess the change in cell concentration for a longer period of time. The mutant *tbc1-11* was used to repeat this experiment as it showed the severest temperature sensitivity. The lower panel in Fig.3.10 shows that when monitored up to 8 hours, the cells started to show a severe phenotype and the increase in cell concentration became slower. This result was slightly different from other typical microtubule mutants, as the growth defect appeared much later in *tbc1* mutants. Growth seemed to be normal for up to 4 hours, and only when we incubated it for longer and up to 8 hours was there a stark difference. This could be a key to elucidating the nature of Tbc1 and how it regulates the microtubules within the cell.

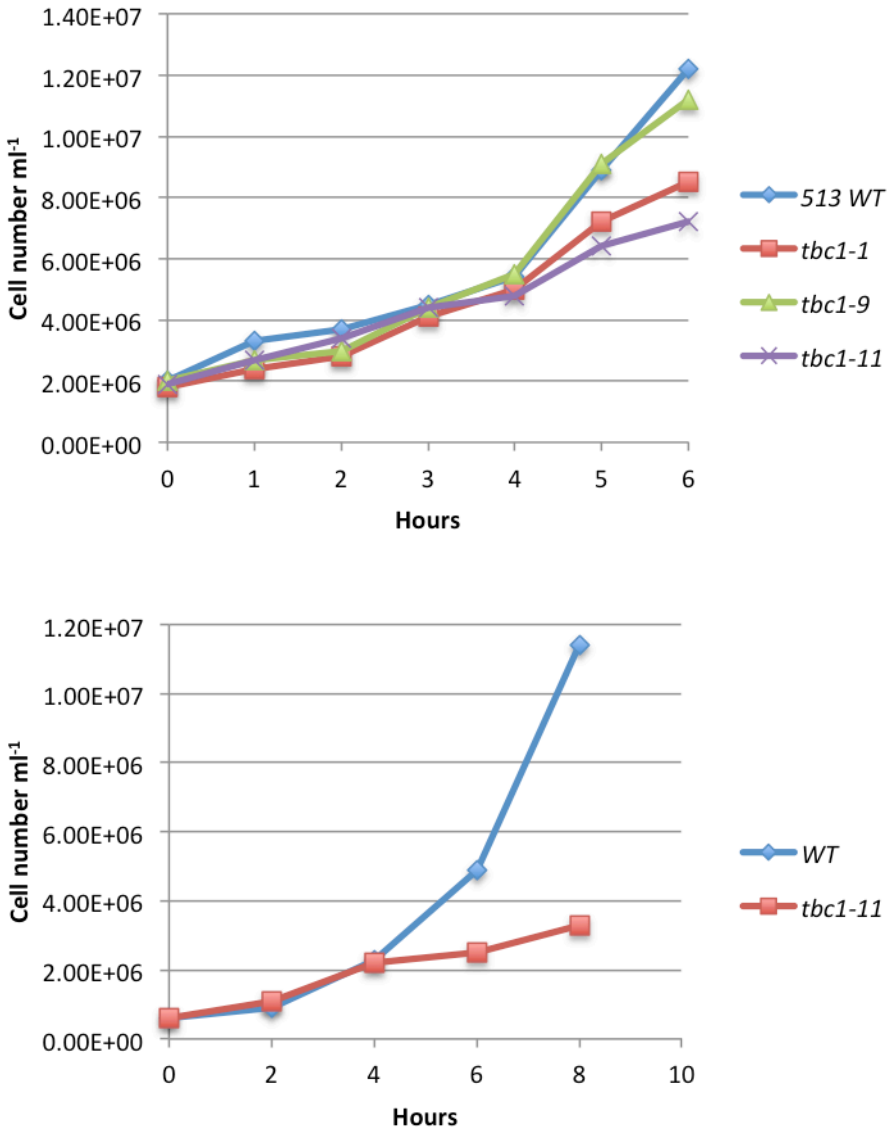

Figure 3.10 Growth curves for *tbc1* ts mutants

The number of cells per ml of each of the chosen *tbc1* ts mutants were counted and monitored over time. The upper panel shows 3 ts mutants and the wild-type strain plotted over the course of 6 hours after the shift to restrictive temperature. 0 hours indicates moment of shift-up. Lower panel shows the repeated experiment where *tbc1-11* and the wild-type strain were incubated for a longer time course up to 8 hours. Data plotted are representative means from 3 independent experiments.

3.4.5 Microtubule phenotypes of *tbc1* mutants

To confirm that Tbc1 has a role in the tubulin folding cofactor pathway, the microtubule phenotypes of the ts mutants were observed. The mutants were crossed with a strain with α-tubulin Atb2 tagged with GFP. Conventionally due to its ease of use and visualisation, we first attempted to cross it with a strain that expressed GFP-Atb2 under the endogenous promoter, but this proved to be unsuccessful as the isolated strain was severely sick even at the permissive temperature. Therefore a different strain containing SV40-GFP-Atb2, which expresses the GFP fusion under a viral promoter (Jones et al., 1988; Pardo and Nurse, 2005), was used. Throughout this study I found great difficulty in tagging Tbc1 with various tags, this case being an example, and even if the tagging was successful it was difficult to cross these strains to introduce any other tags. Therefore we could not use any other fluorescent tags to observe other cellular structures such as the spindle pole body. Using the SV40-GFP-Atb2 however, allowed the strain to be used for observation of microtubules in the mutant as it showed no defects at the permissive temperature.

Consistent with the growth curve, the morphology phenotype of *tbc1-11* also only appeared after 6 hours of incubation at 36°C. The cells were incubated for a further 2 hours until 8 hours, to enable a higher percentage of the cells to show a stronger phenotype. The cells were taken and observed under the fluorescence microscope for the GFP signal - Fig.3.11 shows both wild-type and mutant cells at the permissive and restrictive temperature after 8 hours. Wild-type microtubules are seen for the wild-type strain, both at 27°C and 36°C. In contrast, *tbc1-11* shows a clear loss of microtubules at 36°C. Morphologically, the cells looked elongated, branched, or significantly shorter. Both these phenotypes were similar to those of the other tubulin cofactor mutants. It is interesting to see that even at 27°C, the microtubules look somewhat weaker and slightly broken compared to the wild-type cells, suggesting that the microtubules are already fragile. This suggests that *tbc1* mutations already render the microtubule structures highly unstable. Upon quantification, I found that nearly 75% of the cells showed complete microtubule loss, and a further 18% showing no microtubules but bright GFP dots within the cell as shown in (b). The only signals of GFP-Atb2 seen

were that of some very bright dots within the cell. These dots often located close to the nucleus – and are thought to be where the microtubules tried to nucleate, but failed to do so and resulted in a local accumulation of tubulin. The rest of the cells retained their microtubules, although they appeared shorter than the wild-type microtubules. This lack of microtubules can be explained due to the defects in tubulin folding pathway – there is a reduced number of functional heterodimers folded for elongation of the microtubules. The TBZ sensitivity of *tbc1-11* also correlates well with this phenotype (Fig.3.8, 3.9), as defects in microtubule structure commonly lead to sensitivity for the drug.

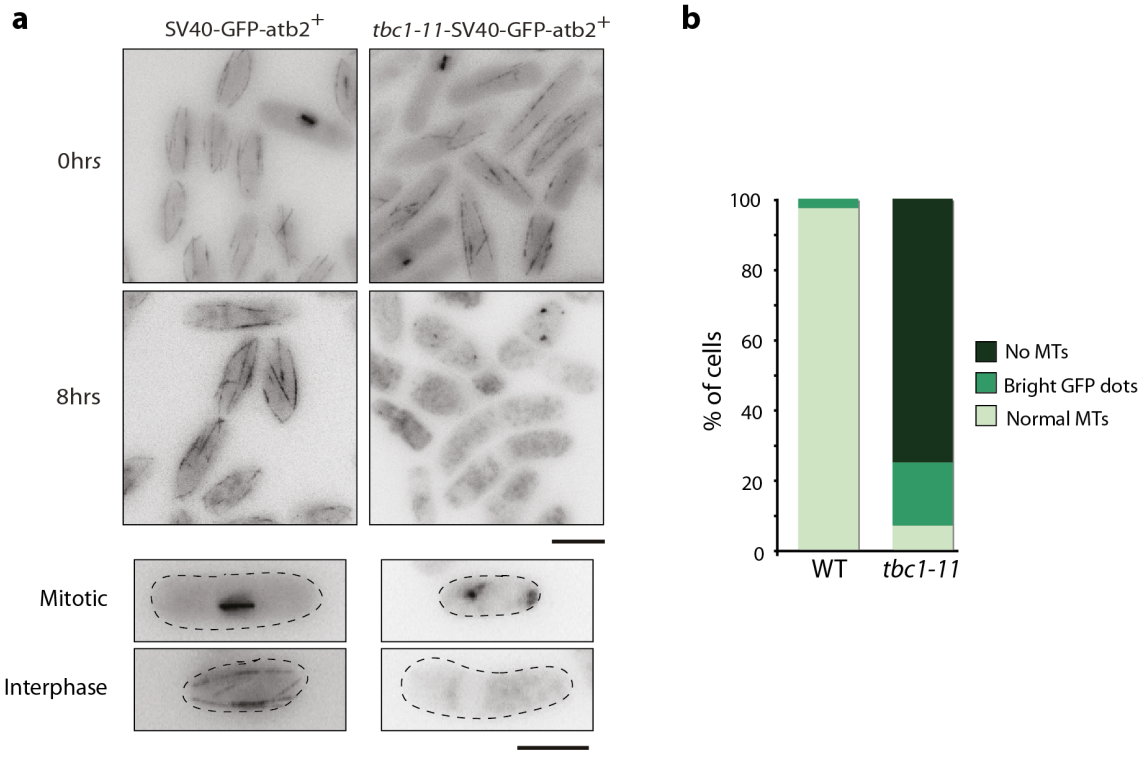

Figure 3.11 Microtubule phenotypes of *tbc1-11*

(a) *tbc1-11* with GFP labelled Atb2 was incubated at 36°C for 8 hours and observed under the fluorescence microscope. Fifteen sections were taken along the Z-axis at 0.2 mm intervals. These images were further processed using deconvolution and then projected into a single projection with the maximum intensity algorithm. (b) shows the quantification of 300 cells each for both wildtype and mutant strain. Bar = 5 μm.

3.4.6 Mitochondria distribution is defective in *tbc1-11*

It was clear from the above result that there were severe microtubule defects within the mutant *tbc1-11*. In order to further analyse the effects of this dysfunction within *tbc1-11*, Mitotracker was used to stain the actively respiring mitochondrion within the cell. In fission yeast, mitochondria are distributed by microtubules and therefore they are usually seen to roughly co-localise with them (Yaffe et al., 1996) (Fig.3.12a). Fig 3.12b shows that mitochondria in *tbc1-11* were still stained after 8 hours incubation at 36°C, suggesting that these organelles are still functional. Their morphology and distribution however were largely impaired. *tbc1-11* mitochondria appeared fragmented, compared to the long filamentous organisation see in wild-type cells. Clusters of mitochondria also accumulated at the tips of the cells, instead of spanning across their length. This further confirms the microtubule defects within the cells.

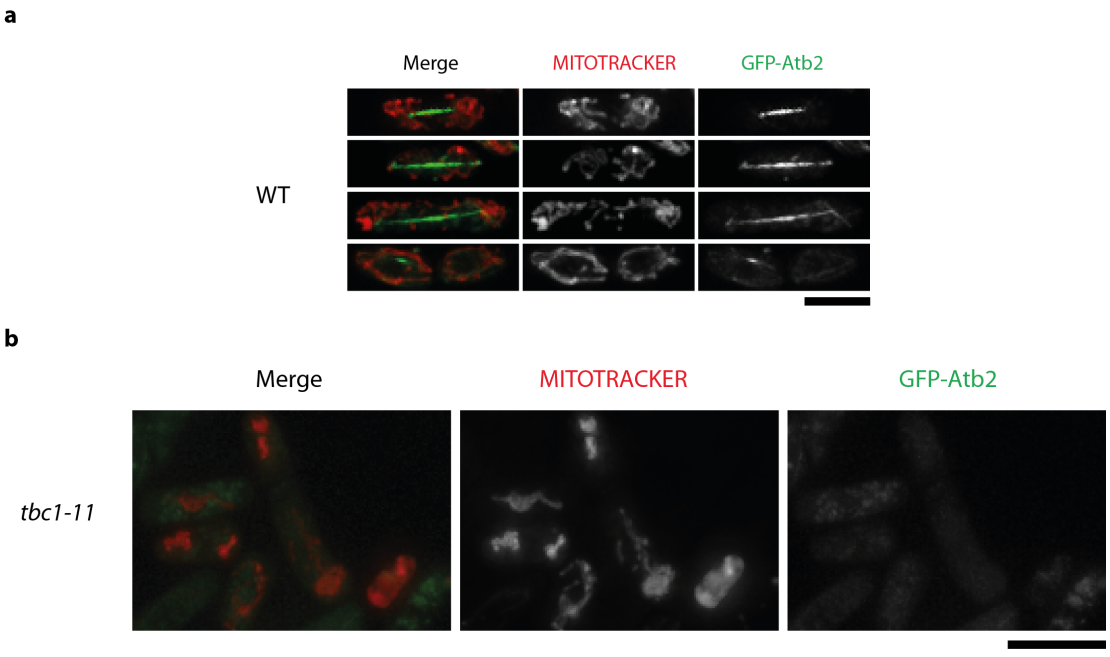

Figure 3.12 Mitotracker staining of *tbc1-11*

tbc1-11 and the wild-type strain were incubated for 8 hours at 36°C and stained with Mitotracker. The cells were observed under the fluorescence microscope and the GFP and RFP channels used to take images. The images were deconvoluted and projected as previously described. (a) single wild-type cells imaged at different points within the cell cycle are shown. (b) *tbc1-11* shows defective distribution of mitochondria as well as lack of microtubules.

3.5 Rescue of *tbc1-11* mutant with human cofactor C and RP2

To observe if Tbc1 could be rescued by human cofactor C or RP2, overexpression plasmids (gifted from Prof Mike Cheetham) of each were transformed into the mutant *tbc1-11* to determine if there was any rescue of the temperature sensitivity of the mutant. Although high conservation of the domains are seen as previously described, the human homologues were not able to rescue the phenotypes as seen in spot test in Fig.3.13.

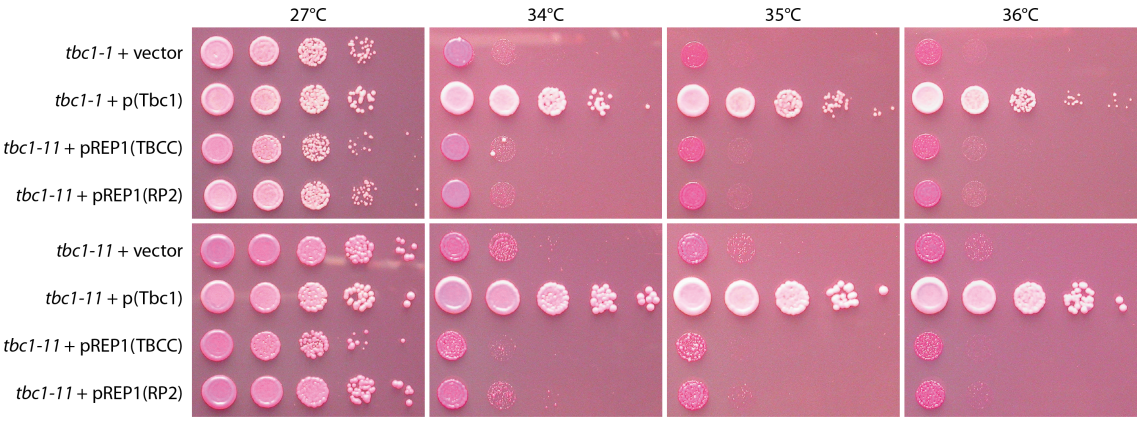

Figure 3.13 Human homologues of Tbc1 transformed into *tbc1* mutants

tbc1-1 and *tbc1-11* were transformed with overexpression vector pREP1 containing the human homologues cofactor C and RP2. They were also transformed with multicopy plasmids of fission yeast Tbc1 as a positive control and empty vector as a negative control. Each strain was spotted onto YE5S plates containing phloxine B. Plates were incubated at 27°C, 34°C, 35°C and 36°C for 3 days and images taken.

3.6 Discussion

The fission yeast homologue for tubulin folding cofactor C has been identified and named *tbc1*. This protein has been found to share the conserved domains with the human related proteins cofactor C, RP2 and TBCCD1, and furthermore shown conservation amongst other organisms. I have shown that it is able to interact with the

fission yeast homologues of cofactor D and cofactor E, proving that it is able to form the supercomplex that comes together at the end of the tubulin folding pathway.

The ts mutants isolated for *tbc1* showed a phenotype that was commonly seen for the other tubulin folding cofactor mutants. The mutant for the cofactor D homologue Alp1 also showed significant loss of microtubules together with the bent morphological phenotype (Hirata et al., 1998). The other cofactor homologues studied also showed this phenotype, which places *tbc1* in the cofactor pathway. However, the *tbc1* mutant phenotype appeared significantly later than the other cofactor mutants. This could be because Tbc1 only appears at the later stage of the cofactor pathway. A sufficient pool of tubulin that has gone through the pathway up until the stage of supercomplex formation may be available for the cell to consume for a few cell cycles before it is depleted and the phenotype starts to show. This may also explain the bright dots of GFP tubulin seen in the mutant cells – there is a sufficient amount of tubulin that accumulates at the point of nucleation but cannot elongate into functional microtubules because of the defect of the heterodimer release caused by defective Tbc1. Another possibility is that, depending on the effect of the mutation of my *tbc1-11* mutant, supercomplex formation may be still partly functional. If the ability to bind Alp1 and Alp21 are not lost in this mutant, heterodimers may still be folded. The true effect of the mutant, for example in its activity as a GAP (which will be discussed later in this study), may only appear later, causing this delayed effect.

The TBZ sensitivity of the *tbc1* mutants correlate with the microtubule defects seen within the cells, suggesting further the involvement of Tbc1 with microtubule regulation. Uneven mitochondria distribution also proved that the microtubules were dysfunctional, as mitochondria rely heavily on the microtubules for distribution and regulation.

Many of the randomly mutagenized mutants showed the same point mutation upon sequencing, and many of these point mutations lie in the C-terminus of the protein. This may address the fact that the C-terminus of Tbc1 is important for the function of this protein, probably as a GAP. The domain structure of Tbc1 remains unclear, but the structure of RP2 allows us to identify the important regions for the function of this protein as a GAP and as a microtubule binding protein. The C-terminus which contains

the TBCC domain, is clearly crucial for the fission yeast homologue Tbc1, which is also likely to be the reason why it is so difficult to tag Tbc1 at its C-terminus.

Considering the above results, I decided to study Tbc1 further and explore its possible roles as a GAP. The domain is clearly crucial for proper cell morphology as well as microtubule function, and its similarity to cofactor C and RP2 suggests that it has a G protein partner. In order to do this, I decided to carry out any consequent analysis on the mutant *tbc1-11*, this mutant contained its mutation close to the arginine that lies very close to the arginine finger which is crucial for GAP function. The mutant also had a very strong phenotype and was consistent with the other cofactor mutants, so it was the perfect mutant to investigate.

Chapter 4. Isolation of *alp41* temperature sensitive mutants

4.1 *S.pombe* Alp41 is the orthologue of human Arl2

Tbc1 is predicted to be a GTPase activating protein (GAP), similar to human RP2 and cofactor C. Upon searching for a G protein that could be the interactor of Tbc1, we identified fission yeast Alp41, the othologue of human Arl2.

Fig.4.1 shows the alignment between human Arl2, fission yeast Alp41, *D. melanogaster* Arf84S and human Arl3, which was carried out using Clustal W2 and then adjusted by hand. Much of the sequence is highly conserved amongst the species, with many amino acids having an exact match or if not related. The main domains of the protein are also conserved, notably the P-loop and the two switch regions which are the characteristic GTPase features of the Arl family of proteins.

Alp41 shares 55% identity with human Arl2 and 47% with human Arl3. This high sequence conservation suggests that not only are the Arl proteins very conserved between one another but they are also highly conserved amongst different species. The fact that there is only one orthologue in fission yeast of the G protein Alp41 and tubulin cofactor Tbc1 suggests multifunctionality of these proteins in fission yeast.

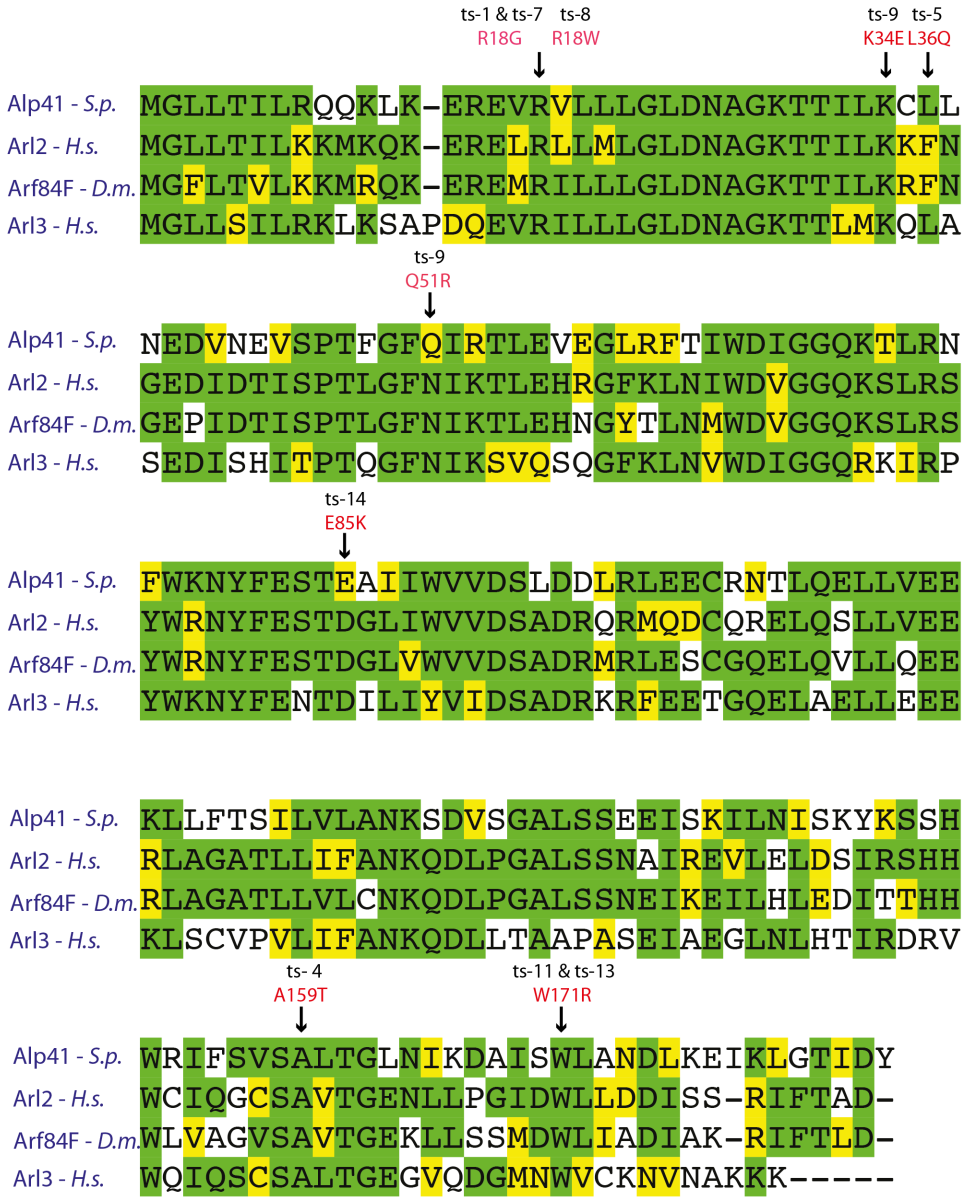

Figure 4.1 Sequence alignment of Alp41 and its orthologues in various organisms

The genome sequence of Alp41 and its orthologue in *H. sapiens* and *D. melanogaster* were aligned using the ClustalW2 program as a base and then adjusting by hand. Alignment also includes human Arl3, and related protein Arl2. Residues marked with green show exact conservation, while yellow marks the residues with related amino acid properties. Mutations of temperature sensitive mutants isolated (see Chap.4.3) are indicated in red.

4.2 Alp41 localises to the cytoplasm and nucleus

Alp41 was tagged at the N-terminus with GFP under the *nmt1* promoter using the *pFA6a-nmt1-GFP* plasmid. The colonies formed containing the integrant was streaked onto EMM plates with or without added thiamine to observe the growth when the promoter was off or on. As Fig.4.2a shows, there was no difference in growth after 2 days of incubation. This indicated that neither the overexpression of Alp41 nor the N-terminal tag was toxic to the cells.

To observe the localization of Alp41 within the cell, the strain was grown in plus thiamine conditions overnight, then washed and incubated under minus thiamine conditions for a further 18 hours and observed for GFP signal. This time there was a clear difference in signal between the cells grown in minus and plus thiamine, and a strong and bright signal seen. As shown in Fig.4.2b, there is both clear GFP signal in the cytoplasm, and a significantly stronger signal in the nucleus. This was observed throughout the cell cycle in both interphase and mitotic cells (lower panels). This ubiquitous localisation could be explained by the requirement of tubulin throughout the cell and throughout its life cycle. The nuclear signal could be due to the possible requirement of tubulin within the nucleus during mitosis. On the other hand, there is a tendency for cytoplasmic proteins to accumulate in the nucleus when overepressed, so it remains unclear if this is a specific signal for Alp41.

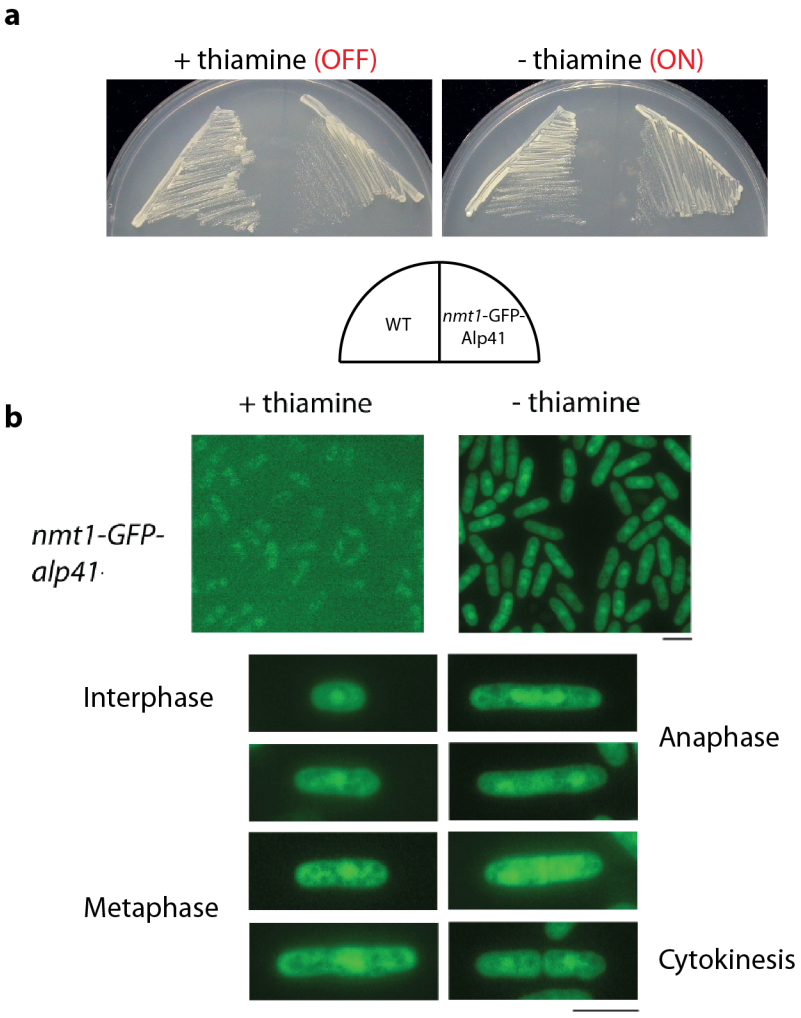

Figure 4.2 Overexpression of GFP-Alp41

(a) Cells expressing Alp41 under its own promoter (left) or over-expressing it under the control of the *nmt1* promoter (right), were streaked onto minimal medium with or without thiamine. (b) Localisation of GFP-Alp41 observed by wide field microscopy under repressed (+ thiamine) or repressed (-T) conditions. Upper panel shows a field of cells and the lower panel individual cells at various stages of the cell cycle under minus thiaine conditions. Bar = 5 μm.

4.3 Isolation and characterisation of *alp41* temperature sensitive mutants

By sequence analysis we have confirmed that Alp41 is indeed the fission yeast orthologue of Arl2, suggesting that the interacting G protein of Tbc1 may be Alp41. This interaction is investigated further in Chapter 5. Alp41 has been studied in fission yeast previously (Radcliffe et al., 2000b) but apart from its role in microtubule regulation it was not clear how it played a role in the tubulin folding pathway. Now that we had a possible interactor for this protein, we decided to create a mutant of it and study it together with the *tbc1* mutant.

Like Tbc1, Alp41 is essential for cell viability. Therefore temperature sensitive mutants were isolated by random mutagenesis with the same procedure as described in Chapter 3. Within 4 independent trials, 10,000 colonies were screened for temperature sensitivity. 14 colonies were picked up and further characterised.

4.3.1 Temperature sensitivity

The temperature sensitivity of each of the strains was tested by serial dilution spot test. Each ts candidate as well as a positive (wild-type) control was spotted onto each YE5S + phloxine B plate. Fig.4.3 shows plates incubated at 27°C, 32°C, 34°C and 36°C. A range of temperature sensitivity was seen amongst the strains, with some strains only showing a slight pink colour at the higher temperatures and others showing no growth. The severest sensitivity was seen in *alp41-4, alp41-7, alp41-8* and *alp41-14*. Generally the severity of these mutants were weaker compared to that of the *tbc1* ts mutants, with a varying range of sensitivity at the higher temperatures. *alp41-10, alp41-11, alp41-12* and *alp41-13* seemed to show a very weak phenotype at 36°C, with the colony growing with a light pink colour close to the wild-type strain (summarised in Fig.4.5).

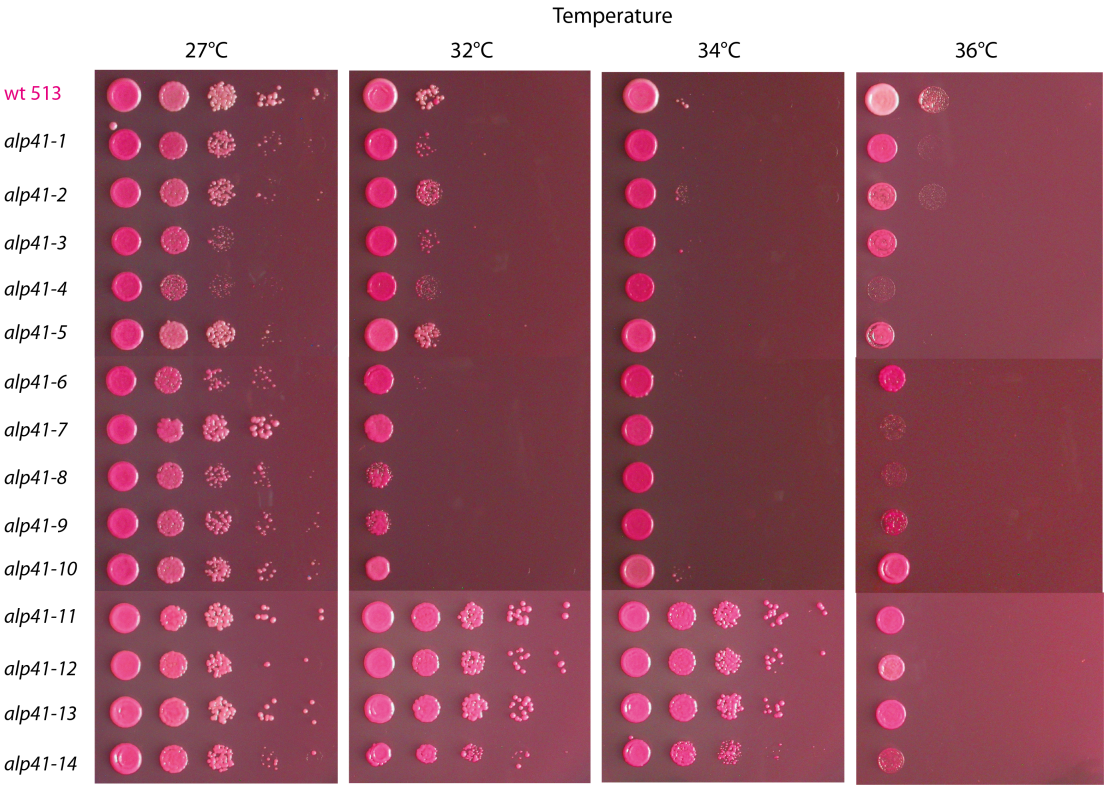

Figure 4.3 Serial dilution spot test for temperature sensitivity for all *alp41* ts candidates

The 14 candidates were tested for temperature sensitivity by spot test on rich YE5S media with added phloxine B. Plates were incubated for 3 days at the temperatures shown. Pink colour indicates normal growth, dark red colour indicates cell death. The degree of colour correlates to strength of temperature sensitivity.

4.3.2 Thiabendazole sensitivity

In addition to observing temperature sensitivity, TBZ (microtubule drug) sensitivity was also assessed with the serial dilution spot test. YE5S plates with increasing concentrations of TBZ were spotted with the mutant candidates and imaged after incubation at 27°C for 2 days (Fig.4.4). Compared to the wild type strain, the mutants showed varied sensitivity to the drug, although no strains grew at the highest concentration of 20 μg/ml (data not shown).

Consistent with temperature sensitivity, *alp41-4* and *alp41-14* showed very high sensitivity, with very little growth at 10 μg/ml. *alp41-9* and *alp41-12* showed high sensitivity to TBZ although they were not as sensitive to the drug as they were to temperature. Some mutants such as *alp41-1*, *alp41-2*, *alp41-5*, *alp41-7* and *alp41-10* did not show much TBZ sensitivity compared to the wild-type control, and therefore were not picked up for further analysis.

TBZ sensitivity can give an idea about the function of the gene within the cell, and the clear sensitivity of some of the *alp41* mutants strongly suggested that *alp41* would be involved in microtubule regulation as well as possibly the tubulin cofactor pathway. The sensitivity of these mutants has been summarised in Fig.4.5.

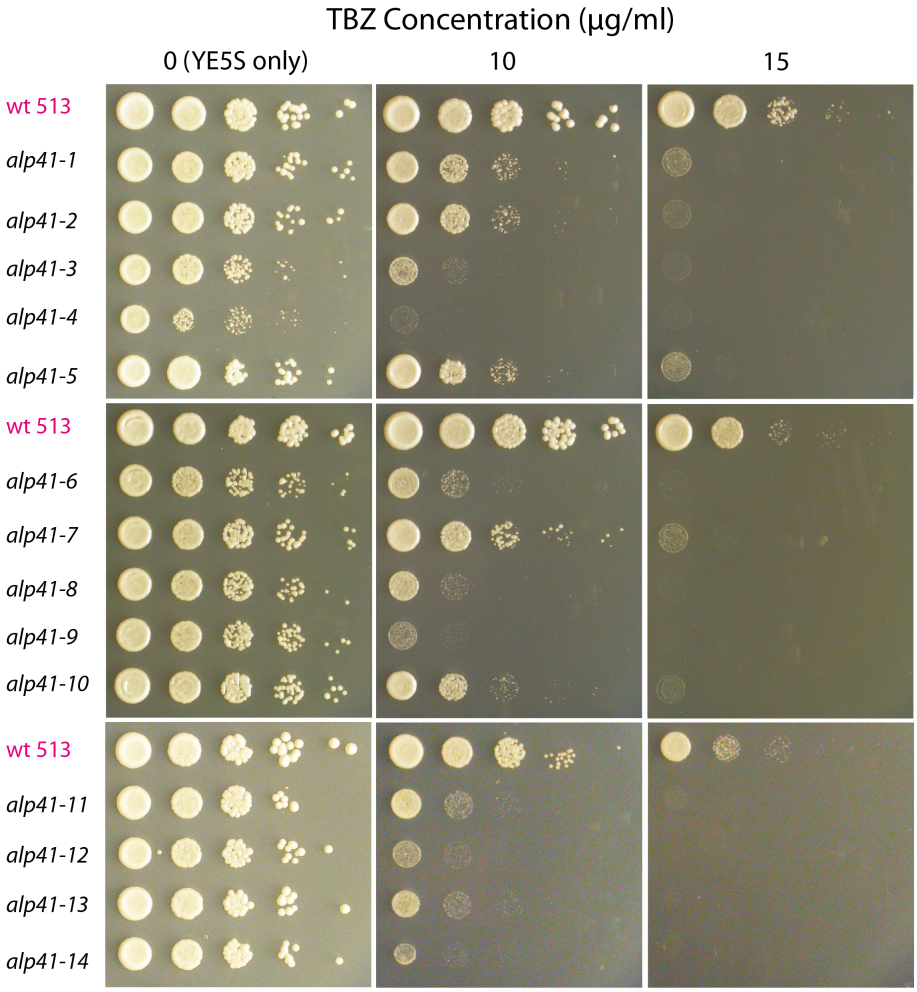

Figure 4.4 Serial dilution spot test for TBZ sensitivity for all *alp41* ts candidates

All ts candidates were spotted onto YE5S plates containing 10 or 15 µg/ml of TBZ. The plates were then incubated at 27°C for 2 days.

4.3.3 Sequencing of *alp41* mutants

In order to further investigate the effects of defective *alp41* function, the 14 mutant alleles were sequenced. The mutations are summarised in Fig.4.5 and highlighted in Fig.4.1 to show degree of conservation. Five of the alleles were mutated in the intron region, so were eliminated from further analysis (as expected these were the alleles with relatively weaker temperature and TBZ sensitivity). There were 2 alleles – *alp41-1* and *alp41-7,* that had the same point mutation – R18G, that lies just before the P-loop region. This same amino acid residue was also mutated in *alp41-8* – where instead of the arginine being mutated into a glycine, it was mutated into a tryptophan. This was interesting as there was a completely opposite phenotype in TBZ sensitivity in these two mutants, where *alp41-7* was not sensitive and *alp41*-8 was highly sensitive. There were also two of the same mutations found in *alp41-11* and *alp41-13*, which both had a W171R mutation. The only clear domains known in Alp41 are at the N-terminal of the protein, so there was no clear indication of how these mutations may affect the protein structure. *alp41-4* showed a mutation at A159T, and *alp41-5* at L36Q. *alp41-9* was the only mutant with 2 mutations at K34E and Q51R. This mutant was interesting as there was a strong sensitivity in TBZ but not so much for the temperature. Finally, *alp41-14* showed a point mutation at E85K, which lies just after the Switch II region.

In order to remove any possibility of extragenic mutations causing temperature or TBZ sensitivity, the mutants were back-crossed with a wild-type strain and the co-segregation of temperature sensitivity and hygromycin resistance observed. Consequently I found that co-segregation was not seen in *alp41-4*, which had shown strong sensitivity in temperature and TBZ, so this mutant was eliminated from further investigation.

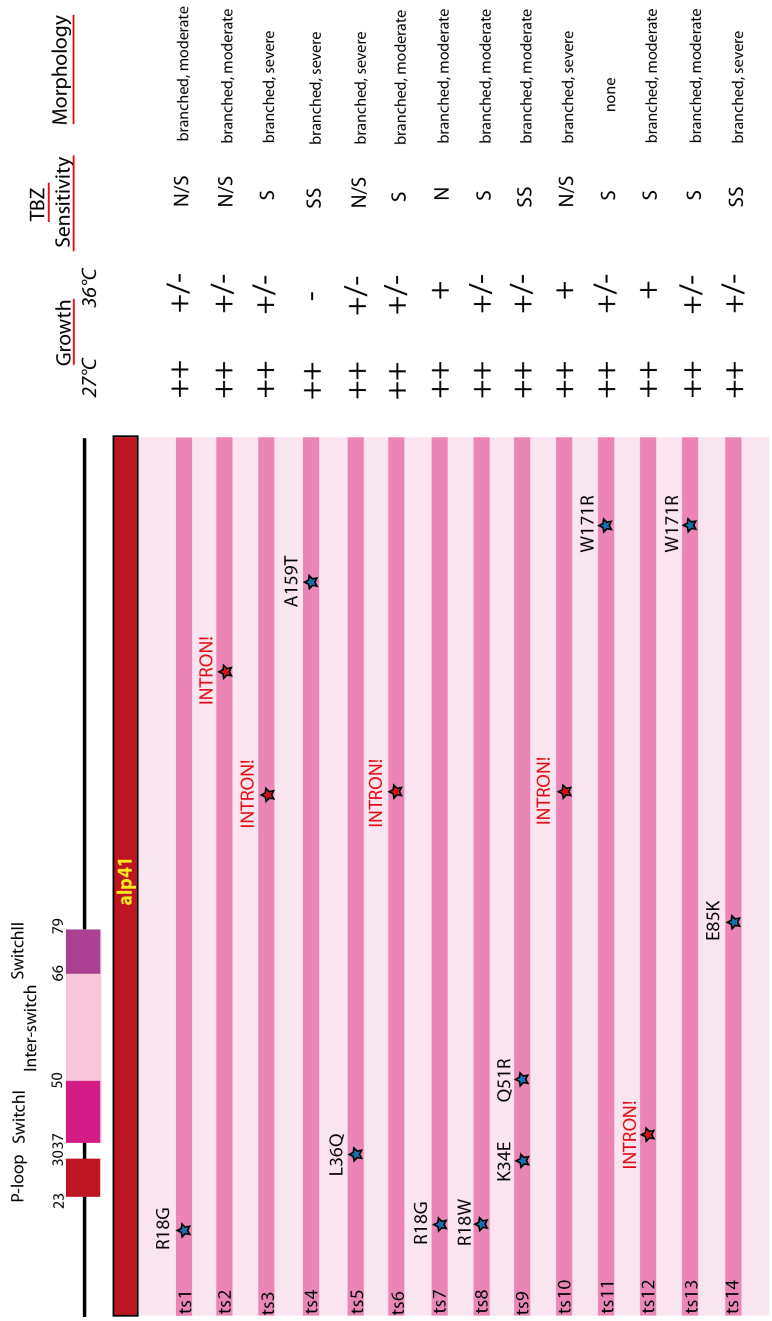

Figure 4.5 Summary of characteristics of *alp41* ts candidates

The 14 ts mutant candidates were sequenced and the mutation sites shown in the scheme. The known domains of Alp41 – the P-loop and the two switch regions, are shown and labelled. Mutations in the intron region are marked in red. Growth at 27°C and 36° are indicated – a '-' indicates no growth at all, '+/-' indicates moderate growth, '+' indicates growth and '++' means significant growth. TBZ sensitivity is described with 'S' for sensitive, 'SS' for significantly sensitive, and 'N' for normal. The morphology observed for cells of each of the candidates is listed on the far right.

4.3.4 Growth curve

In order to determine the cell cycle progression of the mutants, *alp41-1*, *alp41-9* and *alp41-14* were incubated in rich medium from a starting concentration of $2x10^6$ cells per ml at 36°C over 6 hours. Interestingly, there was large variation amongst the mutants as shown in Fig.4.6, with *alp41-1* seeming to grow at the same rate as the wild-type strain but the other two mutants showing a slightly slower growth rate. The lack of phenotype of *alp41-1* was not surprising, as in comparison to the other mutants the severity for temperature or TBZ was milder as shown in Fig.4.3 and Fig.4.4. However even the two other mutants did not show a severe growth defect at 6 hours of incubation at 36°C, so the experiment was repeated independently for *alp41-14* which was incubated for longer up to 14 hours at 36°C (Fig.4.6 lower panel). The mutant started to show a growth defect around 8 hours after incubation at 36°C, and growth continued to slow down for the rest of the monitored time. However growth never completely stalled and the cells were still seen to grow slowly, even at 14 hours of incubation.

This slow appearance of ts phenotype was similar to that of the *tbc1* mutants, which again took more than 6-8 hours of incubation to show slowing of growth. As discussed earlier, this may be due to the pool of heterodimers left in the cell, but in the case of Alp41, its related function to Tbc1 probably holds the key to understanding this phenotype. If we believe that the phenotype of *tbc1* mutants do not appear because it plays a role at the end of the pathway, it would be understandable if Alp41, which it is regulating, was also showing its phenotype late. However it remains interesting to understand why the growth of the *alp41-14* mutant does not cease, even after 14 hours of incubation at the restrictive temperature. How and why this mutant would lead to cell death may be critical to understanding the function of Alp41.

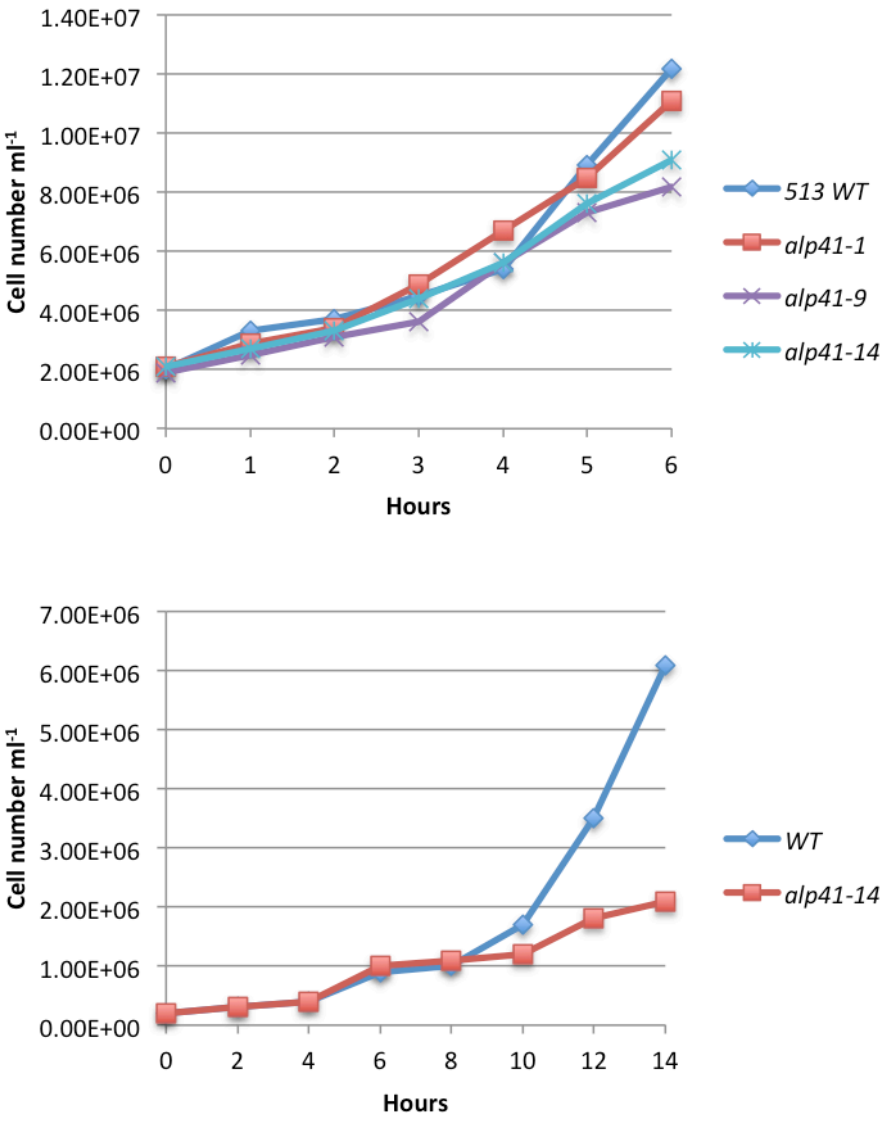

Figure 4.6 Growth curves for *alp41* ts mutants

The number of cells per ml of each of the chosen *alp41* ts mutants were counted and monitored over time. The upper panel shows 3 ts mutants and the wild-type strain plotted over the course of 6 hours after the shift to restrictive temperature. 0 hours indicates moment of shift-up. Lower panel shows the repeated experiment where *alp41-14* and the wild-type strain were incubated for a longer time course up to 14 hours. The number of cells plotted are means from 3 independent experiments.

4.4 There are 2 classes of *alp41* ts mutants

To investigate this slow appearance of phenotype further, we analysed the cellular characteristics of these mutants to decipher what may be causing this unusual phenotype. Upon observing the temperature and TBZ sensitivity of the 14 mutants isolated above, we decided to analyse further the mutants *alp41-5, alp41-7, alp41-8, alp41-9* and *alp41-14*. These mutants showed the highest sensitivity to the restrictive temperature as well as TBZ. The mutants all had a single point mutation apart from *alp41-9* that has two mutations (summarised in Fig.4.5).

In order to observe their microtubule phenotype, the mutants were crossed with a strain tagged with GFP-Atb2 (microtubules) and Sid4-mRFP (spindle pole body, SPB). The cells were incubated overnight at the permissive temperature and shifted to the restrictive temperature for further incubation. Samples were taken as appropriate and observed under the fluorescence microscope.

4.4.1 Class I mutants show loss of microtubules

Upon initial observation of *alp41-5, alp41-7* and *alp41-8*, I found that for all the strains the phenotype started to appear at around 6-8 hours upon incubation at the restrictive temperature. All mutants showed visible morphology defects (see Fig.4.7), with bent, elongated or short cells, similar to that of the *tbc1* ts mutants. There appeared to be dead cells also seen frequently in the samples, and growth seemed to be arrested after 8 hours. The microtubule phenotype resembled that of the *tbc1* ts mutants, in that essentially the microtubules were absent or defective. None of the *tbc1* mutants were left with any microtubules after 8 hours at the restrictive temperature. By contrast, the *alp41* mutants displayed a wider difference in phenotype as seen in Fig.4.7. Some cells had no microtubules at all, some had very few microtubules, and some had microtubules although they were short and disrupted. The different defects were quantified at time points following the switch to the restrictive temperature and classified into five categories: no microtubules, short/defective spindle (mitotic phenotype), curled interphase microtubules, short interphase microtubules, or normal microtubules, as

indicated in Fig.4.8. 300 cells were counted after 4 hours and 8 hours of incubation at 36°C so that the range of severity could be monitored over time. *alp41-5* and *alp41-7* showed a very similar rate of defects at both 4 and 8 hours, with around half of the cell showing short interphase microtubules and 20% with no microtubules at all. After 4 hours of incubation, only around 10-20% of cells showed normal microtubule structures for both mutants, and this number decreased to a further 10% after 8 hours. *alp41-8* showed a similar range of phenotypes, but the phenotypes appeared earlier than the other 2 mutants, with only 5% of the cells showing a normal phenotype already at 4 hours of incubation.

With these class I mutants, the microtubule defects seemed to be causing growth arrest. Similar to the *tbc1* ts mutants, the defective microtubules would result in the branched and bent morphology of the cells. These results were again consistent with the other cofactor mutants.

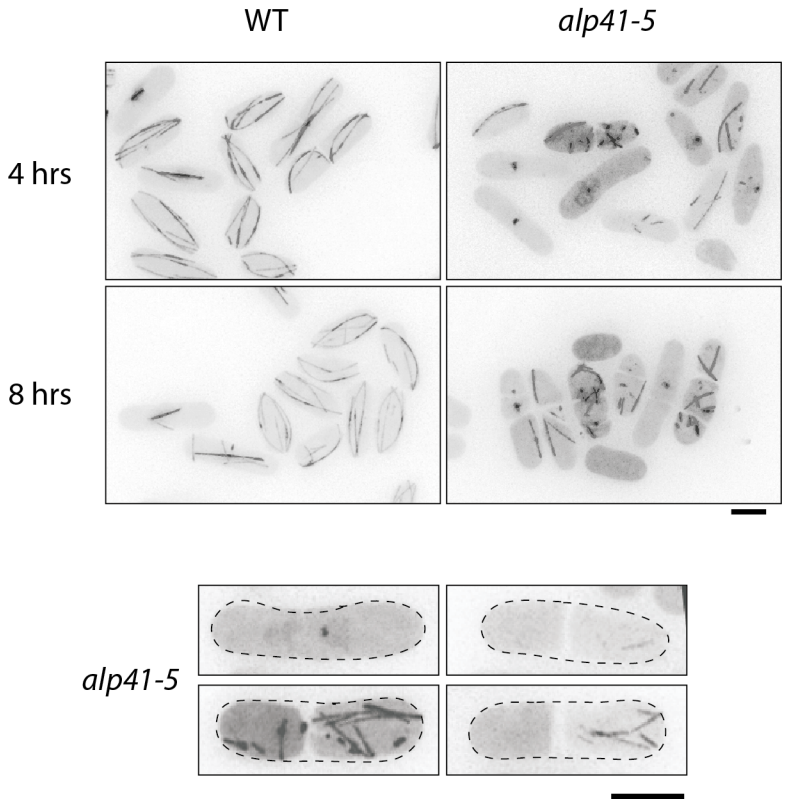

Figure 4.7 Microtubule phenotypes of class I mutant *alp41-5*

A wild-type strain and *alp41-5*, both with Atb2 tagged with GFP, were incubated at the restrictive temperature for up to 8 hours. Samples were taken every 2 hours and observed under the fluorescence microscope. Images shown are those of samples taken after 4 and 8 hours. The lower panel shows four independent mutant cells which have a significant microtubule phenotype. Bars: 5 μm.

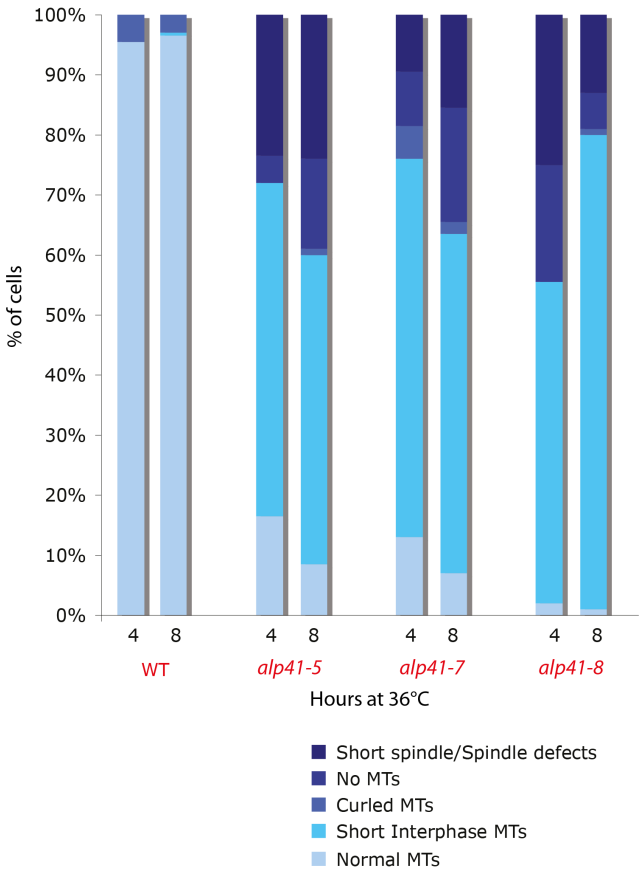

Figure 4.8 Quantifications of microtubule phenotypes of class I mutants.

The microtubule phenotypes observed in Fig. 4.7 were categorised and quantified. Three hundred cells were counted and scored for each strain at 4 and 8 hours. Short spindle/spindle defects indicate mitotic defects seen in the cells, whereas the other categories refer to interphase microtubules. 'Normal MTs' refer to both mitotic and interphase microtubules that looked similar to wild-type conditions. N= 300 cells.

4.4.2 Class II mutants retain their microtubules

In contrast to the class I mutants, the striking phenotype of the class II mutant *alp41-14* was that it showed no phenotype until at least 12 hours of incubation at the restrictive temperature. Therefore all following analyses were done at 14 hours of incubation, where the phenotype was strong enough to assess. The other striking difference was that *alp41-14* showed no loss of microtubules – morphologically, the cells were elongated and bent, forming a 'banana' shape, and the interphase microtubules were retained, although elongated and curled.

Also to note was that there were less microtubule bundles seen, and many of the microtubules seemed to appear more stable, curving around the tip of the cell without undergoing catastrophe (blue arrowheads, lower panel, Fig 4.9a). A small number of other phenotypes including mitotic spindle phenotypes were also apparent, such as irregular spindle formation (red arrowheads, lower panel, Fig.4.9a and b). These included monopolar spindles, mis-oriented spindles, and also cells with some remaining interphase microtubules present even after spindle formation. However, once the phenotypes were characterized and quantified, it was clear that the mitotic phenotypes were only in a minority of the cells, and that the interphase microtubule phenotypes were the major phenotypes seen in a larger number of cells. Overall, from around 8 hours the various phenotypes start to appear in approximately 20% of the cells, which by 14 hours increase to over half of the cells.

The morphology and related microtubule phenotypes were quantified in 300 cells (Fig.4.11c). The cells were categorised into 4 groups – normal morphology/normal microtubules (31%), bent morphology/curled microtubules (35%), bent morphology/normal microtubules (9%) and normal morphology/curled microtubules (25%). Overall, 61% of the cells showed abnormalities in cell shape and/or microtubule phenotype.

In order to characterise this mutant further, a viability assay was carried out to determine the survival rate of these cells after different times under the restrictive

temperature. From 8 hours onwards, a known number of cells were taken every 2 hours from culture and spread on YE5S plates and incubated at 27°C. After 3 days of incubation the formed colonies were counted and a percentage calculated of viable cells. The resulting plot in Fig.4.9c shows that compared to the wild-type, the viability is lower even at the beginning of the experiment, and this viability lowers steadily after 8-12 hours up until 16 hours. Notably, the viability of the wild-type strain also reduces after prolonged incubation at high temperature, but the difference between the 2 strains is significant enough to see the extent of the defect in the mutant. This loss in viability complements the growth curve data, which showed that after approximately 8 hours of incubation the growth started to slow down. However the microtubule phenotype showed no obvious spindle defects, which does not explain how the cells are losing their viability.

In an attempt to understand when this microtubule phenotype was the most detrimental, I counted the proportion of cells at each stage of the cell cycle. This was done after 14 hours incubation at 36°C, after which this strain showed the most obvious phenotype. Curiously, the cells were not blocked at any specific stage of the cell cycle. The mitotic and septation indexes were slightly increased but this did not explain that cells stopped growing and dying.

This microtubule phenotype was unexpected in contrast to the more obvious phenotypes seen in the class I mutants. In addition, it was also unexpected to see this more 'stable' microtubule phenotype when there was a clear TBZ sensitivity seen in *alp41-14*. Mutants of other genes that showed a similar microtubule phenotype where the microtubules appeared more stable, would usually show a resistance to the microtubule drug (Unsworth et al., 2008). To further analyse this mutant, various assays were carried out to observe any other phenotypes.

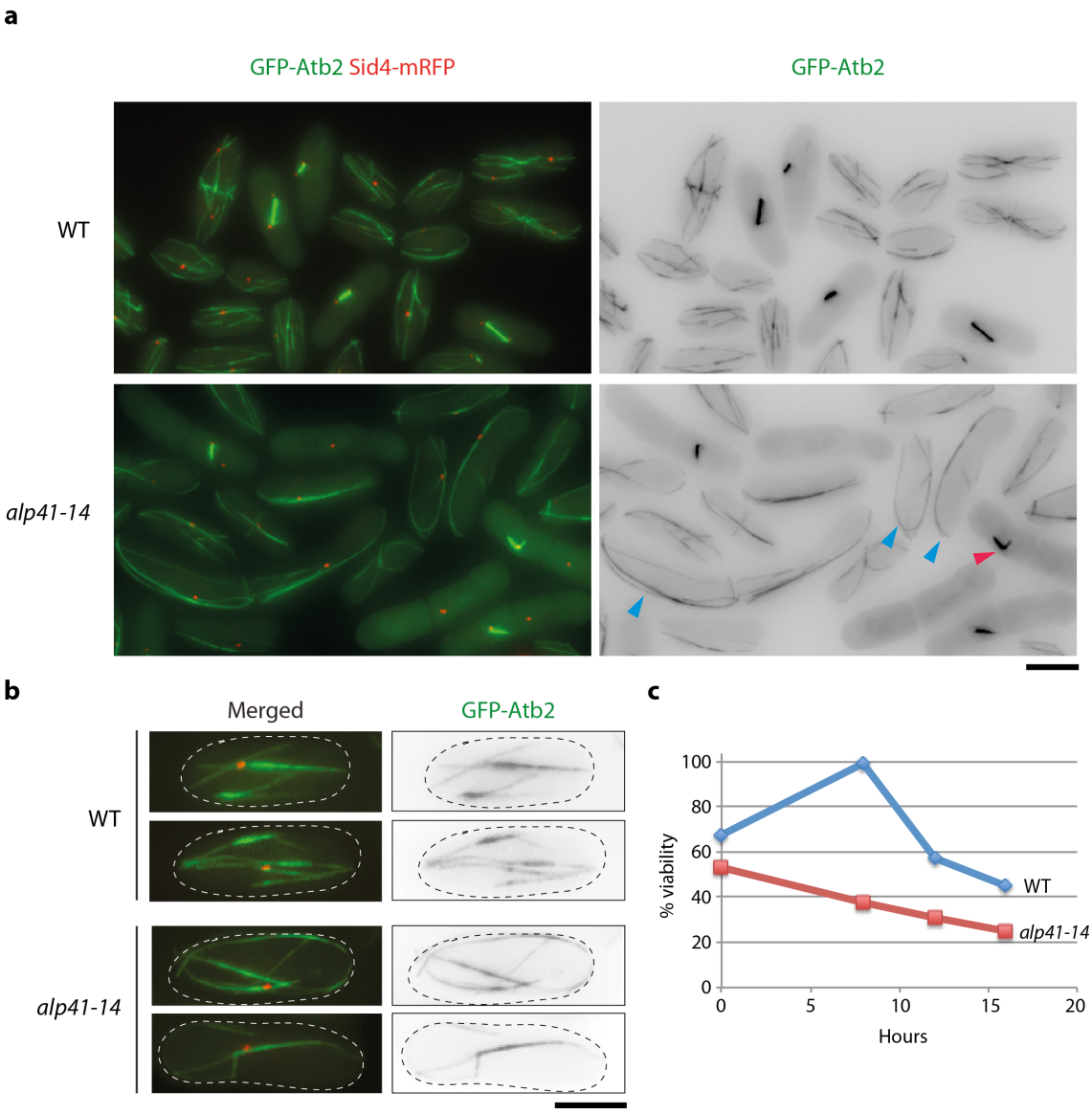

Figure 4.9 Microtubule phenotypes of class II mutants

A wild-type strain and *alp41-14* with GFP-tagged Atb2 and RFP-tagged Sid4 were incubated at 36°C for 14 hours and observed under the fluorescence microscope. Images were processed as previously described. Bars = 5 μm. (a) shows a field of cells. Red arrowhead shows a spindle defect in which a monopolar spindle has started to form in a cell that has not completely divided. Blue arrowheads show "curled" microtubules which have curved around the cell cortex without undergoing catastrophe. (b) shows individual cells where there are obvious curled microtubules in comparison to the wild-type cells. (c) shows the plot of the mean viability of the wild-type and mutant cells taken from two independent experiments.

4.4.2.1 Observation of mitochondria distribution, nuclear signal and nuclear envelope marker

In order to observe any defects in microtubules function, I stained for mitochondrial distribution within this mutant. Mitotracker, a cell permeant probe that labels active mitochondria, was used to see the mitochondria organisation within live cells. Mitochondria within fission yeast are distributed by microtubules, and therefore improper distribution is often seen in microtubule defective cells, as was seen in the *tbc1* mutants. In the wild-type cells, mitochondria loosely co-localise with the microtubules due to their dependency on distribution by microtubules. However Fig.4.10 shows that in *alp41-14*, there were no more smooth and evenly distributed mitochondria, but instead the signal formed aggregates or clusters. In addition, the mitochondria no longer co-localised with the microtubules, even when there were microtubules present. As shown in Fig.4.10b, in close correlation to the microtubule phenotype, the mitochondria phenotype started to appear at around 8 hours of incubation in *alp41-14*. This progressed on to become more severe up until 14 hours of incubation where there were many mitochondrial aggregates seen in the cells.

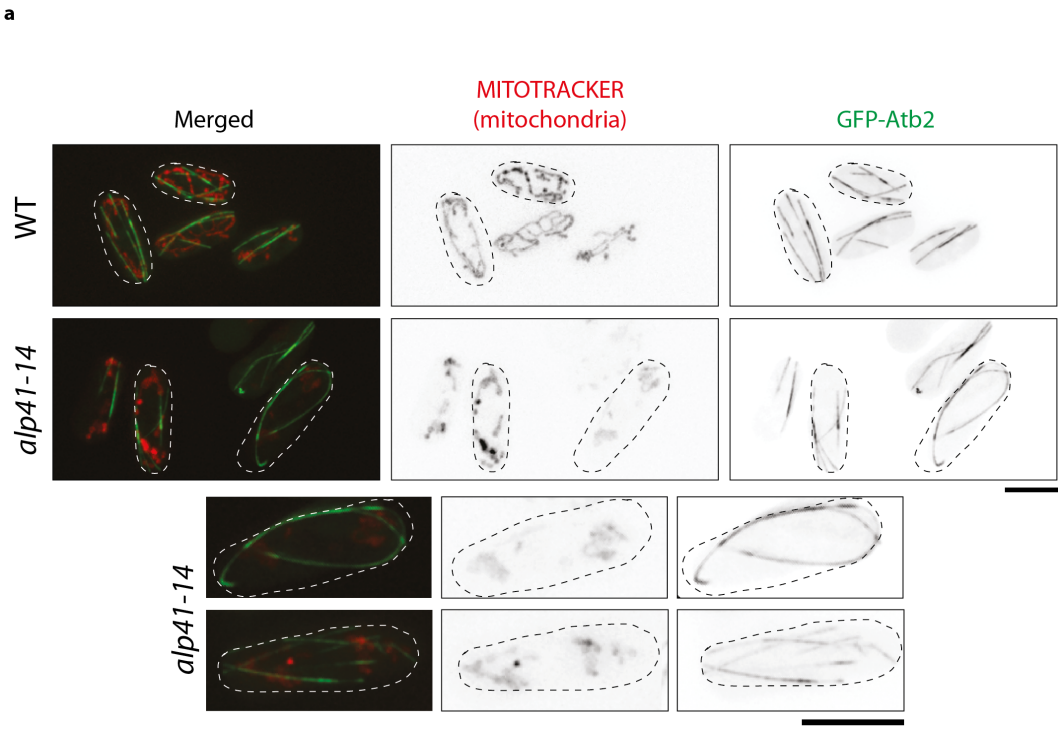
a
Merged
MITOTRACKER
(mitochondria)
GFP-Atb2
WT
alp41-14
alp41-14

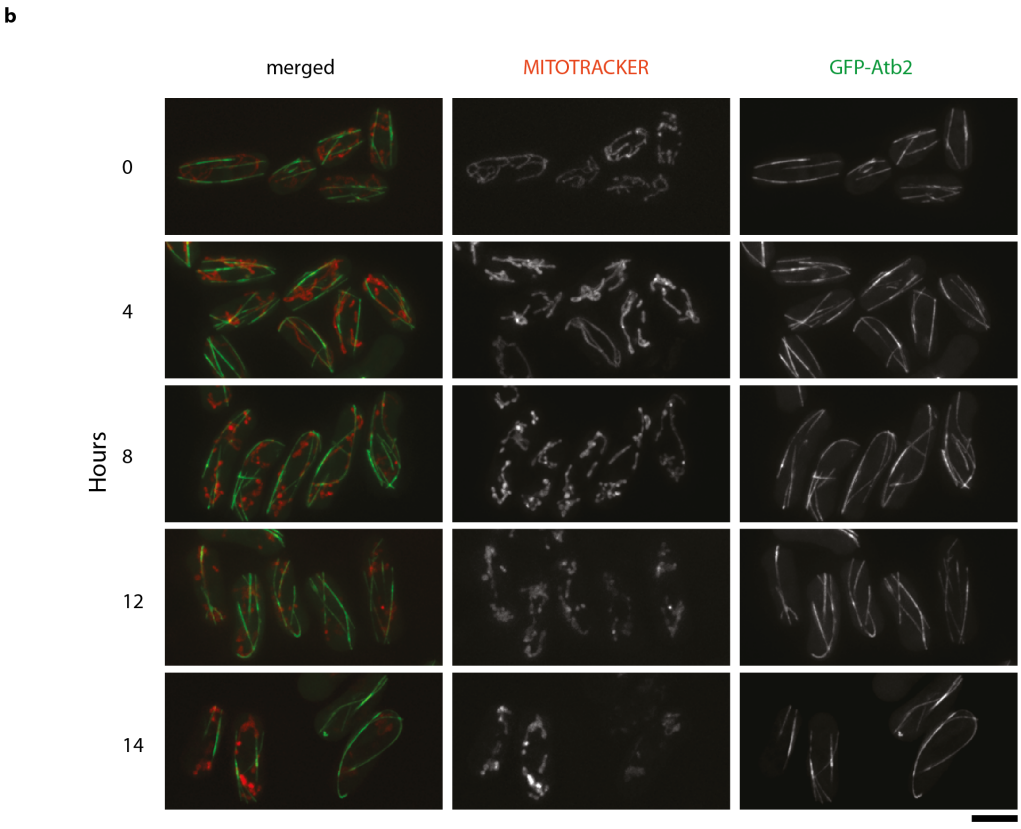
b
merged
MITOTRACKER
GFP-Atb2
Hours
0
4
8
12
14

Figure 4.10 Mitotracker staining of *alp41-14*

A wild-type strain and *alp41-14* were incubated at 36°C for 14 hours and then stained with Mitotracker. (a) shows representative cells from wild-type and mutant cells. Compared to wild-type cells, after 14 hours at 36°C the mutant have defective mitochondria distribution indicated by aggregation. (b) shows images from a time course experiment with mutant samples taken until 14 hours after incubation. *alp41-14* starts to show uneven distribution and aggregations of mitochondria from around 8 hours, which gradually increases by the end of the experiment where the microtubule phenotypes are strongly seen which correlates with the appearance of the microtubule phenotype. Bar: 5μm.

To find further defects, an additional tag of Cut11-CFP (nuclear membrane marker) was introduced into the mutant strain to observe if there were any defects in nuclear shape or misplacement. Nuclear misplacement is commonly caused by defective microtubules, as microtubule dynamics and anchoring are shown to play a vital role in nuclear positioning (Reinsch and Gonczy, 1998). When 300 cells were quantified (Fig.4.11c), 30% of the cells had non-circular Cut11 staining – in wild-type cells, the nuclear envelope forms an even round shape at the middle of the cell. 20% of the cells had fragmented nuclear envelope staining where there was no recognisable shape formed by the cut11, and 6% of the cells appeared to have 'multiple nuclei', showing two, or even three nuclear membrane structures although the cell was not undergoing mitosis (no septum formation).

Hoechst staining was also used to determine if the mutant showed any chromosome mis-segregation. The quantified result is shown in Fig.4.11c. Interestingly, 62% of cells showed defects in nuclear shape. In 42% of the cells the staining appeared fragmented – where there were clusters of nuclear material seen but not in the organised hemispherical shape as seen in the wild-type cells. In addition, 20% of the cells showed dispersed staining, where there were no clear clusters of nuclear material and it appeared dispersed throughout the cytoplasm. This was further confirmed using the histone Hht1 tagged with RFP (data not shown). When observing the Hoechst stained cells, we also noticed a phenotype in the septa that was quantified in Fig.4.11c. Out of the septated cells seen in the 300 cells counted, 27% had septation defects – 13% had more than one septum formed, which indicates that either cytokinesis or segregation did

not occur properly. In addition, 14% had a misplaced septum – where the septum did not form in the middle of the cell as it should in proper cytokinesis. These phenotypes would lead to mis-segregation of the chromosomes and therefore mitotic defects. The position of the division plane in fission yeast is defined by the position of the nucleus (Daga and Chang, 2005), and so this septum defect correlates with the nuclear phenotype.

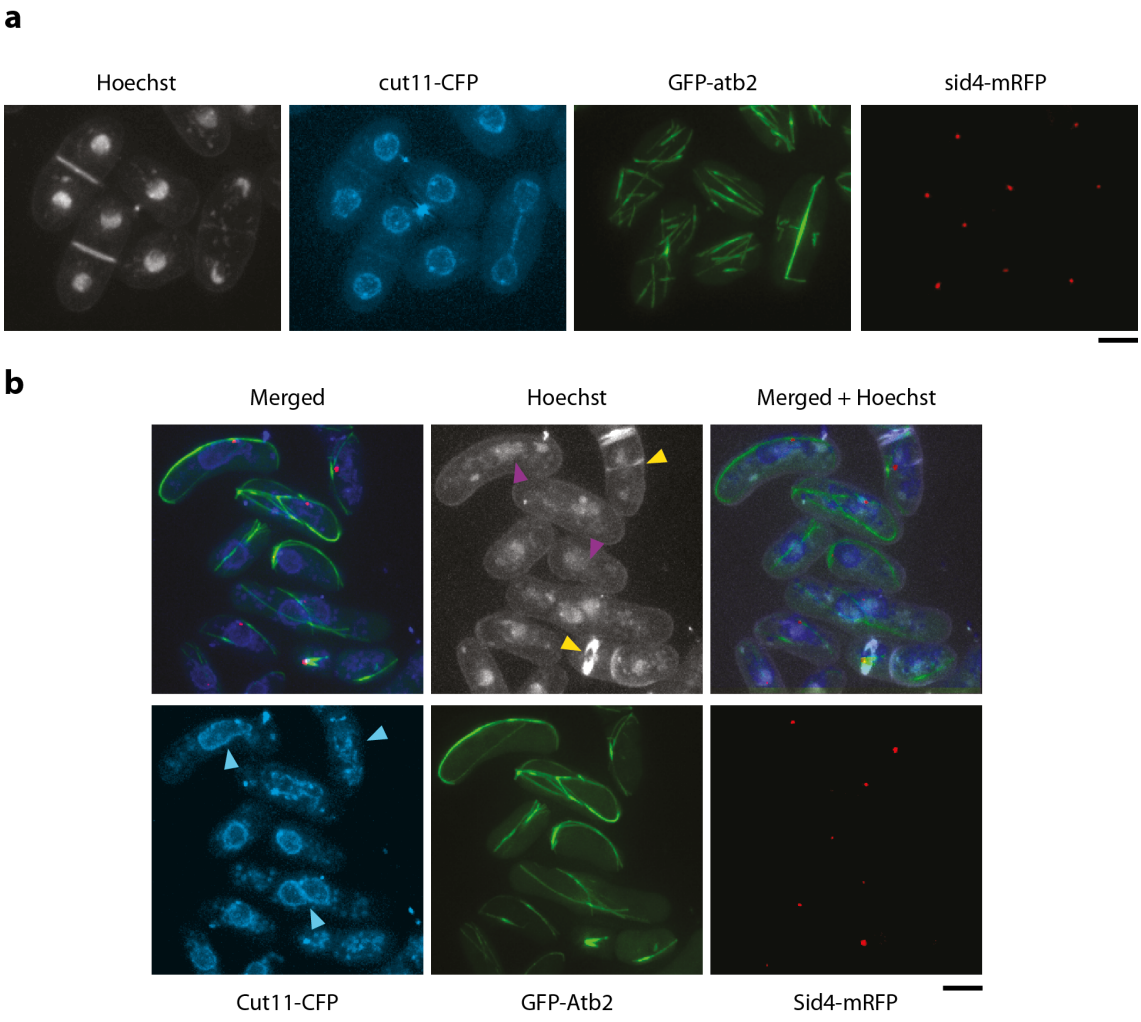

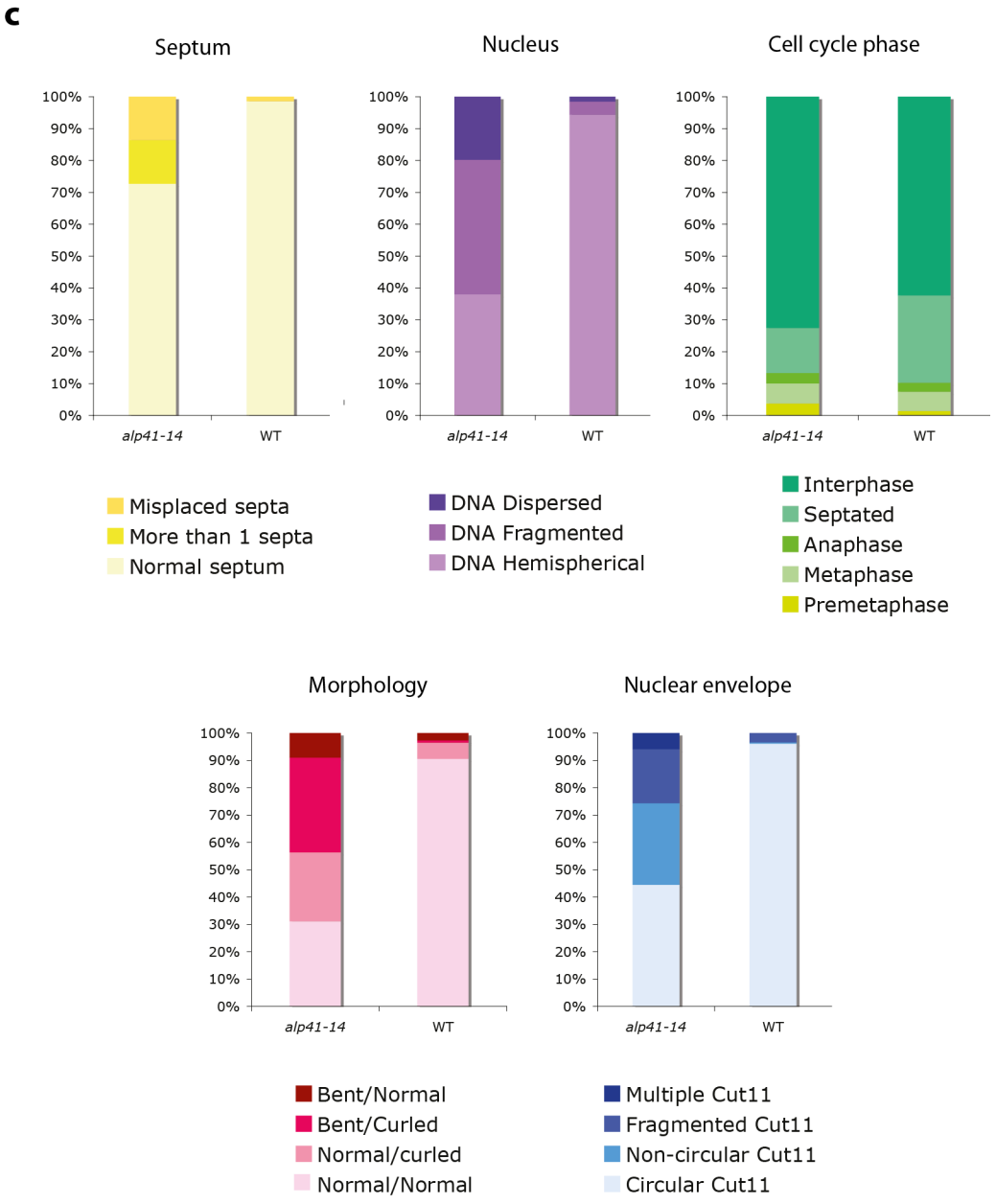

Figure 4.11 Phenotype characterisation of *alp41-14*

alp41-14 crossed with a strain expressing GFP-Atb2, Sid4-mRFP and Cut11-CFP was incubated at 36°C for 14 hours. Samples were taken, stained with Hoechst and observed under the fluorescence microscope. (a) shows wild-type cells, (b) shows the *alp41-14* mutant. The yellow, purple and blue arrowheads show septum, DNA and Cut11 defects, respectively. (c) the phenotypes seen in (b) were quantified by counting 300 cells and scoring them for severity of phenotype. Defects in septum formation were scored as; normal, more than one septum per cell, and misplaced where the septum was seen not in the middle of the dividing cell but elsewhere. Hoechst staining defects were classified by the shape of the staining – wild-type staining would show a hemispherical shape formed within the cell, but in the mutants they were often seen as dispersed, where there was no concentrated region of staining and there was staining across the area of the cell,

or fragmented, where there was more than one cluster of DNA material per cell. The cell cycle phase was also determined for the cells by observing the Sid4 (SPB) signal. 'Morphology' describes the cell morphology as well as the microtubule phenotype. 'Bent/Normal' indicates a bent cell shape but normal microtubules, and 'Bent/curled' a bent cell shape and curled microtubules. 'Normal/curled' indicates a normal cell shape but curled microtubules, and 'Normal/normal' if they look completely wild-type for both cell shape and microtubule phenotype. Cut11-CFP shape has been classified as 'multiple' where there was more than one nucleus in the cell despite it not being at anaphase, 'fragmented' where there was no clear shape which could be distinguished as the nuclear membrane, and 'non-circular' if there was a recognisable shape but it was not completely circular. Bar: 5μm.

4.4.2.2 Class II mutant **alp41-14** *retains its tubulin concentration*

One of the direct results of defects in the tubulin folding cofactor pathway is the lack of proper heterodimer formation. This is thought to cause a range of effects on microtubule structure or organisation – and may upset the balance of the α- and β- tubulin monomer/heterodimer pool. To assess if this was the case in the ts mutants isolated for both *tbc1* and *alp41*, I measured the different levels of tubulin in these mutants as well as for mutants for *alp1*, *alp11*. Protein was extracted from ts mutants *tbc1-11*, *alp41-14*, *alp1-1315* and *alp11-924* and 30 μg of each run on an SDS-PAGE gel. The cofactor mutants *alp1-1315* and *alp11-924* were used as positive controls, as both previously showed a decrease in α-tubulin (Chap.1.8). The separated protein was transferred onto a membrane that was blotted against α-tubulin. The intensity of the band was calculated using Adobe Photoshop CS4 whilst normalising to a Cdc2 band and plotted for comparison. Two samples of each protein was assessed – at 0 hours after switching to the restrictive temperature and a further 8 hours after incubation. *alp1-1315* and *alp11-924* both show a characteristic microtubule defect (Hirata et al., 1998), (Radcliffe and Toda, 2000). As *tbc1-11* also showed this very similar phenotype, the similar decrease in relative intensity of α-tubulin shown in Fig. 4.12 all correlates with the microtubule phenotype. Interestingly but not surprisingly, there was no obvious decrease in the intensity of *alp41-14*. As the mutant is able to retain its microtubules, there would not be any difference with the wild-type cells.

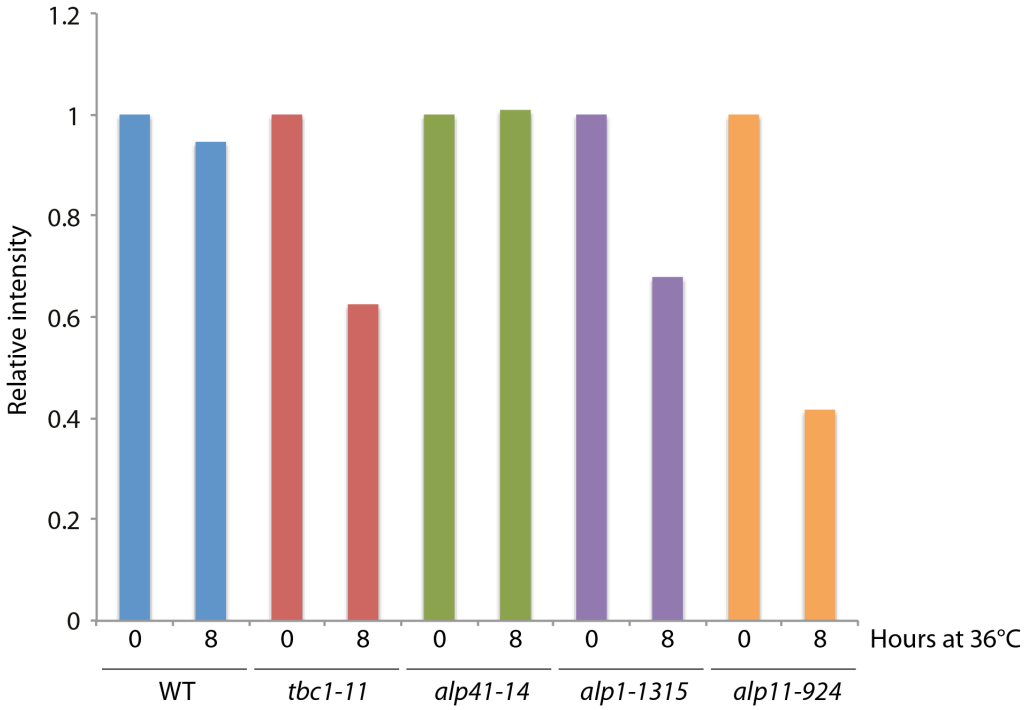

Figure 4.12 Tubulin concentration in cofactor mutants

The α-tubulin concentration of each of the cofactor mutants shown were determined by loading 30 μg of protein extract from each mutant after 0 and 8 hours of incubation at 36°C onto an SDS-PAGE gel and performing a western blot against α-tubulin. The intensity of each band was calculated using Adobe Photoshop CS3, normalised against a control protein band and plotted on a bar chart.

4.5 Discussion

Alp41, the fission yeast homologue of Arl2, was identified as the candidate G protein that Tbc1 is the GAP for. In order to study the two proteins together, first, ts mutants were isolated for the *alp41* gene. The morphological phenotypes and sensitivity to TBZ were slightly weaker than that of the *tbc1* ts mutants, but the mutants showed microtubule defects, thereby confirming the involvement of Alp41 in the tubulin folding pathway.

Interestingly, many of the mutants shared point mutations, or mutations around the same region of the gene. Not much is known about the domains within the Alp41 protein so it cannot be determined what the implications these mutations have, but a lot of the mutations were seen around the N-terminus where the switch regions and P-loop are – the features of a G protein. This may also help us understand the defects that Alp41 have may in relation to its interaction with Tbc1.

When looking at the microtubules, I made an interesting observation that out of the 14 mutants isolated, there were strikingly different microtubule phenotypes between some of the mutants - some mutants lost their microtubules, and some on the contrary had seemingly stabilised microtubules. I classified the mutants into two main categories – class I and class II, depending on the microtubule phenotype.

The class I mutants were very similar to the *tbc1* ts mutants – they lost their microtubules after incubation at restrictive temperature, which would understandably lead to cell death. However the class II mutant *alp41-14* was much more difficult to fathom – its observed phenotypes were different, almost opposite to the class I mutants. The length of time required for the phenotype to occur was much longer, and the morphology showed a more bent and elongated shape than the characteristic branched shape of the other mutants. Upon observing this phenotype and the contradictory TBZ sensitivity (as often an "over-stable microtubule phenotype" would result in resistance to the microtubule drug), we hypothesised that maybe although the microtubules were retained, they were not functional. Various assays were carried out to further analyse this, and indeed the mutant showed a high rate of chromosome mis-segregation as well as defective mitochondrial distribution and nuclear displacement. This may also explain why the mutant takes so long for the phenotype to appear – if the microtubules are still present there may not be any immediate effects on the cells such as cell division or organelle distribution, but once these defects are accumulated over time, the strain starts to lose viability. More importantly, *alp41-14* showed no decrease in α-tubulin concentration. The other cofactor mutants, including that of *tbc1,* showed a clear decrease. This highlights the possibility that Alp41 may have additional roles besides the one it plays in the tubulin folding pathway – *alp41-14* is clearly defective, but it

may still be folding heterodimers for microtubule formation. The mutation in this mutant could be causing defects in a separate function. It remains to be addressed if the class I mutants would show a decrease in tubulin concentration – it is strongly likely that this is the case. This possibility that Alp41 may have different roles may explain this anomalous nature of *al41-14,* which is clearly not so straightforward as the class I mutants.

Although no data has been shown here, there was also another interesting mutant – *alp41-9*. The mutant also failed to show a phenotype until after 10 hours incubation at the restrictive temperature – they appeared slightly earlier than *alp41-14* but later than the class I mutants. However the microtubule and morphological phenotype was much milder than that of *alp41-14*, and only curved microtubules were seen (no mitotic spindle phenotypes were seen). This classed *alp41-9* as an intermediate mutant between the two classes. *alp41-9* is the only mutant where there are two mutations within the gene, and appears to be different to the other mutants. This may be an explanation for its behaviour, but this has not been pursued much further.

The characterisation of the *alp41* mutants strongly suggests its involvement in the tubulin folding pathway. In order to identify how it is involved together with Tbc1, I next looked at the two proteins together.

Chapter 5. Tbc1 is a GAP for Alp41 and the GTP/GDP cycle is crucial for Alp41 function

The results obtained from the mutant analysis of *tbc1* and *alp41* places them both in the tubulin folding pathway and microtubule regulation. The sequence of Tbc1 suggests strongly that it is a GAP, as it possesses the characteristic TBCC domain and arginine finger. Alp41, the fission yeast orthologue of Arl2, has the characteristic motifs of a G protein. Taking this into account, I hypothesised that Tbc1 acts as a GAP for Alp41. In order to confirm this, I used various techniques to assess if the 2 proteins interacted biochemically and genetically.

5.1 Tbc1 and Alp41 co-immuno-precipitate in whole cell extract

First, the interaction between the two proteins was assessed by immuno-precipitation. Strains with 3HA-tagged Tbc1 and GFP-tagged Alp41 were constructed and protein extracted from the cells. An overexpression strain of Alp41 was used (in order to compare with other Alp41 interactions which will be discussed later in Chapter 6) and therefore the cells were grown in minimal media to allow overexpression by wash-out of thiamine. IP was performed against GFP and Fig.5.1 shows the resulting blot. In the single-tagged control strain, no protein was co-immuno-precipitated with GFP-Alp41. By contrast, a specific band corresponding to Tbc1-3HA co-immuno-precipitated with GFP-Alp41. This shows that there is a very strong possibility that Alp41 is involved in the regulation of Tbc1 or vice versa.

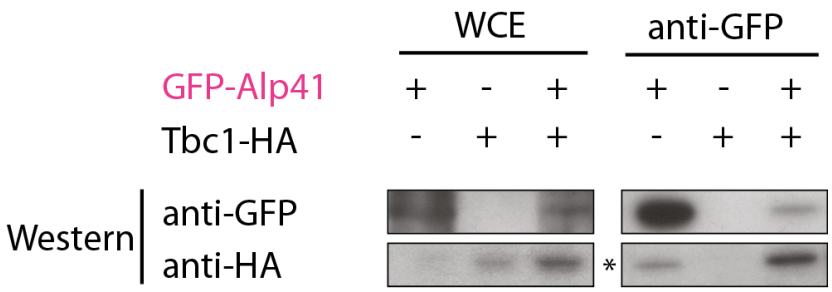

Figure 5.1 Immuno-precipitation of Alp41 and Tbc1

IPs were performed using double tagged strain expressing GFP-Alp41 and Tbc1-3HA. First lane shows control strain expressing GFP-Alp41 only. Second lane shows control strain expressing Tbc1-3HA only. The third lanes show the double tagged strain. WCE = whole cell extract. Asterisk shows unspecific band.

5.2 Tbc1 and Alp41 interact by peptide array assay

In order to show that the Tbc1-Alp41 interaction is direct, we checked if they could bind one to one using an *in vitro* peptide array assay. The advantage of this system is that it involves purified recombinant proteins and that, contrarily to the IP described above, no other interfering proteins such as MAPs or tubulin could make them indirectly interact.

The peptide array synthesised covered the entire of Tbc1 or Alp41. 20 amino acid residues per spot was spotted onto a cellulose membrane with 2 residue increments between the spots. HIS-tagged Alp41 and Tbc1 were expressed in BL-21 *E.coli* and purified using a nickel column. The membranes were incubated with the purified protein overnight at 4°C. After several washes to remove any unbound protein, the specific interactions were detected using an anti-HIS antibody by western blot.

As seen from Fig.5.2, there is clear interaction between both Tbc1 peptide and Alp41 protein, and *vice versa*. Simultaneously, this also allowed us to determine the domains that are important for binding between the two proteins, which was previously unknown. In the case of Alp41, the largest interacting region lies in the N-terminal of the protein,

where the P-loop and the 2 switch regions lie. These are the regions that are important for G protein activity, which would further strengthen our result that Tbc1 is a GAP for Alp41. On the other hand, on analysing the interaction for the Tbc1 peptide incubated with Alp41 protein, we found that the interacting regions span along the entire of the protein, with some of the regions lying at the end of the coiled coil domain, some lying in the GAP domain at the C-terminal of the protein, and some in between these two domains. Therefore I would conclude that the interacting region of Tbc1 spans the whole protein. The disadvantage of the peptide array assay is that it does not take into account the structural folding of the protein. Therefore it cannot be determined how, in a structural conformation, the residues interact. However it did confirm that these two proteins interact, and taken together with the IP data, regulate one another both *in vivo* and *in vitro*.

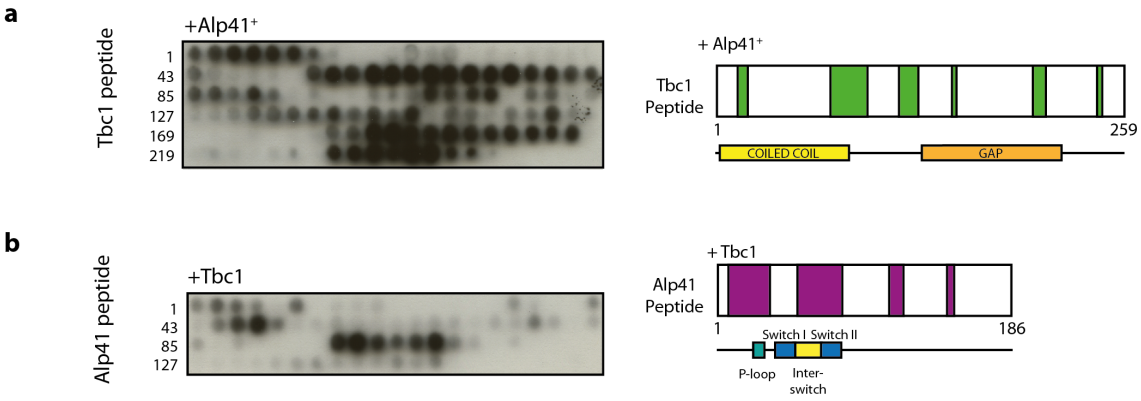

Figure 5.2 Tbc1 and Alp41 interact by peptide array assay

Recombinant Alp41 and Tbc1 proteins were purified from *E.coli* and a peptide array assay performed. The blots are shown on the left and after analysis a schematic was constructed marking the regions of interaction. Numbers on the blot mark the amino acid number at the beginning of the row. (a) Cellulose membrane spotted with Tbc1 peptide was incubated with Alp41 protein. (b) Cellulose membrane spotted with Alp41 peptide was incubated with Tbc1 protein. Both peptides have their known regions illustrated.

5.3 Double mutants of *tbc1* and *alp41* show mutual rescue of the ts phenotype

To investigate further the regulation between *tbc1* and *alp41*, I next took the genetic approach and crossed the strongest ts mutants of both genes to observe any rescue of the temperature sensitive phenotype.

If we hypothesise that Tbc1 is a GAP for Alp41, Tbc1 is interacting with the active form of Alp41, aiding its GTP hydrolysis and rendering it inactive. Therefore if Tbc1 loses its GAP activity (as in *tbc1-11*), Alp41 will not be converted and will accumulate in its GTP-active form. Assuming that the *alp41* mutant may be locked in its GDP-inactive form, then the double mutant *tbc1-11 alp41* should restore the balance between GTP and GDP and show a wild-type phenotype. To observe if this was the case, we crossed *tbc1-11* and the class I mutant *alp41-8*, and class II mutant *alp41-14*.

Figure 5.3 shows the spot test with the single and double mutants. *tbc1-11* shows a stronger sensitivity at 36°C than the *alp41* mutants, as previously shown. The double mutant between *tbc1-11* and *alp41-14* showed a significant rescue of the phenotype, with it growing almost at a similar extent to the wild-type strain. This could also be seen in the TBZ sensitivity. This mutual rescue of phenotype confirms that the two proteins are related in function and possibly play an antagonistic role.

Interestingly, as shown in Fig.5.3a, we found that the class I mutants of *alp41* showed no rescue. This could have been due to the difference in the nature of the ts phenotype, clearly seen with the microtubule morphology. If the mutation causes a different effect in the GTP/GDP balance, this may not be so simply to rescue by the *tbc1-11* mutant. The class I mutants show a much stronger morphological and microtubule phenotype than the class II mutant. This could be reflected in the varied ability to rescue the *tbc1* mutant.

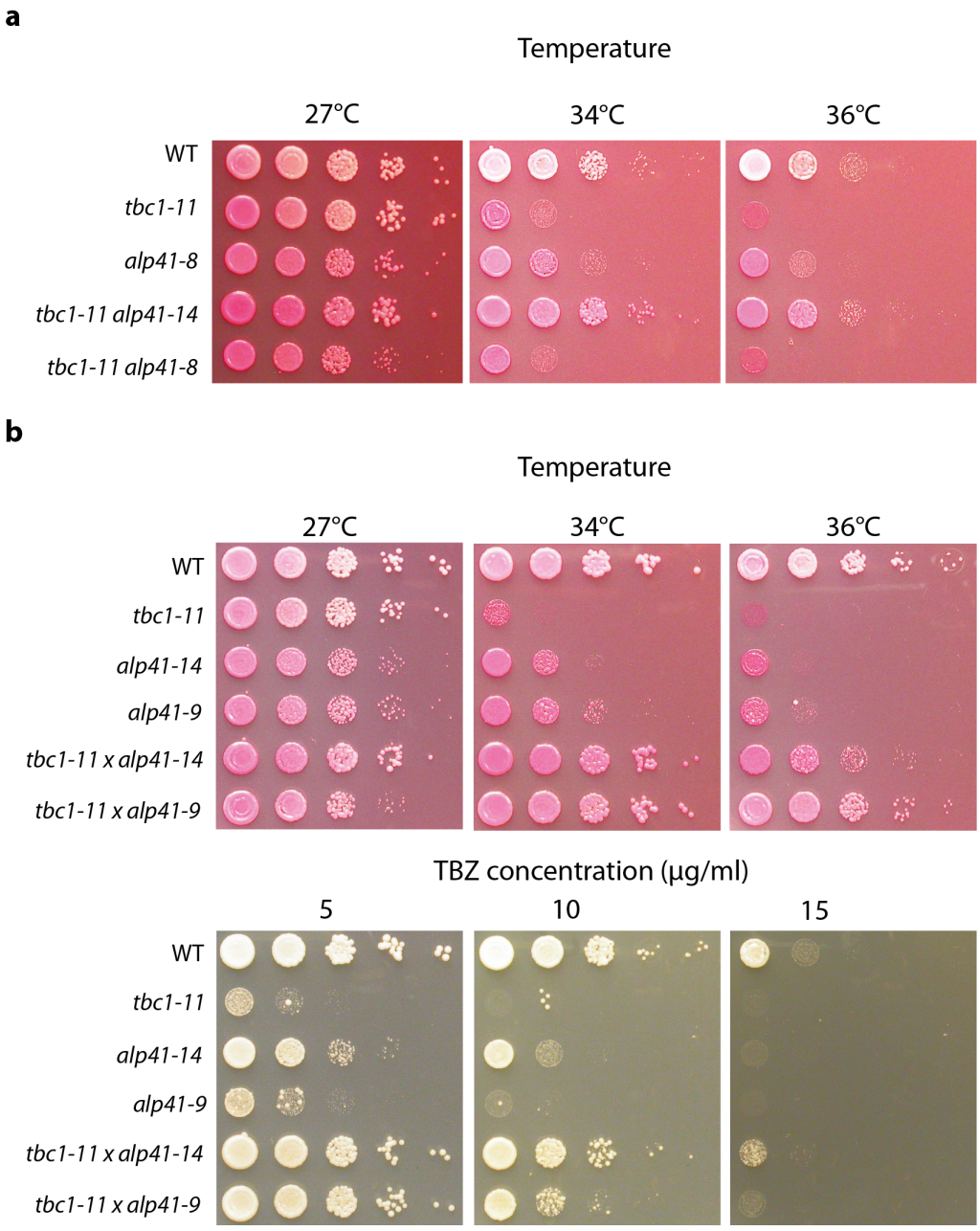

Figure 5.3 Double mutants of *tbc1* and *alp41*

Double mutants were spotted onto YE5S plates with added phloxine B or TBZ. Plates were incubated at various temperatures for 3 days and image taken.
(a) Class I mutant *alp41-8* was crossed with *tbc1-11*. (b) class II mutant *alp41-14* was crossed with *tbc1-11*. The cross with *alp41-9* also shows rescue.

5.4 *alp41-14* is able to rescue the *tbc1* deletion strain

As previously mentioned, *tbc1* is an essential gene which upon deletion leads to cell death. Therefore a strain in which the genomic *tbc1* gene was deleted but was kept viable by introduction of $tbc1^{+}$ on episomal plasmids was constructed. When we crossed this deletion strain with *alp41-14,* the lethality of the strain was overcome and the double mutant was viable. This meant that the *tbc1* deletion became viable in the absence of $tbc1^{+}$ containing plasmids by the *alp41-14* mutation.

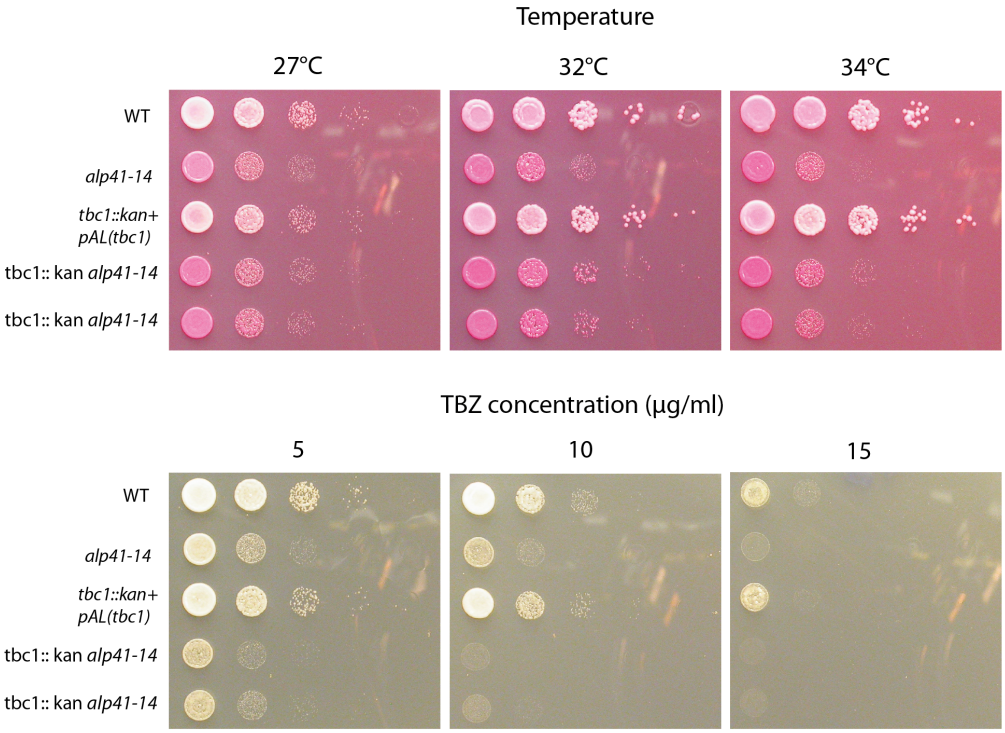

Figure 5.4 *alp41-14* is able to rescue *tbc1* deletion mutant

The *tbc1* deletion mutant was crossed with *alp41-14*. Random spore analysis produced viable spores which were restreaked and spotted onto YE5S plates containing phloxine B or TBZ. The plates were incubated at various temperatures for 3 days and images taken. Plate shows 2 independent clones spotted.

5.5 The overexpression of GTP and GDP bound forms of Alp41 both result in similar microtubule loss

Having gathered evidence that Tbc1 does regulate Alp41 as a GAP, the effect of defective Alp41 regulation was investigated further. Alp41 is a small G protein, which implies that it can exist in either of two states – in the active GTP bound or inactive GDP bound form. To determine how this would affect the microtubules or cell morphology, mutations were introduced into *alp41* which would render Alp41 to be either constitutively GTP or GDP bound. These mutations were gathered from the literature of the related G proteins such as Arl3 and Arl2 (Bhamidipati et al., 2000). These mutations included Q70L, a GTPase deficient form of Alp41 rendering it constitutively GTP bound, T30N which loses the ability to bind with GTP and therefore is constitutively GDP bound, and T47A which induces a defect in the effector loop which inhibits the switching from GDP to GTP. These forms of Alp41 were placed into plasmids with the inducible promoter pREP1 and transformed into a wild-type strain. Upon overexpression, the GDP forms (T30N and T47A) started to show a strong phenotype at 20 hours after incubation in minus thiamine (overexpression condition) and the GTP form (Q70L) showed a strong phenotype after 24 hours of incubation. Strikingly, although the protein is in the opposite state, the phenotypes in cell morphology appeared identical – the cells were severely branched, bent or elongated. The strains were spotted onto EMM plates with or without thiamine to elucidate what the effect of overexpression showed – as Fig.5.5 shows, overexpression of these plasmids is toxic.

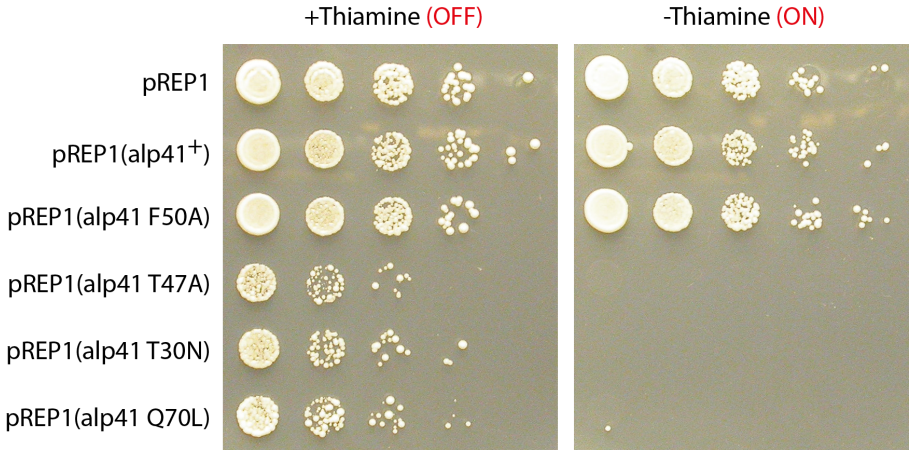

Figure 5.5 Overexpression of GTP/GDP fixed forms of Alp41 was toxic.

Plasmids expressing constitutively GTP or GDP bound forms of Alp41 were transformed into wild-type cells and transformants were spotted onto EMM plates with or without thiamine. Plates were incubated at 27°C for 2 days and images taken.

To observe if microtubule defects were causing this toxicity, the plasmids were transformed into strains with GFP-tagged Atb2 and mCherry-tagged Cut11 (nuclear envelope marker). After incubation in minus thiamine, there was a notable loss of microtubules observed in both states – they were similar to those found in the ts mutants isolated for *tbc1* and the class I mutants of *alp41*. Although there was a range of severity due to the overexpression being via plasmid and not integration (plasmid copy numbers vary among the individual cells), the majority of cells either had no microtubules at all or short defective microtubules – as shown by the representative cells in Fig.5.6b. In order to monitor the timing of induction of this phenotype, cells were observed from 20 hours until 32 hours, every 4 hours. Live cells were taken and observed under the fluorescence microscope as shown in Fig.5.6a. There was a gradual loss of microtubules seen over this time span, although the phenotype appears earlier at 20 hours in Alp41 (T30N) in comparison to Alp41 (Q70L), which does not show a very strong loss of microtubules until 28 hours of incubation. This was further confirmed by quantification, where the cells with microtubule defects were counted for all four time-points (Fig.5.6c). When quantified, it was clear that for both states, after 28 hours of

incubation in minus thiamine less than 20% of the cells contained 'normal' microtubules. Half of the remaining cells showed either no microtubules, and the rest short/broken microtubules.

These microtubule and morphological phenotypes were not seen when the plasmid containing the wild-type Alp41 was overexpressed within these cells (first column, Fig.5.6a). This was also informative as it showed that whichever form the wild-type Alp41 is in within the cells, this was not toxic to the cells, consistent to the result seen in Fig.4.2.

Furthermore, there was also a nuclear membrane phenotype seen upon overexpression (Fig.5.6d) – when quantified, we found that in correlation to the microtubule phenotypes found in the cells, the Cut11 signal showing the nuclear membrane of these cells were either mis-shapen, broken or collapsed. This could be explained by the lack of microtubules resulting in misplacement of the nucleus in interphase cells. In many of the cells it was not possible to find a circular nuclear membrane at all, as it was disintegrated into an aggregate.

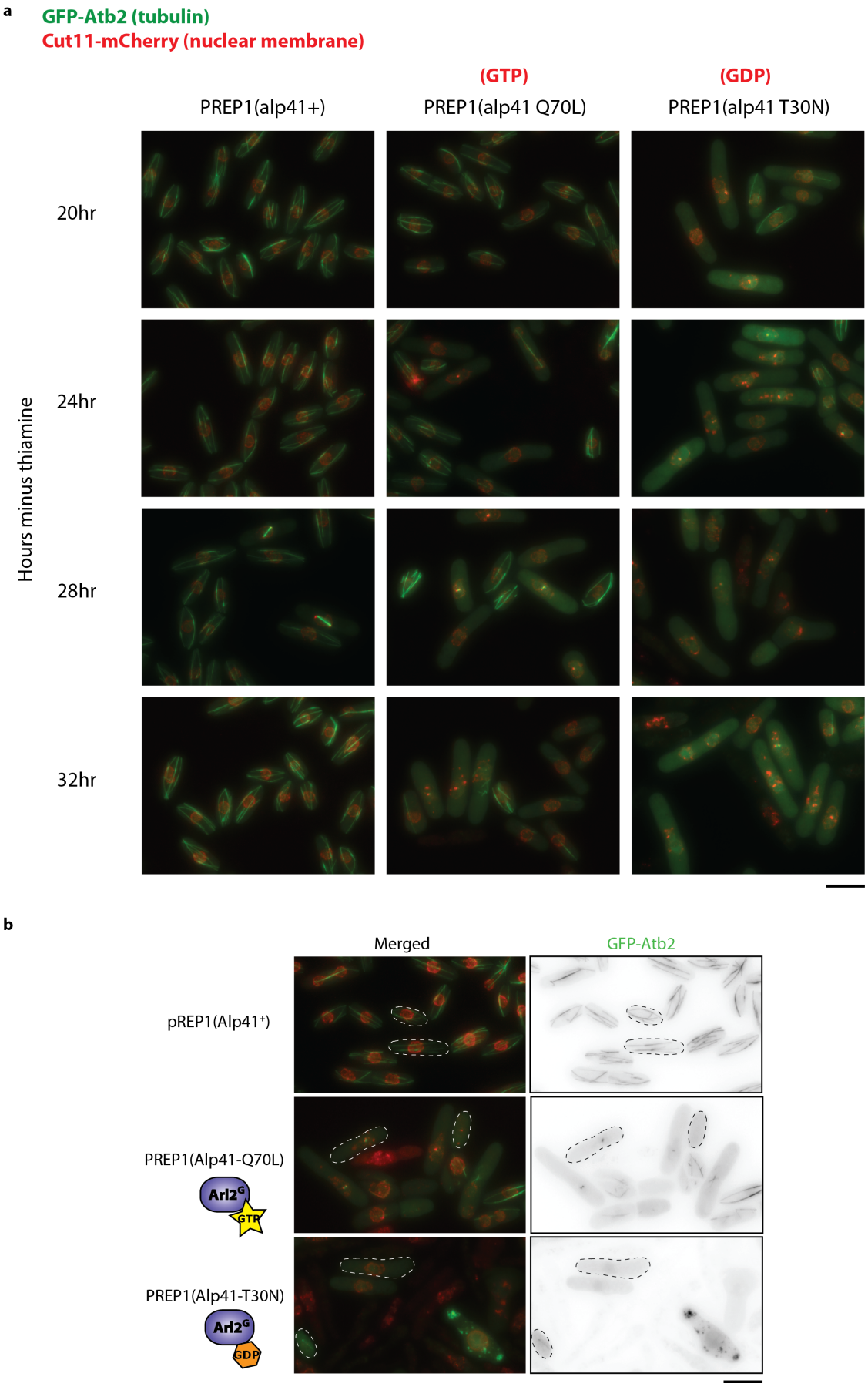
a
GFP-Atb2 (tubulin)
Cut11-mCherry (nuclear membrane)
(GTP)
(GDP)
PREP1(alp41+)
PREP1(alp41 Q70L)
PREP1(alp41 T30N)
20hr
24hr
28hr
32hr
Hours minus thiamine
b
Merged
GFP-Atb2
pREP1(Alp41+)
PREP1(Alp41-Q70L)
Arl2G
GTP
PREP1(Alp41-T30N)
Arl2G
GDP

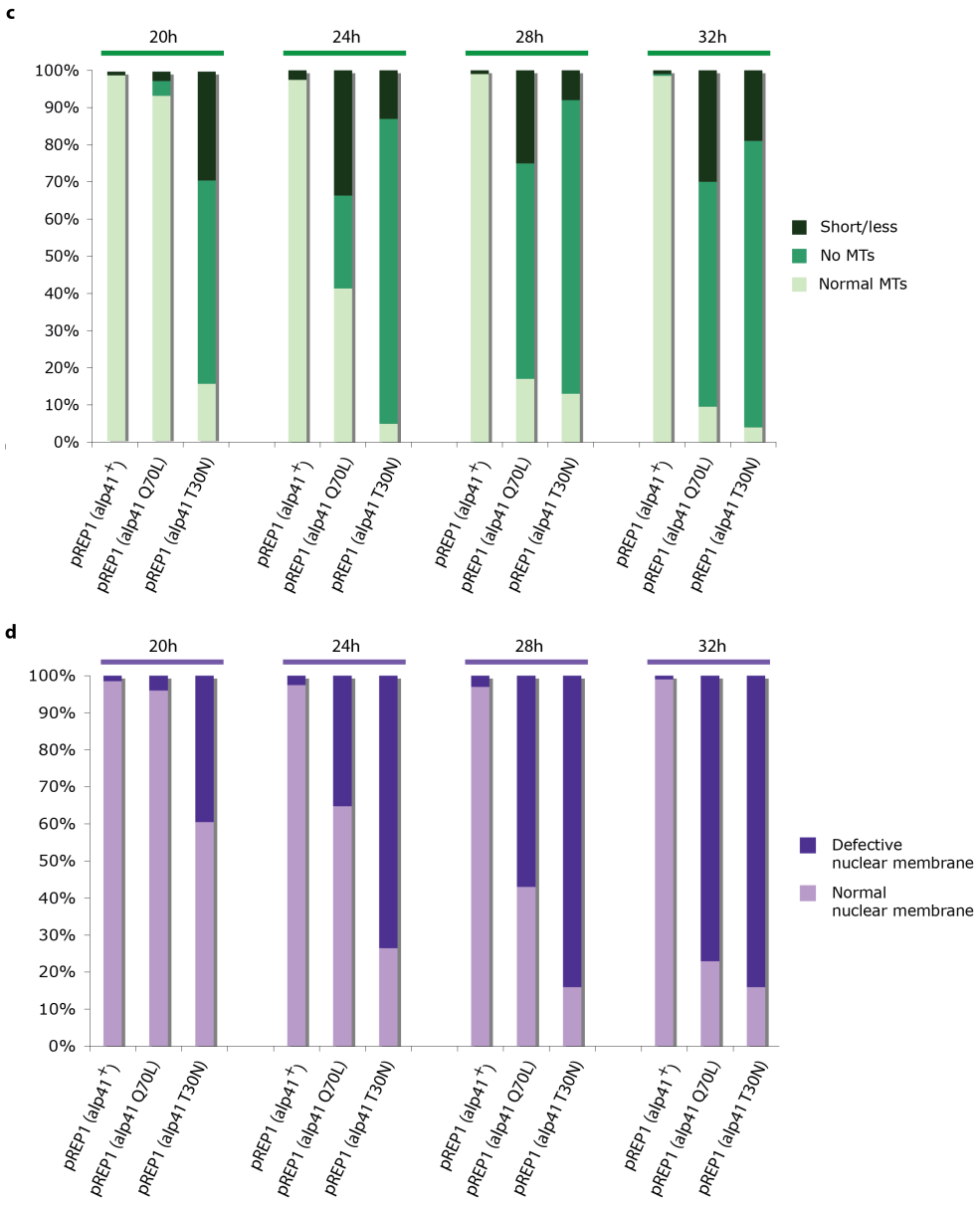

Figure 5.6 Overexpression of GTP/GDP forms of Alp41 lead to microtubule loss

Strains containing GFP-Atb2 and Cut11-mCherry were transformed with exogenous plasmids overexpressing constitutively GTP (Alp41-Q70L) or GDP (Alp41-T30N) bound forms of Alp41. Strains were incubated in minus thiamine conditions for over 20 hours. (a) Every 4 hours, samples were taken and observed under the microscope for microtubule phenotypes. (b) shows a representative figure of cells after 32 hours at minus thiamine. (c) Microtubule phenotypes were quantified by counting 300 cells and classified into 3 classes – short/less microtubules, no microtubules at all or normal microtubules. (d) Cut11-RFP was observed to determine if there was any defect in nuclear membrane shape. "Defective" nuclear membrane phenotypes varied from an abnormal shaped nucleus, no apparent membrane signal, or more than one nuclear membrane structure per cell. Bar: 5μm.

5.6 Overexpression of GTP or GDP bound Alp41 shows varied levels of rescue in temperature sensitive mutants

The overexpression of the GTP or GDP-bound forms of Alp41 causes severe microtubule defects and is clearly detrimental for the cell. From these data I hypothesised that either of these states may be mimicking the various mutants of *alp41* isolated, and may even be able to rescue the ts phenotypes. The plasmids were therefore transformed into both class I and class II mutants and observed to see if there was any rescue of phenotype.

The resulting data was interesting yet somewhat puzzling. There indeed was some rescue amongst some of the mutant/plasmid combinations, but the degree of rescue varied amongst the strains. Fig.5.7 shows the spot tests that were carried out with each of the transformants.

Of the two class I mutants tested, there were different levels of rescue seen. *alp41-7* showed rescue only with the GDP-bound form of Alp41 and the wildtype Alp41 control. However, the complete opposite was seen in *alp41-8,* which was rescued by the GTP-bound form. On the other hand, the class II mutant *alp41-14* was rescued by all forms of Alp41. This distinct difference in rescue emphasised the complexity of these mutants and again suggested that Alp41 may be playing several roles in the cell (discussed further in discussion Chap.5.8).

a

	Class I	Class I	Class II
	alp41-7	*alp41-8*	*alp41-14*
Vector only	-	-	-
pREP1(alp41+)	+	+	+
pREP1(alp41 Q70L)	-	+	+
pREP1(alp41 T30N)	-	-	+
pREP1(alp41 T47A)	+	-	+
pREP1(alp1+)	-	-	-
Mutation	R18G	R18W	E85K

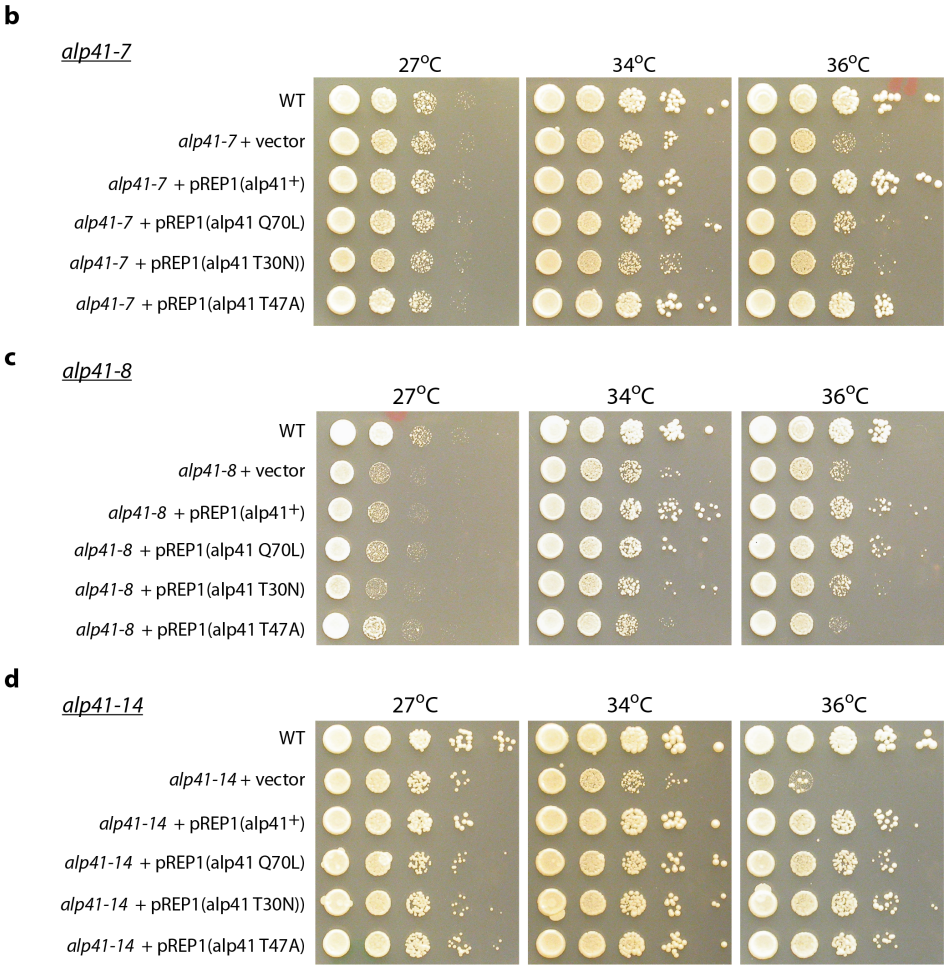

Figure 5.7 Overexpression of GTP/GDP fixed form of Alp41 in *alp41* ts mutants

Class I and class II *alp41* ts mutants were transformed with overexpression plasmids of GTP/GDP bound forms of Alp41. (a) Summary of rescue in all mutant strains. '+' indicates rescue, '-' indicates no rescue. (b)*alp41-7* (c) *alp41-8* (e) *alp41-14* were transformed with pREP1(Alp41-Q70L), pREP1(Alp41-T30N), pREP1(Alp41-T47A), pREP1(Alp41^{+}), or empty pREP1. Transformants were spotted onto YE5S plates and incubated at various temperatures for 3 days.

5.7 Tbc1 interacts with both GTP and GDP bound forms of Alp41

In order to determine if the GTP or GDP state of Alp41 affects its interaction with Tbc1, I used the peptide array assay to see if the *in vitro* binding was affected. The GTP/GDP bound form of Alp41 was purified from *E.coli* and incubated with Tbc1 peptide spotted on the cellulose membrane. Fig.5.8 shows that both forms of Alp41 showed an interaction with the Tbc1 peptide. Furthermore, the interacting regions are similar in both forms, and also with the wild-type Alp41 protein shown previously in Fig.5.2. This shows that at least in *in vitro* conditions, Tbc1 is able to interact with Alp41 whatever state it is in. This is not unexpected, as Tbc1 will be bound to Alp41 in the GTP form before its activity and then to the GDP form, and the region that it interacts is likely to be unchanged in this circumstance. However it will be interesting to see if this balance of GTP or GDP bound Tbc1 is affected by any other interactors of Alp41, for example resulting in competition for binding to Alp41. This was further investigated by searching for potential interactors of Alp41 (see chapter 6).

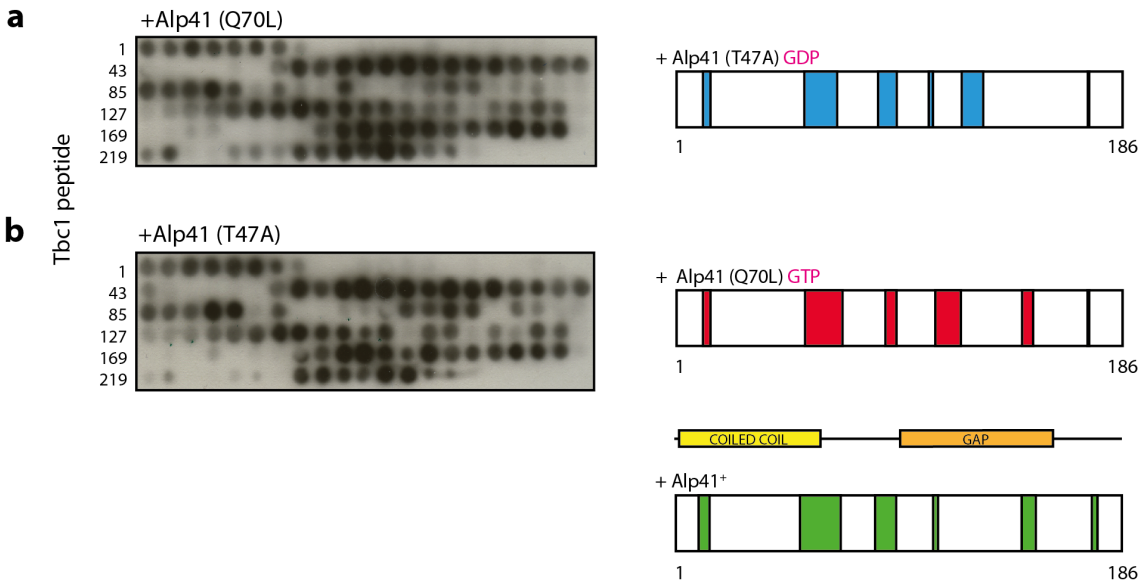

Figure 5.8 Peptide array assay with Tbc1 peptide and various Alp41 proteins

Peptides for Tbc1 were synthesised and spotted onto cellulose membranes. Recombinant HIS-tagged GTP/GDP bound forms of purified Alp41 were incubated overnight with the membrane and a Western blot performed using anti-HIS antibody. The developed films were analysed and a scheme constructed illustrating the regions of binding within the Tbc1 peptide. The scheme from wild-type Alp41^{+} is also shown for comparison.

5.8 Discussion

The genetic interaction between the mutants of *tbc1* and *alp41* suggest that they are involved in the same pathway. The data from the IP and peptide array assay also confirm this, and deducing from the sequence analysis, we conclude that Tbc1 acts as a GAP for the Alp41 G protein.

Due to the nature of Alp41 as a small G protein, we investigated how the GTP or GDP state of the protein affected the cell when overexpressed. We achieved this by constructing overexpression plasmids by point mutation according to literature. Initially, we had expected the phenotypes to differ between the two states, but on observing the microtubules, we found that the phenotypes were identical despite there being some discrepancy in timing of appearance. These identical phenotypes shown in both the GTP and GDP bound state of Alp41 was unexpected yet striking. The two conditions should render the G protein to be in complete opposite states to one another, but they showed the same phenotype. This could be explained by the importance of the G protein continuously cycling within the two states (Fig.5.9). Examples of such G proteins can be seen in fission yeast Ran GTPases such as Spi1, where the balance of the GTP and GDP-bound forms is important through continuous cycling (Matynia et al., 1996). This may also be the case for Alp41, where at least for the microtubule phenotype, the importance lies in the cycling between the two states and their balance. This could also explain the similar phenotypes seen in the *tbc1* ts mutants – if Tbc1 cannot function properly as a GAP, it will interfere with this balance. More specifically, in the case of the *tbc1* mutants, Alp41 would be fixed in the GTP form, as its GAP function would be compromised meaning it would not be able to aid GTP hydrolysis.

Why this results in the loss of microtubules is a point of interest, and will be further investigated in Chapter 6 by observing the possible interactors of Alp41 and its role in microtubule formation. It was however clear that in both cases, the microtubules were either gone or defective. Any microtubules that were left were short, defective or disorganised, and almost no proper microtubules were seen during interphase. This was

similar to the class I *alp41* mutants and the *tbc1-11* mutant. It was also notable that there were almost no mitotic cells in the cells observed.

Hypothesising that maybe the *alp41* mutants could be rescued by the overexpression of either the GTP or GDP bound form of Alp41, these plasmids were transformed into the mutants. However data showed varied levels of rescue amongst the different *alp41* mutants isolated, even within the same class. This apparent discrepancy between the same type of mutant was intriguing – the two mutants clearly showed the same microtubule phenotype but the degree of rescue was so different. This may be explained by the phenomenon seen in the previous section – the two mutants may be defective in opposite forms – one may be mimicking the GTP form of Alp41 and the other the GDP form. Therefore even if one of the forms of Alp41 is sufficient, the balance cannot be kept if the mutant is defective in cycling – the opposite overexpression plasmid may be able to rescue each nucleotide form, but the microtubule phenotype may be the same due to defective cycling. Also interesting is that these two mutants are actually mutated at the exact same residue, just into two different amino acids – R18G and R18W, respectively. The fact that such a small difference in mutation can make such a huge impact on the cell and its fate is interesting. What sort of defect these mutations cause may be the key to understanding this. In order to characterise and distinguish the difference between the mutations in the different *alp41* mutants, we attempted to map the mutation site on the structure of the G protein based upon the structure of the Arl3-RP2 interaction (Evans et al., 2005). However, we were unable to predict an obvious or clear structural or functional defect that these mutations could have, and so it remains elusive how the mutations may affect the function of Alp41.

Considering that *alp41-14* was an outlier regarding microtubule phenotype, the difference in rescue may not be so unexpected. This mutant obviously is defective in an alternative way to the other mutants, and the fact that it can be rescued by any form of Alp41 may suggest that it is somehow a milder mutant in terms of G protein function – for example it may be cycling-competent but defective in another microtubule related function.

Also interesting to note was the fact that the overexpression of these plasmids were unable to rescue the *tbc1* mutant (data not shown). Assuming that this mutant has defective GAP activity, it was clear that providing either the GTP or GDP bound form of Alp41 was not enough to recapitulate the wild-type phenotype. Tbc1 is able to interact with both the GTP and GDP bound forms of Alp41 – this may suggest that in wild-type situations Tbc1 is able to, and is required to, interact with both cycling forms of Alp41.

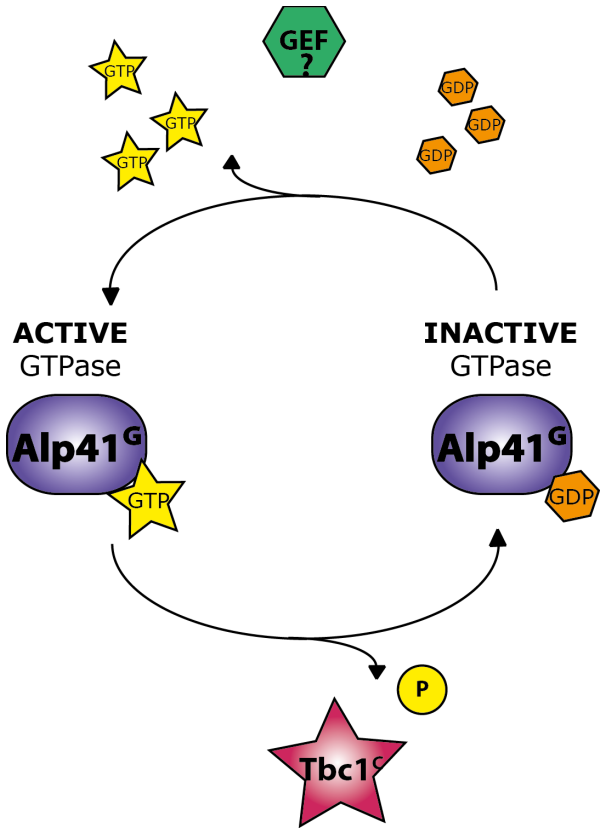

Figure 5.9 The GTP/GDP cycle must be circulating for proper Alp41 function

For proper function of Alp41 there must be constant cycling between the GTP and GDP state. Tbc1 acts as a GAP for Alp41 to render it inactive after hydrolysis. At the moment, how Alp41-GDP is converted to Alp41-GTP is unclear, as the GEF which exchanges the GTP to GDP remains unidentified.

Chapter 6. Alp41 has an important role in Alp1 regulation

So what exactly is the function of Alp41? Data suggested its involvement in the tubulin folding pathway, but how and when still remained unclear. Its role as a G protein may be to regulate the other cofactors in the pathway, or potentially other proteins in microtubule regulation. By looking for potential interactors of Alp41, this question was pursued.

6.1 Yeast 2-Hybrid Screening resulted in no potential candidates for interactors of Alp41

In order to look for an interactor, a Yeast 2-Hybrid (Y2H) screen was carried out using Alp41 as a bait (See Materials and Methods for details). From the first set of screening, 12 positive clones shown in Fig.6.1 were picked up and sequenced. The hits included Ado1 – an adenosine kinase, translation elongation factor eEF3, Plb1 – a phospholipase B homologue, Uhp1 – a ubiquitinated histone-like protein, ATPase beta subunit Atp2, and some predicted phosphatase activator or cell surface glycoproteins. None of the hits were clearly involved in the cofactor pathway or microtubule regulation, and therefore the hits were dismissed as either being false positives or interactors that would not be involved in microtubule biogenesis.

Although the screening did not give any obvious hits, the idea that Alp41 must have other interacting partners was not dismissed. It is clear that the screening can produce false positives, as well as miss obvious hits. For example this screening did not pick up Tbc1, which by IP clearly interacted with Alp41. Therefore although the Y2H screen may in cases yield some useful candidates, unfortunately in this case it was not fruitful.

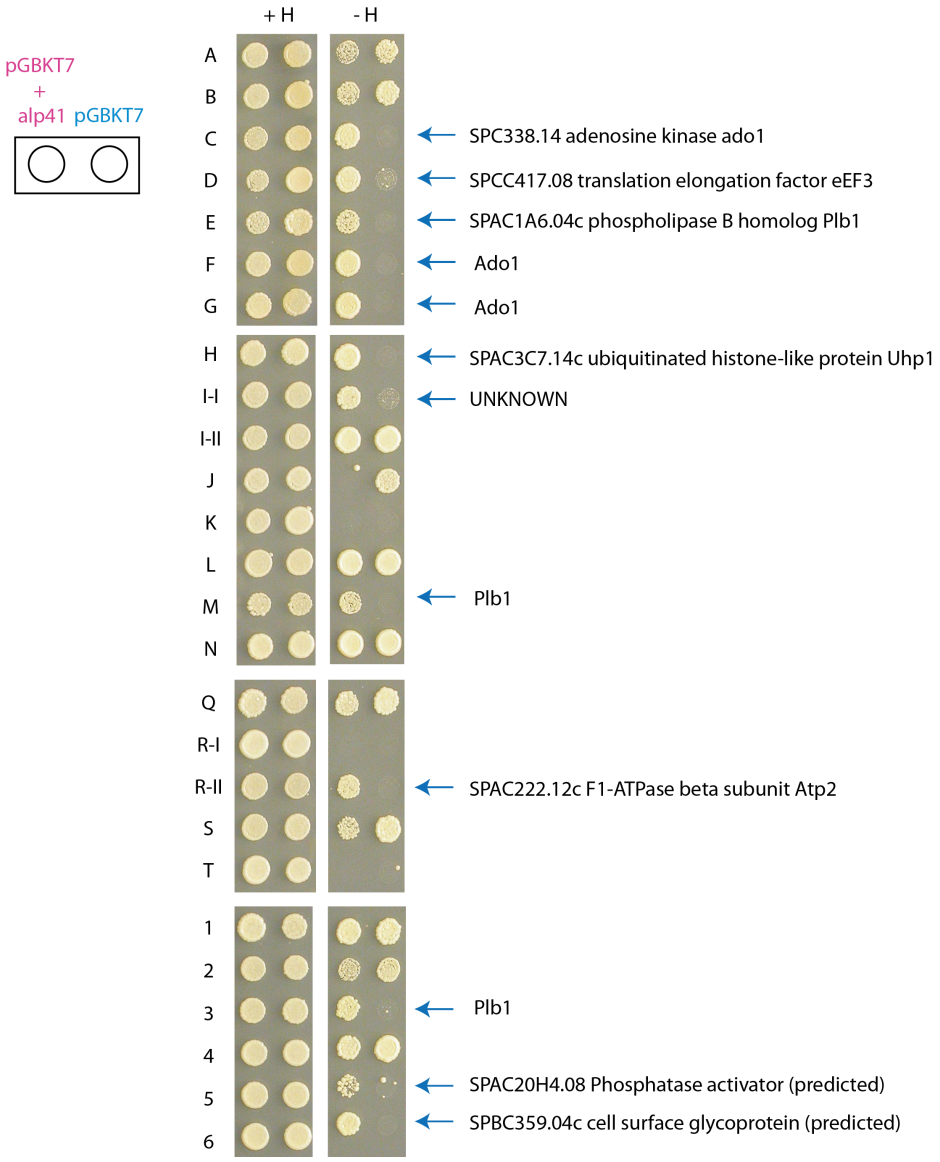

Figure 6.1 Yeast 2-Hybrid screening for Alp41 interactors

The isolated candidate plasmids were transformed into pGBKT7 (*alp41*) and pGBKT7 (empty) strains and the transformants spotted onto plates with or without histidine as shown in the schematic. If there was growth of the strain containing *alp41* but not on the empty strain, it was determined as being positive and the isolated plasmids were sequenced. The result of the sequencing is shown adjacent to each of the positive spots.

6.2 Alp41 did not interact with the other cofactors by Yeast 2-Hybrid

Whilst carrying out the Y2H screening, I had constructed a bait plasmid for Alp41 which was transformed into a yeast strain. By constructing and transforming prey plasmids of the other cofactors – Alp1, Alp21 and Alp11, into the strain containing the bait plasmid pGBKT7-*alp41*, I looked for potential interactions between these combinations.

However, as seen from Fig.6.2, none of the cofactors showed an interaction under various concentrations of 3AT (See Materials and Methods). This was interesting, as the original speculation was that Alp41 was involved in the regulation of one or more of the cofactors. However it did also strengthen the idea that Alp41 was not directly involved in the cofactor pathway – and it could therefore not be classified as a cofactor. I did not rule out the idea of the cofactors being involved with Alp41 due to the nature of the Y2H assay being inconclusive, so I decided to investigate further by different techniques to find what Alp41 could be regulating.

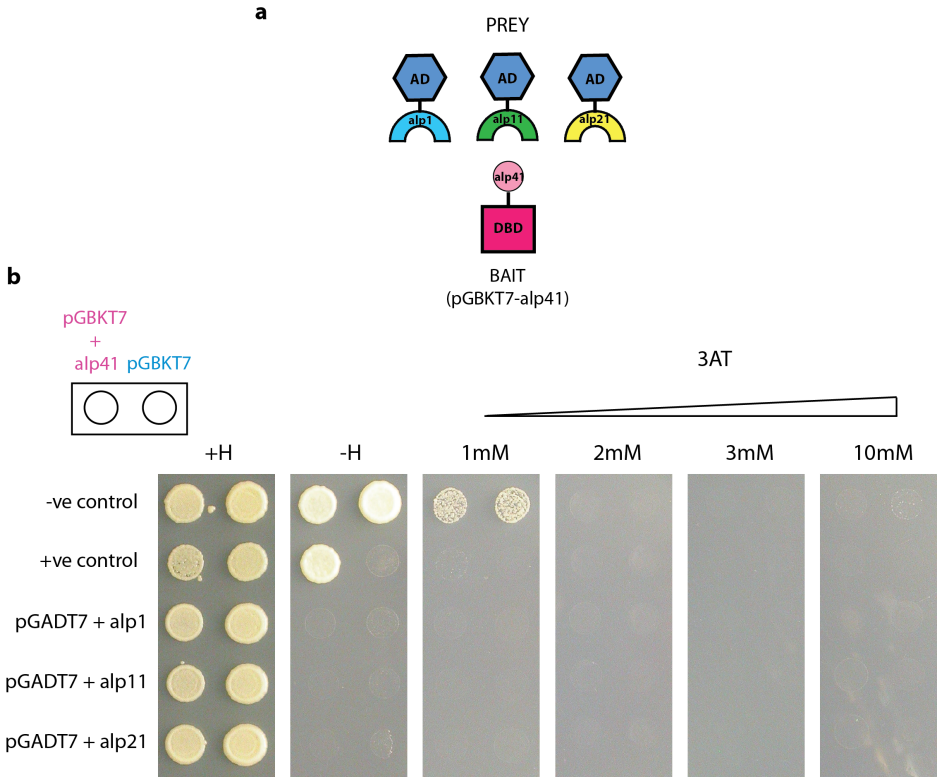

Figure 6.2 Alp41 and its interactions with the other cofactors by yeast-two-hybrid

Plasmids were constructed as shown in (a) and transformed into strains containing pGBKT7(*alp41*) or pGBKT7(empty). They were spotted onto –HIS plates containing increasing concentrations of 3AT and the growth observed after incubation at 27°C for 2 days.

6.3 Alp1 is a potential interactor of Alp41

Since there were no candidates found by Y2H screening, I turned to the literature for potential candidates of Alp41, which stated that its human homologue Arl2 showed an interaction with Cofactor D, the Alp1 homologue (Bhamidipati et al., 2000). Cowan and colleagues showed that these 2 proteins were able to interact by *in vitro* binding. In order to investigate this further, we carried out IPs to observe if this interaction could be seen in our fission yeast system.

6.4 Interaction between Alp41 and Alp1

6.4.1 Alp41 is unable to interact with wild-type Alp1 by IP

Triple tagged strains were constructed in which Alp1 and Alp41 were tagged with 3pk and GFP, respectively (Tbc1 was also tagged with 3HA in this strain but was not used for this experiment). Alp41 was overexpressed in this strain, similar to the strain used in Chap.5.1. Protein was extracted and 5 mg used for each IP reaction against either GFP or pk. Surprisingly, in the IP performed against GFP (Fig.6.3a), no protein was co-immuno-precipitated in either the single-tagged control strain or the double-tagged strain. The reciprocal IP was also performed, but the same result was seen and there was no clear interaction between Alp1 and Alp41.

However, as there was strong evidence from the literature suggesting that Alp41 and Alp1 would interact, I decided to take a different approach to see if they would interact.

6.4.2 Alp41 can only interact with Alp1 when in the GDP-fixed state

Upon observing that Alp1 cannot interact with Alp41 in its wild-type state, I decided to investigate if the GTP/GDP nucleotide state of Alp41 has an effect on the interaction. I therefore constructed strains containing an overexpression plasmid of GFP-tagged GTP/GDP-bound Alp41. The protein was extracted from these strains and an IP performed against GFP.

Strikingly, in the IPs performed under the same conditions with the GTP and GDP bound forms, there was a clear difference in interaction. The GTP bound form using the plasmid containing pREP1(Alp41-Q70L) did not co-immuno-precipitate Alp1, similar to the wild-type plasmid. However for the GDP bound form containing pREP1(Alp41-T47A), we saw a clear interaction with Alp1.

In order to confirm this GDP-bound nucleotide specific interaction, the reciprocal IP was carried out against pk, which Alp1 was tagged with. However, the result was not as clean due to the size of GFP-Alp41 being very close to the size of the heavy chain IgG fragment. Therefore I performed the IP three times to confirm that the results were consistent, using 3 different amounts of protein – 1.5mg, 3mg and 7mg. All these showed the same result for both sets of IPs (Data not shown).

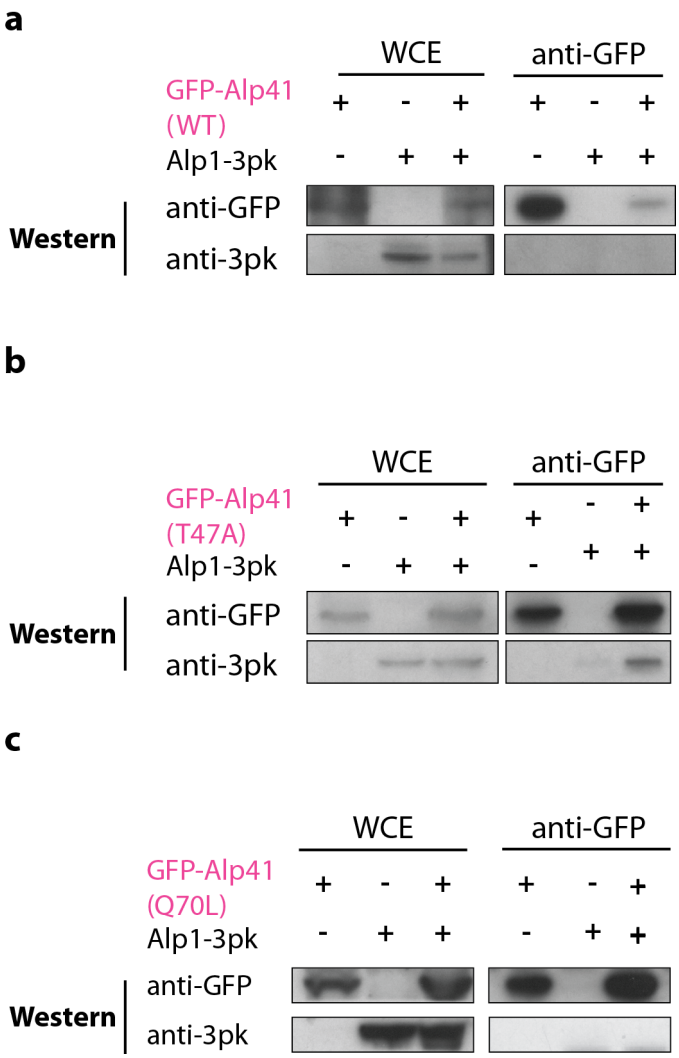

Figure 6.3 Interaction of GTP/GDP bound forms of Alp41 with Alp1

Protein extracts from strains with GFP-tagged Alp41 and 3pk-tagged Alp1 were immuno-precipitated against GFP. For each blot, first lanes contains single tagged control strain, the third the double tagged strain. WCE= whole cell extract, 0.01% compared to IP loading volume. (a) GFP-tagged wild-type Alp41 (b) GDP bound Alp41 (T47A) (c) GTP bound Alp41 (Q70L).

6.4.3 Peptide array shows binding of Alp41 and Alp1

In order to further confirm the interaction between Alp41 and Alp1, I used the *in vitro* peptide array assay to see if this interaction could be seen *in vitro*. The previously described IPs are all performed using whole cell extracts from the yeast strain, so a more direct assay was used for observing such a distinct binding pattern.

Interestingly, when the Alp1 peptide arrays were incubated with recombinant Alp41, the array showed a clear interaction, indicated by the many positive spots seen on the blot in Fig 6.4a. The previous IP showed that the wild-type of Alp41 did not interact with Alp1, so this was unexpected. I then further investigated this interaction to see if this was still seen when the GDP (Fig.6.4b) or GTP (Fig.6.5c) bound form of the recombinant HIS-Alp41 was used instead.

Intriguingly, there was no drastic difference in the interaction between the two forms of Alp41 and its interaction with Alp1. Fig.6.4d shows the merged image of the two forms to accentuate the differences seen in the two binding patterns. Due to the difference in binding in the IP, I was expecting to see a clear difference in the binding patterns. However although there were some ambiguities, similar regions of Alp1 seemed to bind with Alp41. Fig.6.5 shows the summarised map of the interaction regions of the Alp1 protein. As seen from this, the regions were very similar and although there were some small differences, the majority of the regions were almost identical.

Many of these spots were positive, suggesting that it is not a very specific or exclusive site of Alp1 that Alp41 is able to bind to. This is not unexpected, as the peptide array is based on the amino acid residues and does not take into account any of the folding or the 3D structure of the protein. The protein could be folded in such a way that the interacting residues are in close proximity to one another but this would not be shown by the peptide which is solely the amino acids spotted onto the membrane. Simply changing one of the amino acid residues – T47A for the GDP bound form and Q70L for the GTP bound form, may not affect the binding when in the form of simple amino acid residues. Also, because of the nature of the synthesised peptide being 20 amino acids per spot, altering one of them may not have such a huge affect on the interaction,

whereas it may have a drastic effect on the structure. This structural difference may affect the crucial binding sites of the protein, which may affect Alp1 binding.

Although this result could not determine a clear domain in which the proteins interact and did not show the nucleotide specific tendency of the IP, it was an additional result to the IPs that allowed us to confirm that Alp41 and Alp1 do directly interact.

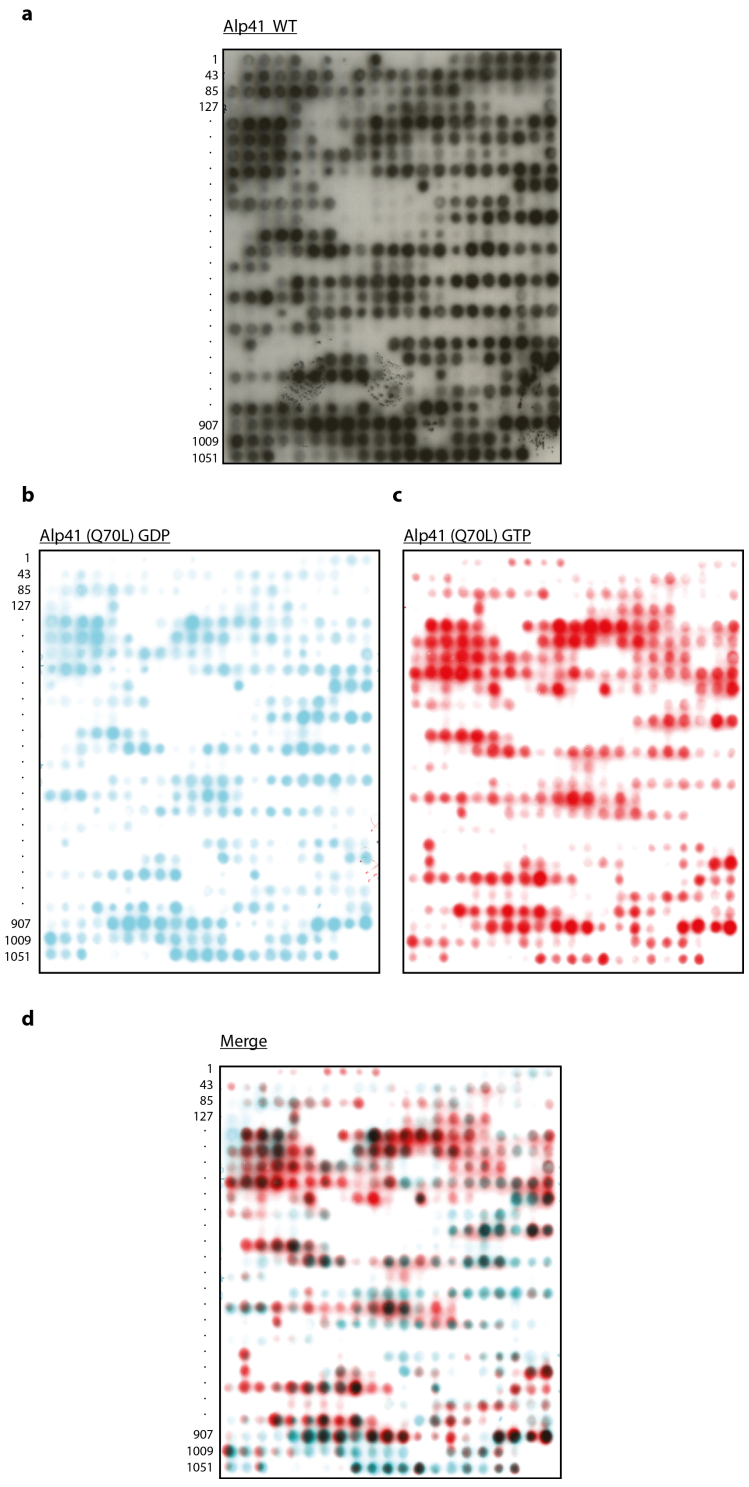

Figure 6.4 Peptide arrays of Alp1 incubated with recombinant Alp41 protein

Alp1 peptides were synthesised and spotted onto a cellulose membrane which was incubated overnight with purified (a) wild-type Alp41 (b) Alp41 (T47A) or (c) Alp41 (Q70L). Spots show regions of interaction. (b) and (c) have been artificially coloured and (d) shows the merged image of these two blots to accentuate the differences in the pattern.

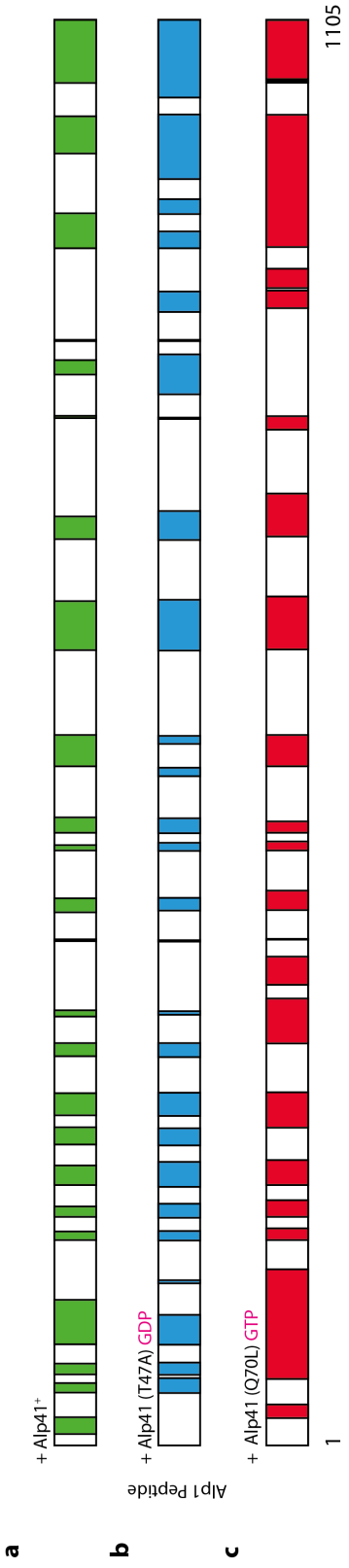

Figure 6.5 Peptide array assay result for Alp1 peptides

Interacting regions from blots shown in Fig.6.4 were analysed from detected blots and summarised into the above schematics.

6.4.4 *alp41* ts mutants are synthetic lethal with the *alp1* ts mutant

In order to further investigate this interaction between Alp1 and Alp41, I crossed the *alp41* ts mutants with the temperature sensitive *alp1-1315* mutant (Hirata et al., 1998) and tetrad analysis performed to see any genetic interactions. Interestingly, all the *alp41* ts mutants tested were synthetically lethal with *alp1-1315*. This was confirmed by random spore analysis where there were no viable spores resulting from the cross between the mutants which were resistant to both selections. This substantiated the finding that Alp1 and Alp41 interact and are involved in regulating one another, and as both *alp1* and *alp41* are essential for cell viability, synthetic lethality suggests that they play roles in the same pathway. It also suggests that both *alp41* and *alp1* may have several roles within microtubule biogenesis that is not solely dependent on this interaction, which is consistent to the idea that Alp41 interacts with Tbc1 whilst Alp1 interacts with other proteins in the pathway.

tbc1	alp1	Viable	Non-viable
+	3pk	28	0
+	-1315	10	7
-11	3pk	19	1
-11	-1315	0	23

tbc1-11 alp1-1315 *tbc1-11 alp1-1315 / tbc1+ alp1-1315*

alp41	alp1	Viable	Non-viable
+	3pk	9	0
+	-1315	6	3
-14	3pk	8	1
-14	-1315	0	9

alp41-14 alp1-1315 *alp41+ alp1-1315*

alp41	alp1	Viable	Non-viable
+	3pk	31	0
+	-1315	12	7
-9	3pk	17	2
-9	-1315	0	31

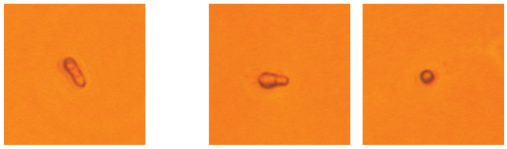

alp41-9 alp1-1315 *alp41-9 alp1-1315 / alp41-9 alp1-3pk*

Figure 6.6 Synthetic lethality of *alp1* double mutants

alp1-1315 was crossed with ts mutants of *tbc1* and *alp41* to observe synthetic lethality. Table shows viable and non-viable spores after incubation, which have been quantified as a chart. The figures below show the non-viable spores. All 3 double mutants show synthetic lethality.

6.5 Overexpression of Alp1 cannot rescue ts mutants of *alp41* nor *tbc1*

Alp1 is known to function in the tubulin folding pathway. However the fact that it interacts with Alp1, and with its GDP form in particular, suggest that Alp1 may have additional roles apart from the capture of β-tubulin and supercomplex formation. I decided to further investigate this Alp41-Alp1 interaction by looking at the function of Alp1.

Firstly, an overexpression plasmid of Alp1 was constructed and transformed into wild-type cells. The overexpression plasmid was used in order to ensure that there was sufficient overexpression. The plasmid allows the cell to have more than 2 copies of the gene – 1 from the endogenous gene, and at least 1 (or more) from the plasmid. As previously reported (Hirata et al., 1998), the overexpression was severely toxic to the cell (Fig.6.7a). I then overexpressed Alp1 in *alp41* mutants to observe if the temperature sensitivity may be rescued. As shown in Fig.6.7b and c, this was not the case. In fact, consistent to the toxicity seen in the wild-type cells, Alp1 in excess rendered *alp41* mutant cells sick (comparing –T and +T), even at the permissive temperature. The fact that Alp1 did not rescue the growth of *alp41* mutants suggests that the role of Alp41 is perhaps not only to regulate Alp1. This would be reasonable, assuming that the GTP bound form of Alp41 must have some other function. Similarly, overexpressed Alp1 was unable to rescue *tbc1* alleles (comparing empty plasmid and plasmid + Alp1; Fig6.7 c). This signifies the importance of Tbc1 in the tubulin folding pathway – excess Alp1 is not enough to overcome the defects in supercomplex formation and possibly the regulation of *alp41* as a GAP. This toxicity of Alp1 was pursued further.

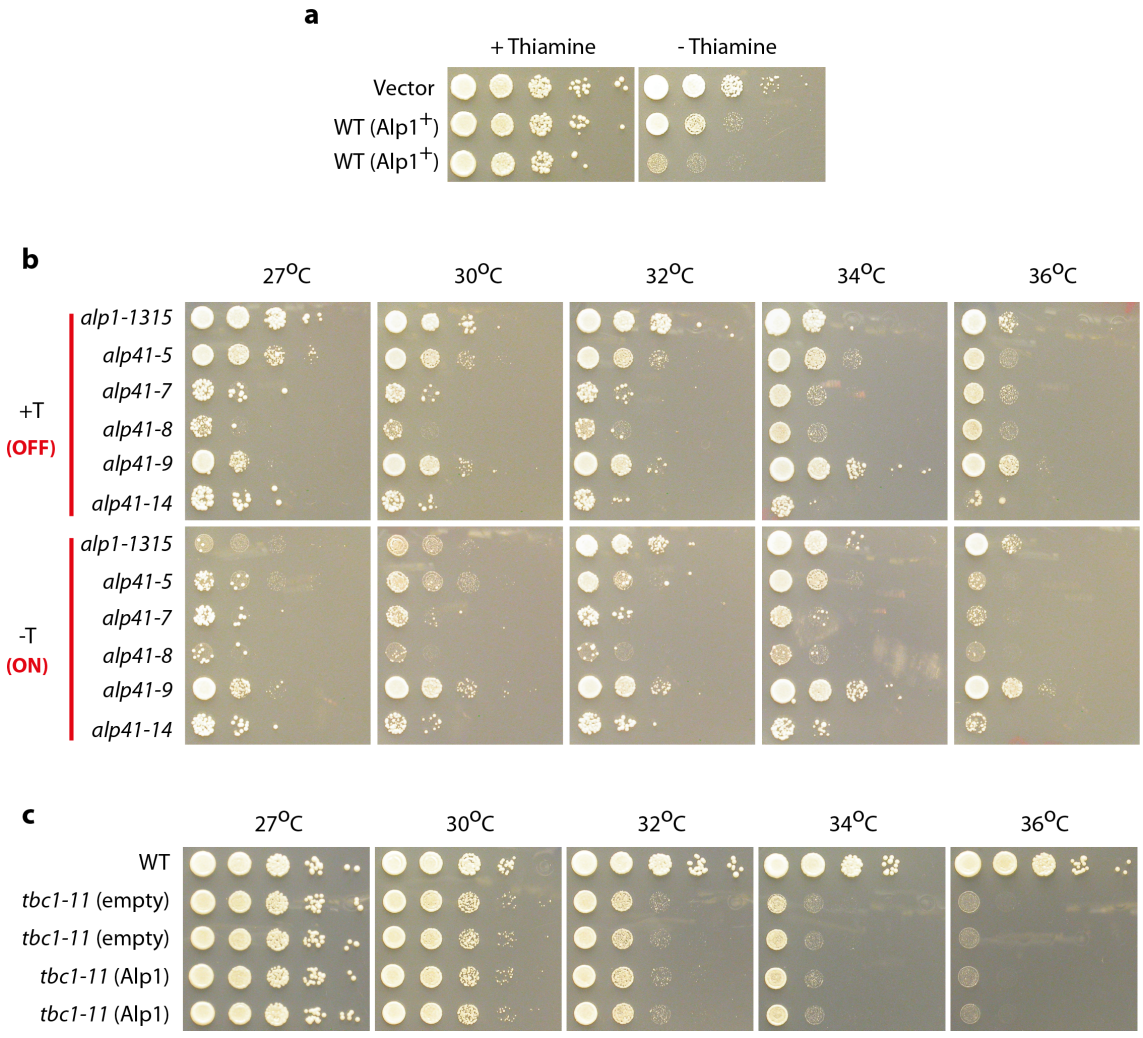

Figure 6.7 Alp1 overexpression in mutants

An overexpression plasmid of Alp1 was transformed into each of the shown mutants and the transformants spotted onto YE5S plates (a,c) or EMM plates with or without added thiamine (b). (a) overexpression of Alp1 in wild-type cells. Two independent transformants are shown. (b) Alp1 overexpression in *alp41* ts mutants. The cells are sicker in –T (overexpression) than +T. (c) Alp1 overexpression in *tbc1-11*.

6.6 Alp1 overexpression causes microtubule defects

In order to investigate the effects of having excess Alp1 in the cell on microtubule morphology, an overexpression plasmid of Alp1 tagged with GFP in a pREP1 background was transformed into a strain with Atb2 tagged with mCherry. The cells were incubated overnight in minimal media with thiamine, washed, and further incubated in minimal media minus thiamine for over 20 hours. The cells were then observed under the fluorescence microscope to observe whether the overexpression of Alp1 had any effect on the microtubule structure or the morphology of the cells.

As seen in Fig.6.8, the cells had an obvious morphological defect. They were drastically elongated or mis-shapen, and appeared bent or branched. The microtubules also showed a strong phenotype – they appeared short and fragmented, or the cells lacked microtubules altogether. Most striking of all, the GFP-Alp1 signal strongly co-localised with the remaining microtubules. The Alp1 signal was very strong, and localised on the microtubules in interphase and mitosis. Previous data suggested that Alp1 may be a microtubule associated protein (Hirata et al., 1998), but it was the first time that this co-localisation had been seen to such an extent.

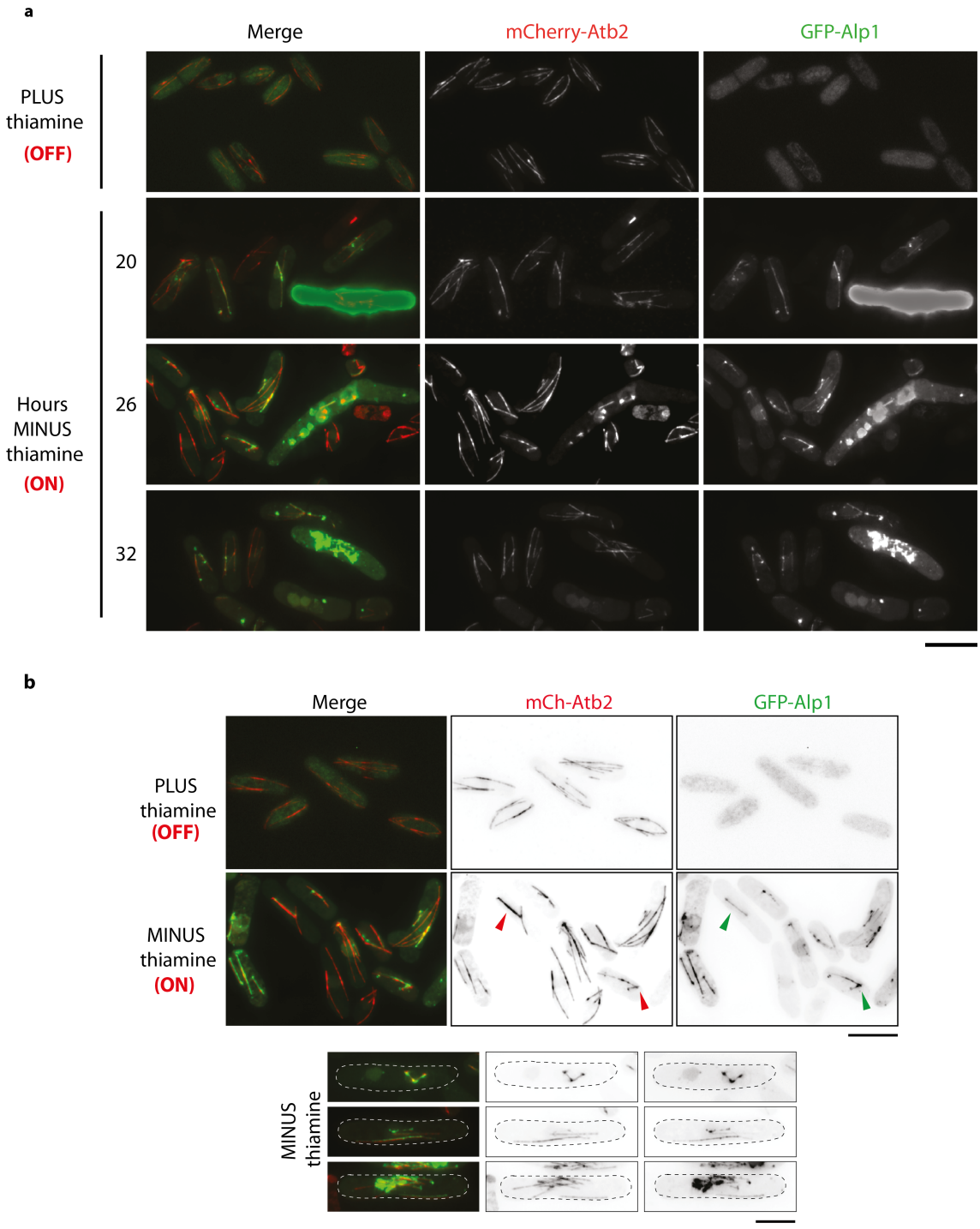

Figure 6.8 Alp1 overexpression causes microtubule phenotypes

Cells transformed with the overexpression plasmid of Alp1 was grown in EMM media minus thiamine for up to 32 hours. (a) Time points were taken at 20, 26 and 32 hours and samples observed under the microscope to follow gradual appearance of phenotype. (b) shows a field of representative cells where the phenotype is clear. Red arrowheads indicate interphase microtubules, green arrowheads show mitotic spindle. Individual cells are also shown in lower panel. Bar: 5μm.

6.7 Discussion

Tbc1 acts as a GAP for Alp41, but what exact function Alp41 has, was previously unclear. In order to search for an interacting partner of Alp41 that could be involved in its regulation, a Y2H screen was carried out which unfortunately did not give us any interesting candidates. However, consulting the literature suggested that Alp41 may bind with Alp1 – *in vitro*, the human orthologues Arl2 and cofactor D were able to interact.

Initially, when we tried to assess this interaction we found that Alp1 did not interact with wild-type Alp41. This was surprising considering the mammalian orthologues showed a clear interaction. However it was suggested in the literature that the GTP/GDP bound forms of Arl2 showed a difference in the interaction with cofactor D – the GDP bound form of Arl2 interacted more readily with cofactor D (Bhamidipati et al., 2000). This led us to believe that in fission yeast there may also be nucleotide dependency in this interaction. Therefore we constructed GDP and GTP bound forms of Alp41 tagged with GFP for further IP experiments. The data showed a clear interaction between the GDP bound form of Alp41 with Alp1, but not for the GTP bound form of Alp41. This was consistent with the mammalian data, and confirmed that Alp1 was an interacting partner of Alp41.

When observed by peptide array assay, the interaction was seen in all forms of Alp41. However, this type of assay does not take into consideration the folding of the protein, and therefore explain the similar binding seen between the forms of Alp41. Also, this maybe suggests that, *in vivo*, another interactor of Alp41 that is blocking the interaction of GTP-Alp41 and Alp1. This interactor would block the interaction seen by IP but not the peptide array assay.

In order to confirm the regulation of Alp41 and Alp1, we crossed mutants of both genes and observed the phenotype. We found that the double mutants were all synthetic lethal. Overexpression of Alp1 was also unable to rescue the mutants of *alp41* and *tbc1*. These

genetic interaction data also enabled us to confirm that these proteins all had roles in the same pathway.

For proper microtubule function I deduced that the continuous nucleotide cycling was important. However in the case of interacting with Alp1, it specifically depended on Alp41 being bound to GDP. This may give us an insight into its regulation – there may be an additional factor that may interact with Alp41 when it is in its GTP form. There stands the possibility that Tbc1 could be this other interacting partner. Previously mentioned data has shown Tbc1 to interact with wild-type Alp41. Deducing from these two results, wild-type Alp41 may preferentially be in the GTP-bound form, interacting with Tbc1. When there is continuous cycling of the pool of the GTP-bound Alp41, and some of it becomes GDP-bound, it may able to bind to and regulate Alp1.

So in what way is Alp41 regulating Alp1? Alp1's known function is to capture the β-tubulin monomer and consequently form the supercomplex with the α-tubulin bound Alp21. The function it plays here is as a tubulin-GAP for the trigger of heterodimer release. However there have been studies suggesting that cofactor D could have a destructive role on microtubules (Bhamidipati et al., 2000). Leading on from this study, Alp1 was overexpressed in wild-type fission yeast cells to observe if such a phenomenon could be observed.

Upon overexpression of GFP-Alp1, the microtubules were depolymerised. The cells showed severe morphological defects and the microtubules were either short, fragmented, or gone altogether. Remarkably, there was significant GFP signal co-localising with the remaining microtubules. It was also visible that the longer we incubated the cells in the overexpression conditions for, the more severe the microtubule phenotype became. In addition, in the shorter and defective remaining microtubules, the co-localising Alp1 signal became stronger. Intriguingly, this suggests that the more Alp1 there is on the microtubule, the more defective the microtubule becomes, and therefore the cells lose their microtubules. This not only confirmed that Alp1 was a MAP, but it also indicated that the localisation of Alp1 on the microtubules possibly led to their depolymerisation. This could be a result of a number of things – the

'painting' of the microtubules with Alp1 may be directly dissociating the heterodimers and/or the protofilaments themselves. Alternatively, the Alp1 binding to the microtubules could be shielding anything else (such as additional heterodimers) from accessing and binding to the microtubule. This would cause the eventual shortening of the microtubule until there remains none in the cell. This confirmed that having excess of Alp1 within the cell is detrimental to the microtubules and therefore the cell itself.

The data suggests that Alp1 has a dual role – it 'creates' and 'destroys' microtubules. This feature of Alp1 is discussed further in the next discussion chapter.

Chapter 7. Discussion

The microtubule is an essential cytoskeletal structure in the cell, required for multiple functions such as cellular transport, cell migration, and importantly, cell division and mitosis. The field is an active area of research and extensive studies have been carried out on aspects such as structure, regulation and function of these flexible and multitasking structures. With new advances in the field and the availability of new research techniques such as microscopy and *in vitro* studies, novel findings are constantly reported.

However, the fundamental aspects of the biogenesis of microtubule subunits are not as well understood. In order for proper microtubule polymerisation to occur, assembly competent α/β tubulin heterodimers must be provided, and to do so, newly folded α- and β- tubulins must go through the tubulin folding pathway. An *in vitro* model of this pathway has been proposed by Cowan and colleagues, but the *in vivo* studies in fission yeast had not been completed as the homologue of cofactor C had not been identified. Nor has the systematic physiological analysis of the pathway been performed in any other organisms. Therefore, in this study, I have identified the fission yeast orthologue Tbc1, constructed and analysed the mutant for this essential protein, and in relation studied its interactor Alp41, the fission yeast orthologue of Arl2. Analysing Alp41 and its mutants led me to investigate the function of Alp1, the orthologue of cofactor D. Intriguingly, Alp1 appeared to have two roles – to fold new heterodimers in the pathway, but also to depolymerise microtubules. These results will be discussed in the context of the overall pathway and its implications.

7.1 The functional characterisation of Tbc1 and its G protein Alp41

The fission yeast orthologues of the tubulin folding cofactors had been previously identified and studied (Hirata et al., 1998; Radcliffe et al., 1998; Radcliffe et al., 1999; Radcliffe et al., 2000a; Radcliffe and Toda, 2000). When a multicopy suppressor screen was carried out for a novel α tubulin mutant (Asakawa, 2005), a candidate was found

for the missing cofactor C which we named Tbc1. Upon mutant isolation we found that the loss of function of cofactor C resulted in microtubule loss, consistent with the effects of losing the other cofactors.

The identification of the fission yeast orthologue of cofactor C allowed us to add to our understanding of the fission yeast tubulin folding pathway. The fact that the loss of function led to the loss of microtubules indicated that the role of Tbc1 was indeed essential for microtubule formation. As the last cofactor to act on the pathway, it clearly has an alternate function to that of the other cofactors which are involved in capturing the α- or β- monomer. In the *in vitro* model, it was shown that cofactor C was able to act in concert with cofactors D and E to trigger GTP hydrolysis on the tubulin itself, triggering release of the heterodimer for incorporation into the plus end of the microtubule. Aside from this, we suspected that cofactor C may have an additional function, acting as a GAP for another G protein.

Upon studying the sequence and identifying the Arginine finger crucial for GAP activity, we turned to the literature to identify the possible small G protein for Tbc1. An ideal candidate was Alp41, the fission yeast orthologue of Arl2. Alp41 carried the consensuses required for it to be identified as a small G protein, and upon ts mutant isolation its microtubule phenotype showed that it was involved in microtubule regulation. RP2 had been identified as a GAP for Arl3. As the sequence conservation between Arl2, Arl3 and Alp41 was so high, we proposed that the small G protein that Tbc1 was acting on was indeed Alp41. This was confirmed by the physical interaction shown between Tbc1 and Alp41 (Fig.5.1, 5.2).

Interestingly, the *alp41* mutants isolated had two very distinct microtubule phenotypes. The class I mutants had a similar phenotype to the *tbc1* and other cofactor mutants, showing defective microtubules. In stark contrast, the class II mutants retained their microtubules, which appeared to curl around the cell tips without undergoing catastrophe. However, further analysis indicated that these microtubules were not functional, showing increased chromosome mis-segregation and defective mitochondria distribution. In contrast to the cofactors, Alp41 is not directly within the tubulin folding

pathway itself (Radcliffe et al., 2000b). Therefore, depending on the effect of the mutations on Alp41 function, there may be differences in the consequent microtubule defects.

This drastic difference in phenotypes may be explained by the nature of the mutation sites seen in these mutants. The mutations in both the class I and class II mutants have been summarised in Fig.4.5, but there was no significant clue in order to establish what effect the mutation had on the function of Alp41. As Alp41 is a small G protein, one of the possibilities is that Alp41 was rendered either GTP or GDP fixed. Otherwise it could be completely unable to bind nucleotides at all. This possible variation in defects could result in different or even opposite phenotypes.

Suggesting that Tbc1 is a GAP for Alp41 which, as previously mentioned, is not strictly part of the tubulin folding pathway, would indicate that Tbc1/cofactor C, has a function apart from that when bound to the other cofactors as part of the supercomplex. This would create another process within microtubule biogenesis, which may not directly influence the heterodimer formation process, but will affect microtubule regulation as seen in the *alp41* mutants. The complexity of the mutants isolated for *alp41* suggested that Alp41 may also be involved in many stages of microtubule regulation.

7.2 Alp41's role in the tubulin folding pathway

Alp41 is a small G protein. Therefore it can exist in the GTP-bound active form or the GDP-bound inactive form. Conventionally, the active GTP-bound form will interact with an effector that would regulate a downstream signalling pathway. The GDP-bound form on the other hand may interact with an additional component, or exist only in its inactive state awaiting activation by conversion into the GTP-bound form.

Following on from the analysis of the *alp41* ts mutants, I investigated what effect it would have on microtubule structure if Alp41 was fixed in either its GTP or GDP bound form. This was in the expectation that maybe the opposing phenotypes seen in the class I and class II mutants could be categorised if they were fixed in either the GTP

of GDP form. Rather unexpectedly, when I constructed the strains overexpressing the GTP or GDP bound form, I saw identical microtubule phenotypes (Fig.5.6). This phenotype mimicked the *tbc1* mutants and *alp41* class I mutants, showing defective microtubules or no microtubules at all depending on the level of overexpression. This led me to propose that it is not the nucleotide state that Alp41 is in that is crucial for its function – but in fact it is the cycling between the two forms that is important. This also explains the rescue experiment in which the different *alp41* mutants had different rates of rescue with plasmids overexpressing GTP or GDP bound Alp41 (Fig.5.7).

These results bring up an important question – is there a GEF for Alp41? At the moment it cannot be said what aids the conversion of the GDP bound to Alp41 to GTP. In order to find some potential candidates, I carried out a Yeast 2-Hybrid screen to find more interacting partners for Alp41. It was already known that its human homologue Arl2 has several interactors, including BART (Zhang et al., 2009), PDEδ (Hanzal-Bayer et al., 2002) and HRG4 (Kobayashi et al., 2003) which all have very different functions within the cell. This suggests that Alp41 may also have numerous partners apart from Tbc1, including a possible GEF. However, the screen did not produce any potentially interesting hits, or any that seemed to be related to microtubule regulation. I believe this is a question that should be addressed again, and will discuss this further in Chap.7.4.

7.3 Alp1's opposing roles and its effects on microtubule dynamics

Upon searching for an interacting partner for Alp41, I picked up Alp1 as being a potential effector. Alp1's human homologue cofactor D had been shown to interact with Arl2 (human orthologue of Alp41), which would indicate a function of Alp1 that would be distinct from its function within the pathway. It would also be reasonable to believe that the interactor of Alp41 could be one of the cofactors, considering its effects in microtubule regulation. This was an interesting prospect to pursue, and so I tried to confirm this interaction. Interestingly, I found that Alp1 and Alp41 did not interact unless Alp41 was in its GDP bound state. This preference of the GDP bound form had

also been shown in the cofactor D-Arl2 interaction, although it was not such a clear difference (Bhamidipati et al., 2000).

Consequently, the purpose of this binding was explored – what effect would it have on the cell if Alp1 was not able to be captured by the GDP-bound Alp41? I mimicked this situation by overexpressing Alp1 within the cell and observing the microtubules, which showed a remarkable result – the GFP-tagged Alp1 was seen to localise on the microtubules, and subsequently depolymerise them (Fig.6.8). This was found in a proportion of the cells observed, with some cells having no microtubules at all after sufficient length of overexpression. This phenotype was consistent in the *tbc1* ts mutants, which, by having defective GAP activity, would result in increased levels of free Alp1 as mimicked by the overexpression.

This data suggested that Alp1 may have dual roles in microtubule regulation – as a cofactor for heterodimer formation, and for the opposing depolymerising function. This led me to propose a model, combining data from Tbc1, Alp41 and Alp1 as shown in Fig.7.1.

At the end of the pathway where the α-tubulin bound Alp21 and β-tubulin bound Alp1 converge to form a supercomplex with Tbc1, two situations can arise. If Tbc1 is readily available to form the supercomplex, GTP hydrolysis for tubulins is triggered by the combined actions of the cofactors, and the newly folded α/β heterodimer is released for incorporation into the plus end of the microtubule. However in the second scenario where Tbc1 is readily acting as a GAP for Alp41, there is excess Alp1 within the cell as supercomplex formation is scarce. This excess Alp1, assuming that the β-tubulin monomer pool is steady, would be free and go on to localise on the microtubules and prevent further polymerisation, leading to eventual depolymerisation of microtubules. This must be inhibited to maintain microtubule dynamics. This is inhibited by the action of Alp41, which is now GDP-bound and able to bind and absorb Alp1.

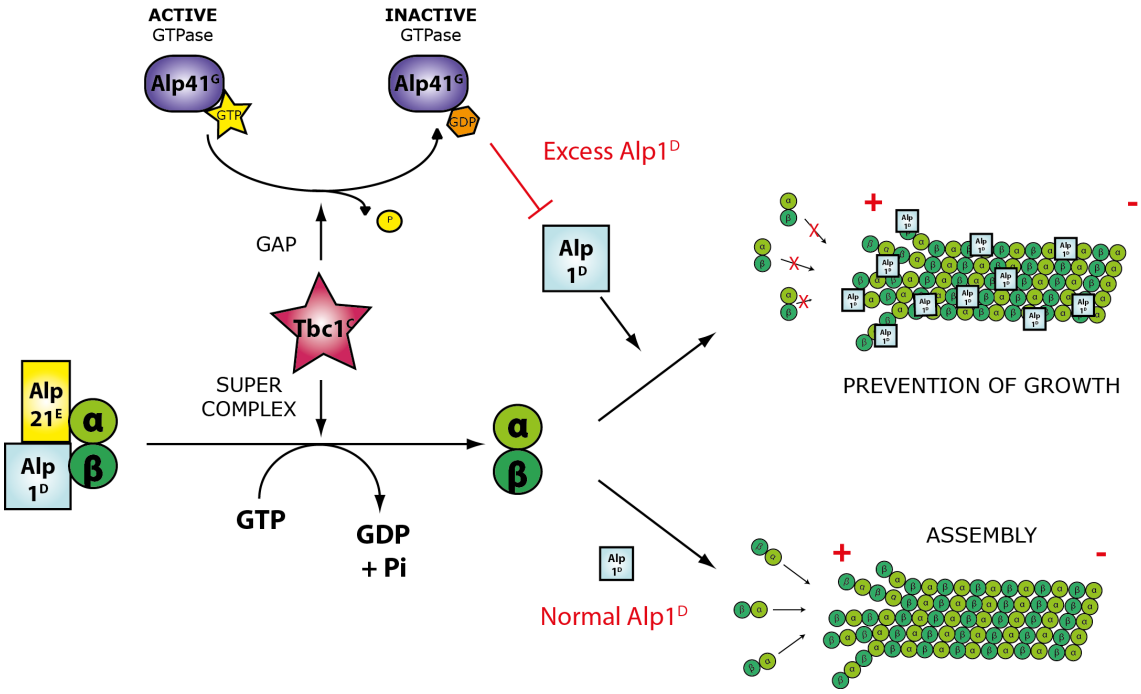

Figure 7.1 The final tubulin folding pathway

The schematic shows the final stage of the tubulin folding pathway after the α-tubulin bound Alp21^{E} and β-tubulin bound Alp1^{D} converge to form the supercomplex as Tbc1^{C} is introduced. Two outcomes are shown – normal assembly of microtubules under normal Alp1 levels, and the prevention of growth caused by excess Alp1 levels in the cell.

This indicates that there are several 'competition' events happening within this section of the pathway. First there is competition of what protein Tbc1 can bind to – Alp41 or the supercomplex. The fact that only GDP-bound Alp41 is able to bind Alp1 shows that when in the wild-type or GTP-bound form, Tbc1 is readily able to bind Alp41. There is also 'competition' for Alp1 – if Tbc1 is not acting as a GAP for Alp41 it is able to form a supercomplex which in turn absorbs the Alp1 within the cell. If there is excess, it is absorbed by GDP-bound Alp41. This intricate balance of Alp1, Alp41 and Tbc1 binding suggests a complex mechanism in order to maintain the tubulin heterodimer pool and microtubule dynamics within the cell.

7.4 Future directions

An important question that arises from this model is, what is the effector of Alp41? The cell clearly has developed a mechanism by which to inhibit microtubules from being destroyed when there is excess Alp1 within the cell. The cause of excess Alp1 within the cell may be a result of several situations, but I propose that in this case it may be from the lack of supercomplex formation due to Tbc1 acting as a GAP for Alp41 instead. This obviously prompts the question of what exactly Alp41 does in regards to its GDP/GTP cycle. There must be an effector that interacts with the active form of Alp41, which, when it needs to be inhibited, will require GAP activity by Tbc1 to render it inactive.

Another remaining mystery is if there is a GEF, or even possibly a GDI, for this reaction. These questions could be answered by performing a different screen in order to look for interactors of Alp41. Performing the Yeast 2-Hybrid screening with a GDP/GTP bound form of Alp41 as a bait could prove to be a more effective way of picking up potential candidates. On the other hand a more direct approach such as a TAP-Tag purification may also be effective in finding interactors. Alp41 is obviously important for microtubule regulation as interfering with its nucleotide cycle has catastrophic impact on the microtubules within the cell. The possibility of other processes that it is involved in with regards to the microtubule would be a point of

interest. A multicopy suppressor screen would also be a possible method of trying to find genetic interactors within this pathway.

Another aspect of this Alp1-Alp41-Tbc1 interaction which remains to be resolved is how exactly Alp1 destroys the microtubules. Evidence suggesting that Alp1 is a MAP was previously seen (Hirata et al., 1998) and this was confirmed in this current study by the overexpression of Alp1 and its co-localisation with the microtubules within the cell. From this data we suggest that this excessive 'painting' depolymerises the microtubules. Interestingly, it has been shown that bovine microtubules can be destroyed by the overexpression of bovine cofactor D, but within the human system this is not the case (Tian et al., 2010). A suggested mechanism is that the excess of cofactor D can dissociate the newly folded heterodimers (Bhamidipati et al., 2000), however this remains to be confirmed. This species dependency and the divergence behind these data suggest that there may be a complex mechanism involving Alp1 and microtubules. It would be interesting to observe this association of Alp1 behaviour as a MAP in greater detail, perhaps on a molecular level by using techniques such as TIRF (total internal reflection fluorescence) microscopy, which allows the *in vitro* observation of single molecules of purified protein on a microtubule (Manneville, 2006).

Interestingly, there have been reports that the other cofactors, namely cofactors B and E, were also able to depolymerise microtubules upon overexpression (Kortazar et al., 2007), which at least for Alp11 was observed in fission yeast (Radcliffe et al., 2000a). Cofactor B has been reported to have a ubiquitin-like domain, which suggests that it may be involved in recycling or degradation of tubulin monomers. Such data imply that there still may be many more functions of the cofactor proteins – molecular chaperones are known to have several functions and this may be the case for the tubulin folding cofactors too.

In this study, I have used the fission yeast model system to observe the effects of loss of function for the tubulin cofactor orthologue Tbc1 and its related G protein Alp41. The two proteins work in concert, with Tbc1 acting as a GAP for Alp41. Alp41 together with Tbc1 regulates the detrimental function of Alp1 to destroy the microtubules within

the cell. Not only has this study confirmed the orthologue of Tbc1 in order to complete the fission yeast tubulin folding pathway, but it has also expanded the knowledge of Alp1, the cofactor D orthologue and what extra importance it plays in microtubule regulation. Its opposing dual roles as a 'creator' and 'destroyer' of microtubules is intriguing, and highlights the necessity of tight regulation of this protein. Further work on Alp1 would allow us to understand the full potential of these tubulin specific chaperonins and their crucial roles within the cell.

7.5 Further implications of the tubulin folding pathway

As mentioned on many occasions, microtubules are essential structures within the cell. Being the fundamental process of tubulin biogenesis, it has become clear that defects in the tubulin folding pathway and the cofactors that compose it can lead to several defects at the organismal level.

Cofactor C has recently been suggested to be involved in cancer. Dumontet and colleagues have shown evidence that the silencing of cofactor C showed reduced tubulin within MCF7 cells, together with higher proliferation and an increased percentage of cells in S-phase. Cofactor C silenced cells also showed higher sensitivity to the S-phase-tageting drug gemcitabine and microtubule-targeting drugs. These results are consistent to the data I have shown for the *tbc1* ts mutants, which showed high sensitivity to TBZ as well as showing a lack of microtubules. This novel discovery that cofactor C may be involved in tumour cell regulation may propel this protein as a potential candidate in drug development (Hage-Sleiman et al., 2010; Hage-Sleiman et al., 2011).

Cofactor D has emerged as a possible centriolar protein, localising at the centrosomes and midbody. When disrupted, there were defects seen in not only spindle organisation but centriole formation itself and ciliogenesis in multiciliated cells (Fanarraga et al., 2010). It was further described as being required for γ-tubulin complex recruitment and anchoring, suggesting possible novel roles in nucleation as well as mitosis (Cunningham and Kahn, 2008). This allows us to speculate that cofactor D may indeed

have several functions in microtubule regulation – especially if they have functions in nucleation. The severe lack of microtubules in the yeast mutants of cofactor D and its toxicity when overexpressed may be related to these functions.

Cofactor B was found to play several interesting and important roles – it has been reported to play important roles in microglia cells in the central nervous system that modulate neurogenesis and neuronal cell death. Cofactor B expression levels have been suggested to act as a microtubule density regulator in these cells (Fanarraga et al., 2009). Defective interactions between cofactor B and α-tubulin have also been reported to cause pachygyria (Tian et al., 2008). Very recently, cofactor B has been associated with EB1, the microtubule plus end protein (Carranza et al., 2012). These neural implications of cofactor B have deemed it an interesting candidate for study.

In addition, cofactor A has recently been suggested to be involved in spermatogenesis and testis maturation (Nolasco et al., 2012). Cofactor E has been linked to disorders such as HRD which is thought to be caused by the lack of functional cofactor E (Tian et al., 2006).

All these studies suggest not only the importance of microtubule function in human disease, but also the widespread effects of defects in the tubulin cofactors. The wide variety of data shown from studies in humans and other organisms show that there are clearly differences in function and characteristics amongst the organismal orthologues. This and my results suggests that the tubulin pathway may to some extent have diverged from the canonical in vitro model proposed from the previous studies. Therefore understanding the fundamentals of cofactor regulation and their microtubule regulation will contribute to several fields of research. I believe that by using the fission yeast system to study these cofactors, I have been able to uncover the details of this complex mechanism, integrating all the cofactors and their roles within microtubule regulation. These very specific small molecular chaperones clearly have very big roles to play within living organisms.

Chapter 8. Reference List

Al-Bassam, J., Kim, H., Brouhard, G., van Oijen, A., Harrison, S.C., and Chang, F. (2010). CLASP promotes microtubule rescue by recruiting tubulin dimers to the microtubule. Dev Cell *19*, 245-258.

Alfa, C.E., and Hyams, J.S. (1991). Microtubules in the fission yeast Schizosaccharomyces pombe contain only the tyrosinated form of alpha-tubulin. Cell Motil Cytoskeleton *18*, 86-93.

Amor, J.C., Horton, J.R., Zhu, X., Wang, Y., Sullards, C., Ringe, D., Cheng, X., and Kahn, R.A. (2001). Structures of yeast ARF2 and ARL1: distinct roles for the N terminus in the structure and function of ARF family GTPases. J Biol Chem *276*, 42477-42484.

Anfinsen, C.B. (1973). Principles that govern the folding of protein chains. Science *181*, 223-230.

Antoshechkin, I., and Han, M. (2002). The C. elegans evl-20 gene is a homolog of the small GTPase ARL2 and regulates cytoskeleton dynamics during cytokinesis and morphogenesis. Dev Cell *2*, 579-591.

Araki, K., and Nagata, K. (2011). Protein folding and quality control in the ER. Cold Spring Harb Perspect Biol *3*, a007526.

Arce, C.A., Rodriguez, J.A., Barra, H.S., and Caputo, R. (1975). Incorporation of L-tyrosine, L-phenylalanine and L-3,4-dihydroxyphenylalanine as single units into rat brain tubulin. Eur J Biochem *59*, 145-149.

Asakawa, K. (2005). The V260I Mutation in Fission Yeast -Tubulin Atb2 Affects Microtubule Dynamics and EB1-Mal3 Localization and Activates the Bub1 Branch of the Spindle Checkpoint. Molecular Biology of the Cell *17*, 1421-1435.

Bahler, J., Wu, J.Q., Longtine, M.S., Shah, N.G., McKenzie, A., 3rd, Steever, A.B., Wach, A., Philippsen, P., and Pringle, J.R. (1998). Heterologous modules for efficient and versatile PCR-based gene targeting in Schizosaccharomyces pombe. Yeast *14*, 943-951.

Barkovich, A.J., Guerrini, R., Kuzniecky, R.I., Jackson, G.D., and Dobyns, W.B. (2012). A developmental and genetic classification for malformations of cortical development: update 2012. Brain *135*, 1348-1369.

Bartolini, F. (2002). Functional Overlap between Retinitis Pigmentosa 2 Protein and the Tubulin-specific Chaperone Cofactor C. Journal of Biological Chemistry *277*, 14629-14634.

Beghin, A., Belin, S., Hage-Sleiman, R., Brunet Manquat, S., Goddard, S., Tabone, E., Jordheim, L.P., Treilleux, I., Poupon, M.F., Diaz, J.J*., et al.* (2009). ADP ribosylation factor like 2 (Arl2) regulates breast tumor aggressivity in immunodeficient mice. PLoS ONE *4*, e7478.

Beghin, A., Honore, S., Messana, C., Matera, E.L., Aim, J., Burlinchon, S., Braguer, D., and Dumontet, C. (2007). ADP ribosylation factor like 2 (Arl2) protein influences microtubule dynamics in breast cancer cells. Exp Cell Res *313*, 473-485.

Belmont, L.D., Hyman, A.A., Sawin, K.E., and Mitchison, T.J. (1990). Real-time visualization of cell cycle-dependent changes in microtubule dynamics in cytoplasmic extracts. Cell *62*, 579-589.

Bhamidipati, A., Lewis, S.A., and Cowan, N.J. (2000). ADP ribosylation factor-like protein 2 (Arl2) regulates the interaction of tubulin-folding cofactor D with native tubulin. J Cell Biol *149*, 1087-1096.

Bitton, D.A., Wood, V., Scutt, P.J., Grallert, A., Yates, T., Smith, D.L., Hagan, I.M., and Miller, C.J. (2011). Augmented annotation of the Schizosaccharomyces pombe genome reveals additional genes required for growth and viability. Genetics *187*, 1207-1217.

Bowzard, J.B., Cheng, D., Peng, J., and Kahn, R.A. (2007). ELMOD2 is an Arl2 GTPase-activating protein that also acts on Arfs. J Biol Chem *282*, 17568-17580.

Brunner, D., and Nurse, P. (2000). CLIP170-like tip1p spatially organizes microtubular dynamics in fission yeast. Cell *102*, 695-704.

Cai, S., O'Connell, C.B., Khodjakov, A., and Walczak, C.E. (2009). Chromosome congression in the absence of kinetochore fibres. Nat Cell Biol *11*, 832-838.

Carazo-Salas, R.E., Antony, C., and Nurse, P. (2005). The kinesin Klp2 mediates polarization of interphase microtubules in fission yeast. Science *309*, 297-300.

Carranza, G., Castano, R., Fanarraga, M.L., Villegas, J.C., Goncalves, J., Soares, H., Avila, J., Marenchino, M., Campos-Olivas, R., Montoya, G.*, et al.* (2012). Autoinhibition of TBCB regulates EB1-mediated microtubule dynamics. Cell Mol Life Sci.

Chang, P., and Stearns, T. (2000). Delta-tubulin and epsilon-tubulin: two new human centrosomal tubulins reveal new aspects of centrosome structure and function. Nat Cell Biol *2*, 30-35.

Chapple, J.P., Grayson, C., Hardcastle, A.J., Bailey, T.A., Matter, K., Adamson, P., Graham, C.H., Willison, K.R., and Cheetham, M.E. (2003). Organization on the plasma membrane of the retinitis pigmentosa protein RP2: investigation of association with detergent-resistant membranes and polarized sorting. Biochem J *372*, 427-433.

Chapple, J.P., Hardcastle, A.J., Grayson, C., Spackman, L.A., Willison, K.R., and Cheetham, M.E. (2000). Mutations in the N-terminus of the X-linked retinitis pigmentosa protein RP2 interfere with the normal targeting of the protein to the plasma membrane. Hum Mol Genet *9*, 1919-1926.

Clark, J., Moore, L., Krasinskas, A., Way, J., Battey, J., Tamkun, J., and Kahn, R.A. (1993). Selective amplification of additional members of the ADP-ribosylation factor (ARF) family: cloning of additional human and Drosophila ARF-like genes. Proc Natl Acad Sci U S A *90*, 8952-8956.

Cunningham, L.A., and Kahn, R.A. (2008). Cofactor D functions as a centrosomal protein and is required for the recruitment of the gamma-tubulin ring complex at centrosomes and organization of the mitotic spindle. J Biol Chem *283*, 7155-7165.

Daga, R.R., and Chang, F. (2005). Dynamic positioning of the fission yeast cell division plane. Proc Natl Acad Sci U S A *102*, 8228-8232.

Daga, R.R., and Nurse, P. (2008). Interphase microtubule bundles use global cell shape to guide spindle alignment in fission yeast. J Cell Sci *121*, 1973-1980.

Daumke, O., Weyand, M., Chakrabarti, P.P., Vetter, I.R., and Wittinghofer, A. (2004). The GTPase-activating protein Rap1GAP uses a catalytic asparagine. Nature *429*, 197-201.

Desai, A., and Mitchison, T.J. (1997). Microtubule polymerization dynamics. Annu Rev Cell Dev Biol *13*, 83-117.

Ding, R., West, R.R., Morphew, D.M., Oakley, B.R., and McIntosh, J.R. (1997). The spindle pole body of Schizosaccharomyces pombe enters and leaves the nuclear envelope as the cell cycle proceeds. Mol Biol Cell *8*, 1461-1479.

Drummond, D.R., and Cross, R.A. (2000). Dynamics of interphase microtubules in Schizosaccharomyces pombe. Curr Biol *10*, 766-775.

Dutcher, S.K., and Trabuco, E.C. (1998). The UNI3 gene is required for assembly of basal bodies of Chlamydomonas and encodes delta-tubulin, a new member of the tubulin superfamily. Mol Biol Cell *9*, 1293-1308.

Ems-McClung, S.C., and Walczak, C.E. (2010). Kinesin-13s in mitosis: Key players in the spatial and temporal organization of spindle microtubules. Semin Cell Dev Biol *21*, 276-282.

Ersfeld, K., Wehland, J., Plessmann, U., Dodemont, H., Gerke, V., and Weber, K. (1993). Characterization of the tubulin-tyrosine ligase. J Cell Biol *120*, 725-732.

Evans, R.J., Chapple, J.P., Grayson, C., Hardcastle, A.J., and Cheetham, M.E. (2005). Assay and Functional Analysis of the ARL3 Effector RP2 Involved in X‐Linked Retinitis Pigmentosa. *404*, 468-480.

Evans, R.J., Schwarz, N., Nagel-Wolfrum, K., Wolfrum, U., Hardcastle, A.J., and Cheetham, M.E. (2010). The retinitis pigmentosa protein RP2 links pericentriolar vesicle transport between the Golgi and the primary cilium. Hum Mol Genet *19*, 1358-1367.

Fanarraga, M.L., Bellido, J., Jaen, C., Villegas, J.C., and Zabala, J.C. (2010). TBCD links centriologenesis, spindle microtubule dynamics, and midbody abscission in human cells. PLoS ONE *5*, e8846.

Fanarraga, M.L., Villegas, J.C., Carranza, G., Castano, R., and Zabala, J.C. (2009). Tubulin cofactor B regulates microtubule densities during microglia transition to the reactive states. Exp Cell Res *315*, 535-541.

Feierbach, B., Verde, F., and Chang, F. (2004). Regulation of a formin complex by the microtubule plus end protein tea1p. J Cell Biol *165*, 697-707.

Feldman, J.L., and Marshall, W.F. (2009). ASQ2 encodes a TBCC-like protein required for mother-daughter centriole linkage and mitotic spindle orientation. Curr Biol *19*, 1238-1243.

Follit, J.A., Tuft, R.A., Fogarty, K.E., and Pazour, G.J. (2006). The intraflagellar transport protein IFT20 is associated with the Golgi complex and is required for cilia assembly. Mol Biol Cell *17*, 3781-3792.

Gao, Y., Melki, R., Walden, P.D., Lewis, S.A., Ampe, C., Rommelaere, H., Vandekerckhove, J., and Cowan, N.J. (1994). A novel cochaperonin that modulates the ATPase activity of cytoplasmic chaperonin. J Cell Biol *125*, 989-996.

Gao, Y., Thomas, J.O., Chow, R.L., Lee, G.H., and Cowan, N.J. (1992). A cytoplasmic chaperonin that catalyzes beta-actin folding. Cell *69*, 1043-1050.

Gao, Y., Vainberg, I.E., Chow, R.L., and Cowan, N.J. (1993). Two cofactors and cytoplasmic chaperonin are required for the folding of alpha- and beta-tubulin. Mol Cell Biol *13*, 2478-2485.

Glotzer, M. (2009). The 3Ms of central spindle assembly: microtubules, motors and MAPs. Nat Rev Mol Cell Biol *10*, 9-20.

Goncalves, J., Nolasco, S., Nascimento, R., Lopez Fanarraga, M., Zabala, J.C., and Soares, H. (2010). TBCCD1, a new centrosomal protein, is required for centrosome and Golgi apparatus positioning. EMBO Rep *11*, 194-200.

Goodwin, S.S., and Vale, R.D. (2010). Patronin regulates the microtubule network by protecting microtubule minus ends. Cell *143*, 263-274.

Grallert, A., Beuter, C., Craven, R.A., Bagley, S., Wilks, D., Fleig, U., and Hagan, I.M. (2006). S. pombe CLASP needs dynein, not EB1 or CLIP170, to induce microtubule instability and slows polymerization rates at cell tips in a dynein-dependent manner. Genes Dev *20*, 2421-2436.

Grayson, C., Bartolini, F., Chapple, J.P., Willison, K.R., Bhamidipati, A., Lewis, S.A., Luthert, P.J., Hardcastle, A.J., Cowan, N.J., and Cheetham, M.E. (2002). Localization in the human retina of the X-linked retinitis pigmentosa protein RP2, its homologue cofactor C and the RP2 interacting protein Arl3. Hum Mol Genet *11*, 3065-3074.

Grynberg, M., Jaroszewski, L., and Godzik, A. (2003). Domain analysis of the tubulin cofactor system: a model for tubulin folding and dimerization. BMC Bioinformatics *4*, 46.

Hagan, I., and Yanagida, M. (1995). The product of the spindle formation gene sad1+ associates with the fission yeast spindle pole body and is essential for viability. J Cell Biol *129*, 1033-1047.

Hagan, I.M. (1998). The fission yeast microtubule cytoskeleton. J Cell Sci *111 (Pt 12)*, 1603-1612.

Hagan, I.M., and Hyams, J.S. (1988). The use of cell division cycle mutants to investigate the control of microtubule distribution in the fission yeast Schizosaccharomyces pombe. J Cell Sci *89 (Pt 3)*, 343-357.

Hagan, I.M., and Hyams, J.S. (1996). Forces acting on the fission yeast anaphase spindle. Cell Motil Cytoskeleton *34*, 69-75.

Hage-Sleiman, R., Herveau, S., Matera, E.L., Laurier, J.F., and Dumontet, C. (2010). Tubulin binding cofactor C (TBCC) suppresses tumor growth and enhances chemosensitivity in human breast cancer cells. BMC Cancer *10*, 135.

Hage-Sleiman, R., Herveau, S., Matera, E.L., Laurier, J.F., and Dumontet, C. (2011). Silencing of tubulin binding cofactor C modifies microtubule dynamics and cell cycle distribution and enhances sensitivity to gemcitabine in breast cancer cells. Mol Cancer Ther *10*, 303-312.

Hall, J.L., and Cowan, N.J. (1985). Structural features and restricted expression of a human alpha-tubulin gene. Nucleic Acids Res *13*, 207-223.

Hallak, M.E., Rodriguez, J.A., Barra, H.S., and Caputto, R. (1977). Release of tyrosine from tyrosinated tubulin. Some common factors that affect this process and the assembly of tubulin. FEBS Lett *73*, 147-150.

Hanahan, D., and Weinberg, R.A. (2011). Hallmarks of cancer: the next generation. Cell *144*, 646-674.

Hanzal-Bayer, M., Linari, M., and Wittinghofer, A. (2005). Properties of the interaction of Arf-like protein 2 with PDEdelta. J Mol Biol *350*, 1074-1082.

Hanzal-Bayer, M., Renault, L., Roversi, P., Wittinghofer, A., and Hillig, R.C. (2002). The complex of Arl2-GTP and PDE delta: from structure to function. EMBO J *21*, 2095-2106.

Hartl, F.U., Bracher, A., and Hayer-Hartl, M. (2011). Molecular chaperones in protein folding and proteostasis. Nature *475*, 324-332.

Hayashi, A., Ding, D.Q., Tsutsumi, C., Chikashige, Y., Masuda, H., Haraguchi, T., and Hiraoka, Y. (2009). Localization of gene products using a chromosomally tagged GFP-fusion library in the fission yeast Schizosaccharomyces pombe. Genes Cells *14*, 217-225.

Hayashi, I., and Ikura, M. (2003). Crystal structure of the amino-terminal microtubule-binding domain of end-binding protein 1 (EB1). J Biol Chem *278*, 36430-36434.

Heald, R., Tournebize, R., Habermann, A., Karsenti, E., and Hyman, A. (1997). Spindle assembly in Xenopus egg extracts: respective roles of centrosomes and microtubule self-organization. J Cell Biol *138*, 615-628.

Heitz, M.J., Petersen, J., Valovin, S., and Hagan, I.M. (2001). MTOC formation during mitotic exit in fission yeast. J Cell Sci *114*, 4521-4532.

Hiraoka, Y., Toda, T., and Yanagida, M. (1984). The NDA3 gene of fission yeast encodes beta-tubulin: a cold-sensitive nda3 mutation reversibly blocks spindle formation and chromosome movement in mitosis. Cell *39*, 349-358.

Hirata, D., Masuda, H., Eddison, M., and Toda, T. (1998). Essential role of tubulin-folding cofactor D in microtubule assembly and its association with microtubules in fission yeast. EMBO J *17*, 658-666.

Honnappa, S., John, C.M., Kostrewa, D., Winkler, F.K., and Steinmetz, M.O. (2005). Structural insights into the EB1-APC interaction. EMBO J *24*, 261-269.

Honnappa, S., Okhrimenko, O., Jaussi, R., Jawhari, H., Jelesarov, I., Winkler, F.K., and Steinmetz, M.O. (2006). Key interaction modes of dynamic +TIP networks. Mol Cell *23*, 663-671.

Hoog, J.L., Schwartz, C., Noon, A.T., O'Toole, E.T., Mastronarde, D.N., McIntosh, J.R., and Antony, C. (2007). Organization of interphase microtubules in fission yeast analyzed by electron tomography. Dev Cell *12*, 349-361.

Horio, T., and Oakley, B.R. (1994). Human gamma-tubulin functions in fission yeast. J Cell Biol *126*, 1465-1473.

Horio, T., Uzawa, S., Jung, M.K., Oakley, B.R., Tanaka, K., and Yanagida, M. (1991). The fission yeast gamma-tubulin is essential for mitosis and is localized at microtubule organizing centers. J Cell Sci *99 (Pt 4)*, 693-700.

Hoyt, M.A., Macke, J.P., Roberts, B.T., and Geiser, J.R. (1997). Saccharomyces cerevisiae PAC2 functions with CIN1, 2 and 4 in a pathway leading to normal microtubule stability. Genetics *146*, 849-857.

Hoyt, M.A., Stearns, T., and Botstein, D. (1990). Chromosome instability mutants of Saccharomyces cerevisiae that are defective in microtubule-mediated processes. Mol Cell Biol *10*, 223-234.

Hubbert, C., Guardiola, A., Shao, R., Kawaguchi, Y., Ito, A., Nixon, A., Yoshida, M., Wang, X.F., and Yao, T.P. (2002). HDAC6 is a microtubule-associated deacetylase. Nature *417*, 455-458.

Hurd, T., Zhou, W., Jenkins, P., Liu, C.J., Swaroop, A., Khanna, H., Martens, J., Hildebrandt, F., and Margolis, B. (2010). The retinitis pigmentosa protein RP2 interacts with polycystin 2 and regulates cilia-mediated vertebrate development. Hum Mol Genet *19*, 4330-4344.

Hurd, T.W., Fan, S., and Margolis, B.L. (2011). Localization of retinitis pigmentosa 2 to cilia is regulated by Importin beta2. J Cell Sci *124*, 718-726.

Inoue, S., and Salmon, E.D. (1995). Force generation by microtubule assembly/disassembly in mitosis and related movements. Mol Biol Cell *6*, 1619-1640.

Ismail, S.A., Chen, Y.X., Miertzschke, M., Vetter, I.R., Koerner, C., and Wittinghofer, A. (2012). Structural basis for Arl3-specific release of myristoylated ciliary cargo from UNC119. EMBO J *31*, 4085-4094.

Ismail, S.A., Chen, Y.X., Rusinova, A., Chandra, A., Bierbaum, M., Gremer, L., Triola, G., Waldmann, H., Bastiaens, P.I., and Wittinghofer, A. (2011). Arl2-GTP and Arl3-GTP regulate a GDI-like transport system for farnesylated cargo. Nat Chem Biol *7*, 942-949.

Janke, C., and Bulinski, J.C. (2011). Post-translational regulation of the microtubule cytoskeleton: mechanisms and functions. Nat Rev Mol Cell Biol *12*, 773-786.

Janson, M.E., Setty, T.G., Paoletti, A., and Tran, P.T. (2005). Efficient formation of bipolar microtubule bundles requires microtubule-bound gamma-tubulin complexes. J Cell Biol *169*, 297-308.

Jones, R.H., Moreno, S., Nurse, P., and Jones, N.C. (1988). Expression of the SV40 promoter in fission yeast: identification and characterization of an AP-1-like factor. Cell *53*, 659-667.

Keating, T.J., and Borisy, G.G. (1999). Centrosomal and non-centrosomal microtubules. Biol Cell *91*, 321-329.

Keating, T.J., Peloquin, J.G., Rodionov, V.I., Momcilovic, D., and Borisy, G.G. (1997). Microtubule release from the centrosome. Proc Natl Acad Sci U S A *94*, 5078-5083.

Keays, D.A., Tian, G., Poirier, K., Huang, G.J., Siebold, C., Cleak, J., Oliver, P.L., Fray, M., Harvey, R.J., Molnar, Z.*, et al.* (2007). Mutations in alpha-tubulin cause abnormal neuronal migration in mice and lissencephaly in humans. Cell *128*, 45-57.

Khodjakov, A., Cole, R.W., Oakley, B.R., and Rieder, C.L. (2000). Centrosome-independent mitotic spindle formation in vertebrates. Curr Biol *10*, 59-67.

Kim, D.U., Hayles, J., Kim, D., Wood, V., Park, H.O., Won, M., Yoo, H.S., Duhig, T., Nam, M., Palmer, G.*, et al.* (2010). Analysis of a genome-wide set of gene deletions in the fission yeast Schizosaccharomyces pombe. Nat Biotechnol *28*, 617-623.

Knoblich, J.A. (2010). Asymmetric cell division: recent developments and their implications for tumour biology. Nat Rev Mol Cell Biol *11*, 849-860.

Kobayashi, A., Kubota, S., Mori, N., McLaren, M.J., and Inana, G. (2003). Photoreceptor synaptic protein HRG4 (UNC119) interacts with ARL2 via a putative conserved domain. FEBS Lett *534*, 26-32.

Komarova, Y., De Groot, C.O., Grigoriev, I., Gouveia, S.M., Munteanu, E.L., Schober, J.M., Honnappa, S., Buey, R.M., Hoogenraad, C.C., Dogterom, M.*, et al.* (2009). Mammalian end binding proteins control persistent microtubule growth. J Cell Biol *184*, 691-706.

Komarova, Y., Lansbergen, G., Galjart, N., Grosveld, F., Borisy, G.G., and Akhmanova, A. (2005). EB1 and EB3 control CLIP dissociation from the ends of growing microtubules. Mol Biol Cell *16*, 5334-5345.

Kortazar, D., Fanarraga, M.L., Carranza, G., Bellido, J., Villegas, J.C., Avila, J., and Zabala, J.C. (2007). Role of cofactors B (TBCB) and E (TBCE) in tubulin heterodimer dissociation. Exp Cell Res *313*, 425-436.

Kubelka, J., Hofrichter, J., and Eaton, W.A. (2004). The protein folding 'speed limit'. Curr Opin Struct Biol *14*, 76-88.

Kühnel, K., Veltel, S., Schlichting, I., and Wittinghofer, A. (2006). Crystal Structure of the Human Retinitis Pigmentosa 2 Protein and Its Interaction with Arl3. Structure *14*, 367-378.

Laskey, R.A., Honda, B.M., Mills, A.D., and Finch, J.T. (1978). Nucleosomes are assembled by an acidic protein which binds histones and transfers them to DNA. Nature *275*, 416-420.

Linari, M., Hanzal-Bayer, M., and Becker, J. (1999). The delta subunit of rod specific cyclic GMP phosphodiesterase, PDE delta, interacts with the Arf-like protein Arl3 in a GTP specific manner. FEBS Lett *458*, 55-59.

Liou, A.K., and Willison, K.R. (1997). Elucidation of the subunit orientation in CCT (chaperonin containing TCP1) from the subunit composition of CCT micro-complexes. EMBO J *16*, 4311-4316.

Llorca, O., Martin-Benito, J., Ritco-Vonsovici, M., Grantham, J., Hynes, G.M., Willison, K.R., Carrascosa, J.L., and Valpuesta, J.M. (2000). Eukaryotic chaperonin CCT stabilizes actin and tubulin folding intermediates in open quasi-native conformations. EMBO J *19*, 5971-5979.

Llorca, O., McCormack, E.A., Hynes, G., Grantham, J., Cordell, J., Carrascosa, J.L., Willison, K.R., Fernandez, J.J., and Valpuesta, J.M. (1999). Eukaryotic type II chaperonin CCT interacts with actin through specific subunits. Nature *402*, 693-696.

Loiodice, I., Staub, J., Setty, T.G., Nguyen, N.P., Paoletti, A., and Tran, P.T. (2005). Ase1p organizes antiparallel microtubule arrays during interphase and mitosis in fission yeast. Mol Biol Cell *16*, 1756-1768.

Manneville, J.B. (2006). Use of TIRF microscopy to visualize actin and microtubules in migrating cells. Methods Enzymol *406*, 520-532.

Martin, J., Langer, T., Boteva, R., Schramel, A., Horwich, A.L., and Hartl, F.U. (1991). Chaperonin-mediated protein folding at the surface of groEL through a 'molten globule'-like intermediate. Nature *352*, 36-42.

Martin, S.G., McDonald, W.H., Yates, J.R., 3rd, and Chang, F. (2005). Tea4p links microtubule plus ends with the formin for3p in the establishment of cell polarity. Dev Cell *8*, 479-491.

Mata, J., and Nurse, P. (1997). tea1 and the microtubular cytoskeleton are important for generating global spatial order within the fission yeast cell. Cell *89*, 939-949.

Matsuyama, A., Arai, R., Yashiroda, Y., Shirai, A., Kamata, A., Sekido, S., Kobayashi, Y., Hashimoto, A., Hamamoto, M., Hiraoka, Y.*, et al.* (2006). ORFeome cloning and global analysis of protein localization in the fission yeast Schizosaccharomyces pombe. Nat Biotechnol *24*, 841-847.

Matsuyama, A., Shimazu, T., Sumida, Y., Saito, A., Yoshimatsu, Y., Seigneurin-Berny, D., Osada, H., Komatsu, Y., Nishino, N., Khochbin, S.*, et al.* (2002). In vivo destabilization of dynamic microtubules by HDAC6-mediated deacetylation. EMBO J *21*, 6820-6831.

Matynia, A., Dimitrov, K., Mueller, U., He, X., and Sazer, S. (1996). Perturbations in the spi1p GTPase cycle of Schizosaccharomyces pombe through its GTPase-activating protein and guanine nucleotide exchange factor components result in similar phenotypic consequences. Mol Cell Biol *16*, 6352-6362.

Maundrell, K. (1990). nmt1 of fission yeast. A highly transcribed gene completely repressed by thiamine. J Biol Chem *265*, 10857-10864.

Maurer, S.P., Fourniol, F.J., Bohner, G., Moores, C.A., and Surrey, T. (2012). EBs recognize a nucleotide-dependent structural cap at growing microtubule ends. Cell *149*, 371-382.

McEwen, B.F., Heagle, A.B., Cassels, G.O., Buttle, K.F., and Rieder, C.L. (1997). Kinetochore fiber maturation in PtK1 cells and its implications for the mechanisms of chromosome congression and anaphase onset. J Cell Biol *137*, 1567-1580.

McNally, F.J., and Vale, R.D. (1993). Identification of katanin, an ATPase that severs and disassembles stable microtubules. Cell *75*, 419-429.

Meng, W., Mushika, Y., Ichii, T., and Takeichi, M. (2008). Anchorage of microtubule minus ends to adherens junctions regulates epithelial cell-cell contacts. Cell *135*, 948-959.

Meunier, S., and Vernos, I. (2011). K-fibre minus ends are stabilized by a RanGTP-dependent mechanism essential for functional spindle assembly. Nat Cell Biol *13*, 1406-1414.

Mitchison, T., and Kirschner, M. (1984). Dynamic instability of microtubule growth. Nature *312*, 237-242.

Moreno, S., Klar, A., and Nurse, P. (1991). Molecular genetic analysis of fission yeast Schizosaccharomyces pombe. Methods Enzymol *194*, 795-823.

Mori, N., Ishiba, Y., Kubota, S., Kobayashi, A., Higashide, T., McLaren, M.J., and Inana, G. (2006). Truncation mutation in HRG4 (UNC119) leads to mitochondrial ANT-1-mediated photoreceptor synaptic and retinal degeneration by apoptosis. Invest Ophthalmol Vis Sci *47*, 1281-1292.

Muromoto, R., Sekine, Y., Imoto, S., Ikeda, O., Okayama, T., Sato, N., and Matsuda, T. (2008). BART is essential for nuclear retention of STAT3. Int Immunol *20*, 395-403.

Newton, C.N., Wagenbach, M., Ovechkina, Y., Wordeman, L., and Wilson, L. (2004). MCAK, a Kin I kinesin, increases the catastrophe frequency of steady-state HeLa cell microtubules in an ATP-dependent manner in vitro. FEBS Lett *572*, 80-84.

Nolasco, S., Bellido, J., Goncalves, J., Tavares, A., Zabala, J.C., and Soares, H. (2012). The Expression of Tubulin Cofactor A (TBCA) Is Regulated by a Noncoding Antisense Tbca RNA during Testis Maturation. PLoS ONE *7*, e42536.

North, B.J., Marshall, B.L., Borra, M.T., Denu, J.M., and Verdin, E. (2003). The human Sir2 ortholog, SIRT2, is an NAD+-dependent tubulin deacetylase. Mol Cell *11*, 437-444.

Pardo, M., and Nurse, P. (2005). The nuclear rim protein Amo1 is required for proper microtubule cytoskeleton organisation in fission yeast. J Cell Sci *118*, 1705-1714.

Perdiz, D., Mackeh, R., Pous, C., and Baillet, A. (2011). The ins and outs of tubulin acetylation: more than just a post-translational modification? Cell Signal *23*, 763-771.

Perez, F., Diamantopoulos, G.S., Stalder, R., and Kreis, T.E. (1999). CLIP-170 highlights growing microtubule ends in vivo. Cell *96*, 517-527.

Peris, L., Thery, M., Faure, J., Saoudi, Y., Lafanechere, L., Chilton, J.K., Gordon-Weeks, P., Galjart, N., Bornens, M., Wordeman, L.*, et al.* (2006). Tubulin tyrosination is a major factor affecting the recruitment of CAP-Gly proteins at microtubule plus ends. J Cell Biol *174*, 839-849.

Poirier, K., Keays, D.A., Francis, F., Saillour, Y., Bahi, N., Manouvrier, S., Fallet-Bianco, C., Pasquier, L., Toutain, A., Tuy, F.P.*, et al.* (2007). Large spectrum of lissencephaly and pachygyria phenotypes resulting from de novo missense mutations in tubulin alpha 1A (TUBA1A). Hum Mutat *28*, 1055-1064.

Price, H.P., Peltan, A., Stark, M., and Smith, D.F. (2010). The small GTPase ARL2 is required for cytokinesis in Trypanosoma brucei. Mol Biochem Parasitol.

Pulkkinen, V., Bruce, S., Rintahaka, J., Hodgson, U., Laitinen, T., Alenius, H., Kinnula, V.L., Myllarniemi, M., Matikainen, S., and Kere, J. (2010). ELMOD2, a candidate gene for idiopathic pulmonary fibrosis, regulates antiviral responses. FASEB J *24*, 1167-1177.

Radcliffe, P., Hirata, D., Childs, D., Vardy, L., and Toda, T. (1998). Identification of novel temperature-sensitive lethal alleles in essential beta-tubulin and nonessential alpha 2-tubulin genes as fission yeast polarity mutants. Mol Biol Cell *9*, 1757-1771.

Radcliffe, P.A., Garcia, M.A., and Toda, T. (2000a). The cofactor-dependent pathways for alpha- and beta-tubulins in microtubule biogenesis are functionally different in fission yeast. Genetics *156*, 93-103.

Radcliffe, P.A., Hirata, D., Vardy, L., and Toda, T. (1999). Functional dissection and hierarchy of tubulin-folding cofactor homologues in fission yeast. Mol Biol Cell *10*, 2987-3001.

Radcliffe, P.A., and Toda, T. (2000). Characterisation of fission yeast alp11 mutants defines three functional domains within tubulin-folding cofactor B. Mol Gen Genet *263*, 752-760.

Radcliffe, P.A., Vardy, L., and Toda, T. (2000b). A conserved small GTP-binding protein Alp41 is essential for the cofactor-dependent biogenesis of microtubules in fission yeast. FEBS Lett *468*, 84-88.

Raybin, D., and Flavin, M. (1977). Enzyme which specifically adds tyrosine to the alpha chain of tubulin. Biochemistry *16*, 2189-2194.

Reinsch, S., and Gonczy, P. (1998). Mechanisms of nuclear positioning. J Cell Sci *111 (Pt 16)*, 2283-2295.

Rhind, N., Chen, Z., Yassour, M., Thompson, D.A., Haas, B.J., Habib, N., Wapinski, I., Roy, S., Lin, M.F., Heiman, D.I.*, et al.* (2011). Comparative functional genomics of the fission yeasts. Science *332*, 930-936.

Rieder, C.L. (1981). The structure of the cold-stable kinetochore fiber in metaphase PtK1 cells. Chromosoma *84*, 145-158.

Rios, R.M., and Bornens, M. (2003). The Golgi apparatus at the cell centre. Curr Opin Cell Biol *15*, 60-66.

Roobol, A., Sahyoun, Z.P., and Carden, M.J. (1999). Selected subunits of the cytosolic chaperonin associate with microtubules assembled in vitro. J Biol Chem *274*, 2408-2415.

Rosenblatt, J. (2005). Spindle assembly: asters part their separate ways. Nat Cell Biol *7*, 219-222.

Ruiz, F., Garreau de Loubresse, N., and Beisson, J. (1987). A mutation affecting basal body duplication and cell shape in Paramecium. J Cell Biol *104*, 417-430.

Ruiz, F., Krzywicka, A., Klotz, C., Keller, A., Cohen, J., Koll, F., Balavoine, G., and Beisson, J. (2000). The SM19 gene, required for duplication of basal bodies in Paramecium, encodes a novel tubulin, eta-tubulin. Curr Biol *10*, 1451-1454.

Sagolla, M.J., Uzawa, S., and Cande, W.Z. (2003). Individual microtubule dynamics contribute to the function of mitotic and cytoplasmic arrays in fission yeast. J Cell Sci *116*, 4891-4903.

Saibil, H.R., Zheng, D., Roseman, A.M., Hunter, A.S., Watson, G.M., Chen, S., Auf Der Mauer, A., O'Hara, B.P., Wood, S.P., Mann, N.H.*, et al.* (1993). ATP induces large quaternary rearrangements in a cage-like chaperonin structure. Curr Biol *3*, 265-273.

Sato, M., Dhut, S., and Toda, T. (2005). New drug-resistant cassettes for gene disruption and epitope tagging in Schizosaccharomyces pombe. Yeast *22*, 583-591.

Scheffzek, K. (1997). The Ras-RasGAP Complex: Structural Basis for GTPase Activation and Its Loss in Oncogenic Ras Mutants. Science *277*, 333-338.

Schrick, J.J., Vogel, P., Abuin, A., Hampton, B., and Rice, D.S. (2006). ADP-ribosylation factor-like 3 is involved in kidney and photoreceptor development. Am J Pathol *168*, 1288-1298.

Schroder, H.C., Wehland, J., and Weber, K. (1985). Purification of brain tubulin-tyrosine ligase by biochemical and immunological methods. J Cell Biol *100*, 276-281.

Schwahn, U., Lenzner, S., Dong, J., Feil, S., Hinzmann, B., van Duijnhoven, G., Kirschner, R., Hemberger, M., Bergen, A.A., Rosenberg, T.*, et al.* (1998). Positional cloning of the gene for X-linked retinitis pigmentosa 2. Nat Genet *19*, 327-332.

Schwarz, N., Hardcastle, A.J., and Cheetham, M.E. (2012). Arl3 and RP2 mediated assembly and traffic of membrane associated cilia proteins. Vision Res.

Sharer, J.D. (2001). ARL2 and BART Enter Mitochondria and Bind the Adenine Nucleotide Transporter. Molecular Biology of the Cell *13*, 71-83.

Sharer, J.D., and Kahn, R.A. (1999). The ARF-like 2 (ARL2)-binding protein, BART. Purification, cloning, and initial characterization. J Biol Chem *274*, 27553-27561.

Shern, J.F., Sharer, J.D., Pallas, D.C., Bartolini, F., Cowan, N.J., Reed, M.S., Pohl, J., and Kahn, R.A. (2003). Cytosolic Arl2 is complexed with cofactor D and protein phosphatase 2A. J Biol Chem *278*, 40829-40836.

Shultz, T., Shmuel, M., Hyman, T., and Altschuler, Y. (2008). Beta-tubulin cofactor D and ARL2 take part in apical junctional complex disassembly and abrogate epithelial structure. FASEB J *22*, 168-182.

Slep, K.C., Rogers, S.L., Elliott, S.L., Ohkura, H., Kolodziej, P.A., and Vale, R.D. (2005). Structural determinants for EB1-mediated recruitment of APC and spectraplakins to the microtubule plus end. J Cell Biol *168*, 587-598.

Spirek, M., Benko, Z., Carnecka, M., Rumpf, C., Cipak, L., Batova, M., Marova, I., Nam, M., Kim, D.U., Park, H.O.*, et al.* (2010). S. pombe genome deletion project: an update. Cell Cycle *9*, 2399-2402.

Stearns, T., Evans, L., and Kirschner, M. (1991). Gamma-tubulin is a highly conserved component of the centrosome. Cell *65*, 825-836.

Stearns, T., Hoyt, M.A., and Botstein, D. (1990). Yeast mutants sensitive to antimicrotubule drugs define three genes that affect microtubule function. Genetics *124*, 251-262.

Stephan, A., Vaughan, S., Shaw, M.K., Gull, K., and McKean, P.G. (2007). An essential quality control mechanism at the eukaryotic basal body prior to intraflagellar transport. Traffic *8*, 1323-1330.

Sullivan, K.F., and Cleveland, D.W. (1986). Identification of conserved isotype-defining variable region sequences for four vertebrate beta tubulin polypeptide classes. Proc Natl Acad Sci U S A *83*, 4327-4331.

Tamkun, J.W., Kahn, R.A., Kissinger, M., Brizuela, B.J., Rulka, C., Scott, M.P., and Kennison, J.A. (1991). The arflike gene encodes an essential GTP-binding protein in Drosophila. Proc Natl Acad Sci U S A *88*, 3120-3124.

Taniuchi, K., Iwasaki, S., and Saibara, T. (2011). BART inhibits pancreatic cancer cell invasion by inhibiting ARL2-mediated RhoA inactivation. Int J Oncol *39*, 1243-1252.

Tian, G., Bhamidipati, A., Cowan, N.J., and Lewis, S.A. (1999). Tubulin folding cofactors as GTPase-activating proteins. GTP hydrolysis and the assembly of the alpha/beta-tubulin heterodimer. J Biol Chem *274*, 24054-24058.

Tian, G., Huang, M.C., Parvari, R., Diaz, G.A., and Cowan, N.J. (2006). Cryptic out-of-frame translational initiation of TBCE rescues tubulin formation in compound heterozygous HRD. Proc Natl Acad Sci U S A *103*, 13491-13496.

Tian, G., Huang, Y., Rommelaere, H., Vandekerckhove, J., Ampe, C., and Cowan, N.J. (1996). Pathway leading to correctly folded beta-tubulin. Cell *86*, 287-296.

Tian, G., Kong, X.P., Jaglin, X.H., Chelly, J., Keays, D., and Cowan, N.J. (2008). A pachygyria-causing alpha-tubulin mutation results in inefficient cycling with CCT and a deficient interaction with TBCB. Mol Biol Cell *19*, 1152-1161.

Tian, G., Lewis, S.A., Feierbach, B., Stearns, T., Rommelaere, H., Ampe, C., and Cowan, N.J. (1997). Tubulin subunits exist in an activated conformational state generated and maintained by protein cofactors. J Cell Biol *138*, 821-832.

Tian, G., Thomas, S., and Cowan, N.J. (2010). Effect of TBCD and its regulatory interactor Arl2 on tubulin and microtubule integrity. Cytoskeleton (Hoboken) *67*, 706-714.

Toda, T., Adachi, Y., Hiraoka, Y., and Yanagida, M. (1984). Identification of the pleiotropic cell division cycle gene NDA2 as one of two different alpha-tubulin genes in Schizosaccharomyces pombe. Cell *37*, 233-242.

Tran, P.T., Marsh, L., Doye, V., Inoue, S., and Chang, F. (2001). A mechanism for nuclear positioning in fission yeast based on microtubule pushing. J Cell Biol *153*, 397-411.

Unsworth, A., Masuda, H., Dhut, S., and Toda, T. (2008). Fission yeast kinesin-8 Klp5 and Klp6 are interdependent for mitotic nuclear retention and required for proper microtubule dynamics. Mol Biol Cell *19*, 5104-5115.

Van Valkenburgh, H., Shern, J.F., Sharer, J.D., Zhu, X., and Kahn, R.A. (2001). ADP-ribosylation factors (ARFs) and ARF-like 1 (ARL1) have both specific and shared effectors: characterizing ARL1-binding proteins. J Biol Chem *276*, 22826-22837.

Vanneste, D., Ferreira, V., and Vernos, I. (2011). Chromokinesins: localization-dependent functions and regulation during cell division. Biochem Soc Trans *39*, 1154-1160.

Veltel, S., Gasper, R., Eisenacher, E., and Wittinghofer, A. (2008a). The retinitis pigmentosa 2 gene product is a GTPase-activating protein for Arf-like 3. Nature Structural & Molecular Biology *15*, 373-380.

Veltel, S., Kravchenko, A., Ismail, S., and Wittinghofer, A. (2008b). Specificity of Arl2/Arl3 signaling is mediated by a ternary Arl3-effector-GAP complex. FEBS Lett *582*, 2501-2507.

Verhey, K.J., and Gaertig, J. (2007). The tubulin code. Cell Cycle *6*, 2152-2160.

Vetter, I.R., and Wittinghofer, A. (2001). The guanine nucleotide-binding switch in three dimensions. Science *294*, 1299-1304.

Vogel, S.K., Raabe, I., Dereli, A., Maghelli, N., and Tolic-Norrelykke, I. (2007). Interphase microtubules determine the initial alignment of the mitotic spindle. Curr Biol *17*, 438-444.

Vogelsberg-Ragaglia, V., Bruce, J., Richter-Landsberg, C., Zhang, B., Hong, M., Trojanowski, J.Q., and Lee, V.M. (2000). Distinct FTDP-17 missense mutations in tau produce tau aggregates and other pathological phenotypes in transfected CHO cells. Mol Biol Cell *11*, 4093-4104.

Vorobjev, I.A., Svitkina, T.M., and Borisy, G.G. (1997). Cytoplasmic assembly of microtubules in cultured cells. J Cell Sci *110 (Pt 21)*, 2635-2645.

Wadsworth, P., and McGrail, M. (1990). Interphase microtubule dynamics are cell type-specific. J Cell Sci *95 (Pt 1)*, 23-32.

Weisbrich, A., Honnappa, S., Jaussi, R., Okhrimenko, O., Frey, D., Jelesarov, I., Akhmanova, A., and Steinmetz, M.O. (2007). Structure-function relationship of CAP-Gly domains. Nat Struct Mol Biol *14*, 959-967.

Wennerberg, K., Rossman, K.L., and Der, C.J. (2005). The Ras superfamily at a glance. J Cell Sci *118*, 843-846.

Westermann, S., and Weber, K. (2003). Post-translational modifications regulate microtubule function. Nat Rev Mol Cell Biol *4*, 938-947.

Wood, V., Gwilliam, R., Rajandream, M.A., Lyne, M., Lyne, R., Stewart, A., Sgouros, J., Peat, N., Hayles, J., Baker, S.*, et al.* (2002). The genome sequence of Schizosaccharomyces pombe. Nature *415*, 871-880.

Yaffe, M.B., Farr, G.W., Miklos, D., Horwich, A.L., Sternlicht, M.L., and Sternlicht, H. (1992). TCP1 complex is a molecular chaperone in tubulin biogenesis. Nature *358*, 245-248.

Yaffe, M.P., Harata, D., Verde, F., Eddison, M., Toda, T., and Nurse, P. (1996). Microtubules mediate mitochondrial distribution in fission yeast. Proc Natl Acad Sci U S A *93*, 11664-11668.

Yamashita, A., Sato, M., Fujita, A., Yamamoto, M., and Toda, T. (2005). The roles of fission yeast ase1 in mitotic cell division, meiotic nuclear oscillation, and cytokinesis checkpoint signaling. Mol Biol Cell *16*, 1378-1395.

Yanagida, M. (1987). Yeast tubulin genes. Microbiol Sci *4*, 115-118.

Yvon, A.M., and Wadsworth, P. (1997). Non-centrosomal microtubule formation and measurement of minus end microtubule dynamics in A498 cells. J Cell Sci *110 (Pt 19)*, 2391-2401.

Zhang, D., Rogers, G.C., Buster, D.W., and Sharp, D.J. (2007). Three microtubule severing enzymes contribute to the "Pacman-flux" machinery that moves chromosomes. J Cell Biol *177*, 231-242.

Zhang, T., Li, S., Zhang, Y., Zhong, C., Lai, Z., and Ding, J. (2009). Crystal structure of the ARL2-GTP-BART complex reveals a novel recognition and binding mode of small GTPase with effector. Structure *17*, 602-610.

Zhou, Z., Thomsen, R., Kahns, S., and Nielsen, A.L. (2010). The NSD3L histone methyltransferase regulates cell cycle and cell invasion in breast cancer cells. Biochem Biophys Res Commun *398*, 565-570.

Zimmerman, S., Tran, P.T., Daga, R.R., Niwa, O., and Chang, F. (2004). Rsp1p, a J domain protein required for disassembly and assembly of microtubule organizing centers during the fission yeast cell cycle. Dev Cell *6*, 497-509.